



UNCLASSIFIED

67-72

~~OFFICIAL USE ONLY~~

BNWL-292

2-

AEC  
RESEARCH  
and  
DEVELOPMENT  
REPORT

PACIFIC NORTHWEST LABORATORY  
MONTHLY ACTIVITIES REPORT  
JUNE 1966

Division  
of  
Reactor Development and Technology Programs

*P.D. Dusseldorp for 63006 Feb* DEC 7 1966

*A. Hasler ant*




**BATTELLE-NORTHWEST**

BATTELLE MEMORIAL INSTITUTE / PACIFIC NORTHWEST LABORATORY

~~OFFICIAL USE ONLY~~

UNCLASSIFIED

## LEGAL NOTICE

This report was prepared as an account of Government sponsored work. Neither the United States, nor the Commission, nor any person acting on behalf of the Commission:

A. Makes any warranty or representation, expressed or implied, with respect to the accuracy, completeness, or usefulness of the information contained in this report, or that the use of any information, apparatus, method, or process disclosed in this report may not infringe privately owned rights; or

B. Assumes any liabilities with respect to the use of, or for damages resulting from the use of any information, apparatus, method, or process disclosed in this report.

As used in the above, "person acting on behalf of the Commission" includes any employee or contractor of the Commission, or employee of such contractor, to the extent that such employee or contractor of the Commission, or employee of such contractor prepares, disseminates, or provides access to, any information pursuant to his employment or contract with the Commission, or his employment with such contractor.

### PACIFIC NORTHWEST LABORATORY

RICHLAND, WASHINGTON

operated by

BATTELLE MEMORIAL INSTITUTE

for the

UNITED STATES ATOMIC ENERGY COMMISSION UNDER CONTRACT AT(45-1)-1830

PRINTED BY/FOR THE U. S. ATOMIC ENERGY COMMISSION

**UNCLASSIFIED**

BNWL-292

CC-44a,b,c  
Nuclear Technology  
(Special Distribution)

PACIFIC NORTHWEST LABORATORY  
MONTHLY ACTIVITIES REPORT  
FOR JUNE 1966

AEC DIVISION OF REACTOR DEVELOPMENT  
AND TECHNOLOGY PROGRAMS

S. L. Fawcett - Director  
F. W. Albaugh - Associate Director  
R. S. Paul - Associate Director

D. C. Worlton	Manager, Applied Physics and Electronics
H. A. Kornberg	Manager, Biology
M. T. Walling	Manager, Chemistry
H. Harty	Manager, Engineering Development
W. D. Richmond	Manager, Engineering Services
A. R. Keene	Manager, Environmental Health and Engineering
J. J. Fuquay	Manager, Environmental and Radiological Sciences
E. R. Astley	Manager, FFTF Project
D. R. de Halas	Manager, Materials
C. A. Bennett	Manager, Mathematics
J. J. Cadwell	Manager, Metallurgy
F. G. Dawson	Manager, Reactor Physics

July 1966

NOTICE: PRELIMINARY REPORT

This report contains information of a preliminary nature prepared in the course of work under Atomic Energy Commission Contract AT(45-1)-1830. This information is subject to correction or modification upon the collection and evaluation of additional data.

PACIFIC NORTHWEST LABORATORY  
RICHLAND, WASHINGTON

**UNCLASSIFIED**

100

100

100

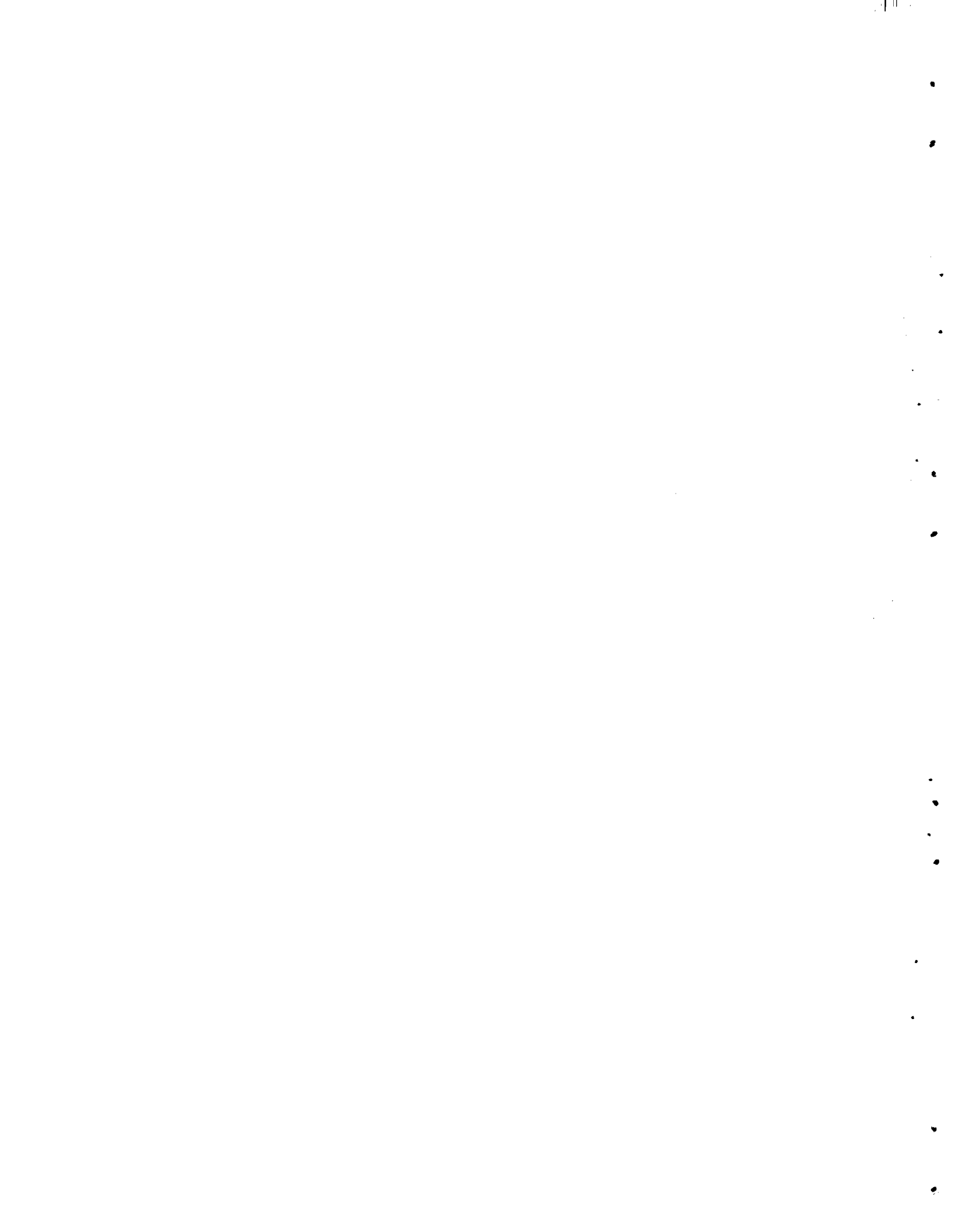
TABLE OF CONTENTS

	<u>Page</u>
SUMMARY . . . . .	4
CIVILIAN POWER REACTORS	
Specific Fuel Cycle Analysis . . . . .	18
Conceptual Reactor Design Studies . . . . .	18
USAEC-AECL Cooperative Program . . . . .	19
APPLIED AND REACTOR PHYSICS	
Plutonium Criticality Studies . . . . .	23
High Temperature Reactor Lattice Physics Studies . . . . .	24
Phoenix Fuel Reactor Program . . . . .	29
REACTOR FUELS AND MATERIALS	
Fast Fuels Oxides and Nitrides . . . . .	32
Basic Swelling Studies . . . . .	33
Nondestructive Testing . . . . .	35
Nuclear Ceramics . . . . .	37
Nuclear Graphite . . . . .	39
Irradiation Damage to Reactor Metals . . . . .	42
ATR Gas Loop Operation and Maintenance . . . . .	48
Metallic Fuels Development . . . . .	51
ENGINEERING DEVELOPMENT	
Neutron Flux Monitors . . . . .	52
Microwave Detection of Coolant Impurities and Measurement of In-Reactor Temperatures . . . . .	54
PLUTONIUM RECYCLE PROGRAM	
Fuels Development . . . . .	55
Fuels Reprocessing Development . . . . .	58
Reactor Physics . . . . .	59
Reactor Engineering Development . . . . .	64
Materials Development . . . . .	65
Cycle Analysis . . . . .	67
Test Reactor Operation . . . . .	70
EBWR Demonstration Program . . . . .	76
Industrial Assistance . . . . .	76
ADVANCED SYSTEMS	
U <sup>233</sup> Fueling of a Fast Compact Reactor . . . . .	76
NUCLEAR SAFETY	
Containment Systems Experiment . . . . .	77
Pressure Vessel Crack Monitoring . . . . .	79
Radioactive Residue Process Developments . . . . .	81
Columbia River Sedimentation Studies . . . . .	82
Waste Solidification Condensate Treatment . . . . .	82
Radioactive Shipment Hazards . . . . .	83
Fission Product Aerosol Containment . . . . .	83
Disposal of Reactor Off-Gas Into Soil Systems . . . . .	84
Reactor Safety Analysis and Evaluation . . . . .	84



CUSTOMER

Assistance to Phillips Petroleum Company . . . . .	86
Assistance to General Atomic . . . . .	86
U. S. Naval Research Laboratory . . . . .	86





SUMMARYCIVILIAN POWER REACTORSSPECIFIC FUEL CYCLE ANALYSIS

Preliminary calculations of the A-C Large Fast Reactor using slab geometry with three core regions, four blanket regions, and one reflector region were completed.

VESTA - Final copies of the report, BNWL-285, "Breeding Isn't Everything - The Economics of Uranium Conservation," are now being cleared for general distribution in August.

DAEDALUS - The code to translate MELEAGER burnup data into a linear programming problem has been written.

CONCEPTUAL REACTOR DESIGN STUDIES

Cost estimates, with the exception of site preparation and special facility charges which may be incurred at the various sites, have been essentially completed, and a draft of the study report is in preparation.

A comment issue report, "Comparison of U<sup>235</sup> and Plutonium Fueling for a Fast Oxide Breeder Reactor," has been prepared.

Work is continuing on drafting a document describing analysis of a nitride fuel cycle in fast breeder power reactors.

USAEC-AECL COOPERATIVE PROGRAM

Hydrogen analyses on the first set of zirconium specimens exposed in the ETR G-7 loop under the cooperative USAEC-AECL program showed effects of alloy and preautoclaving. There was no marked effect of flux on in-reactor hydrogen pickup. Weight gain analysis of the second set of USAEC-AECL specimens is under way at Battelle-Northwest.

The electrically heated test section for studying both turbulent mixing and flow diversion in two interconnected channels was assembled and is in the process of being installed in the experimental facility.

Debugging and modification of the hydrodynamic model for analog computer studies of the BLW-250 nuclear and hydraulic stability were continued. Reasonable agreement between results of the modified analog program and AECL calculations using the HYDNA digital computer code was obtained for simple cases.



The hydrodynamic model being used for the analog computer study of the BLW-250 nuclear and hydraulic stability now shows the salient features expected during transients in reactor power.

Efforts to develop calculational methods for determining parameters for use with a kinetics model based on coupled reactor theory are continuing.

A series of crack propagation tests to determine the effect of the orientation of the starting crack has been initiated.

Tests throughout a range of flow rates continue to show loop pressure fluctuations which are substantially greater than tolerable for precise creep deformation measurements.

### APPLIED AND REACTOR PHYSICS

#### PLUTONIUM CRITICALITY STUDIES

Criticality experiments were continued for determining critical thicknesses of bare and water reflected "infinite" slabs of plutonium nitrate solution. Measurements were performed with the 42-inch water reflected slab vessel in the thickness range of 4.5 - 6.5 inches.

Work was begun on a cooperative research program between the University of Washington and Battelle-Northwest. The program involves conjoint research projects with the Department of Nuclear Engineering and the Critical Mass Physics Section of Battelle-Northwest.

#### HIGH TEMPERATURE REACTOR PHYSICS STUDIES

A contract has been awarded for fabrication of the rare earth oxide-nickel plates for the active element of the safety blades.

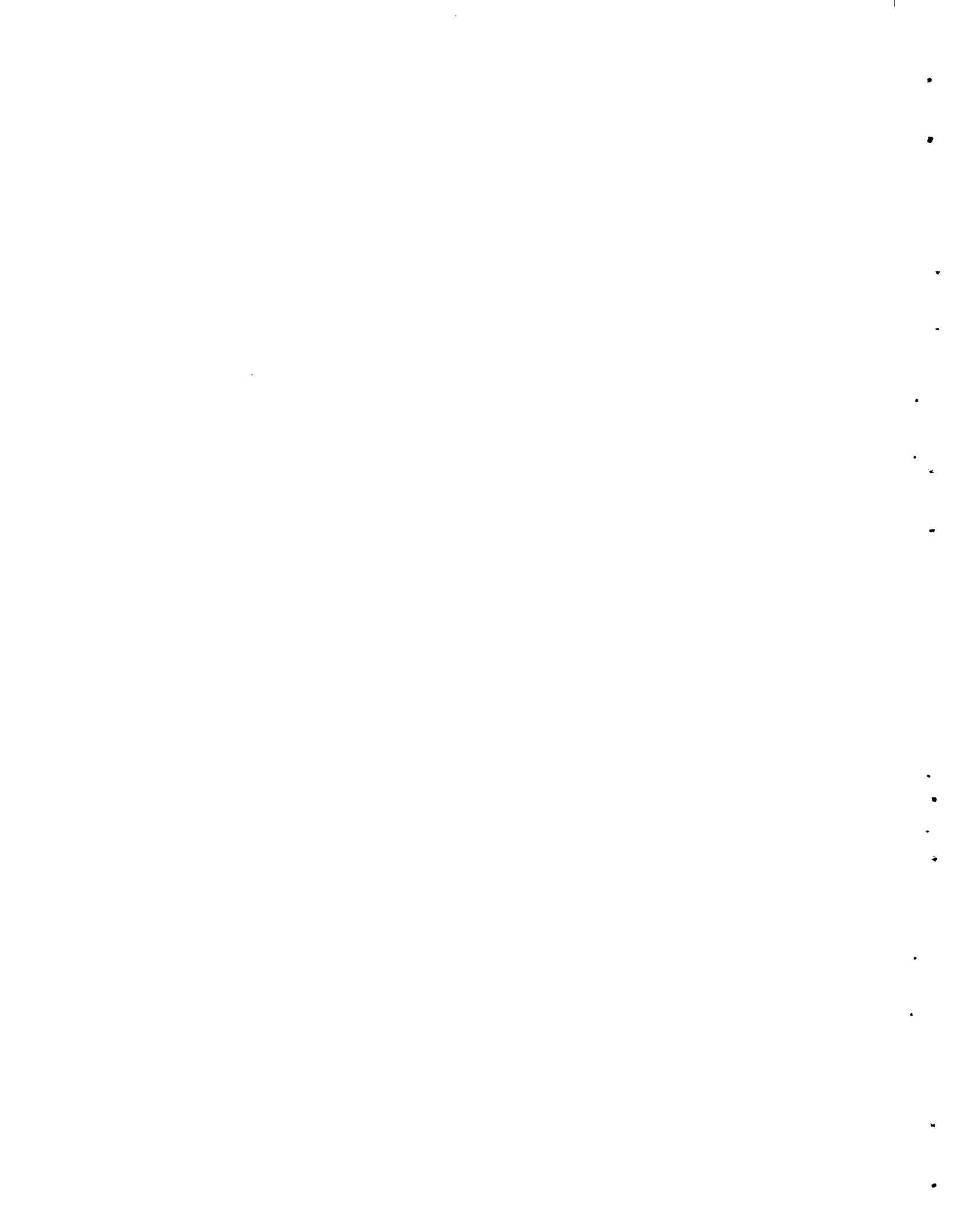
The insulation of the reactor shell has been completed. All graphite for the reactor block has been received and is being stacked to insure against design or machining errors.

An engineering review by Battelle of critical components and systems is complete, and the results are under review.

The instrument system has been accepted from the vendor with exceptions. Debugging and minor modifications continue. A log of component failure has been started for proof of reliability. Programming of the control functions continues.

Design of the couplings between the oscillators and experimental core components has begun.

Cross sections of the many isotopes to be used in analyzing the data from the HTLTR have been extracted from the BNW Master Library



in a form usable with THERMOS. They have been collected for eight temperatures from 100 °K to 2000 °K.

#### PHOENIX FUEL REACTOR PROGRAM

A meeting was held with MTR personnel at NRTS to discuss the MTR-Phoenix experiment. No major problems with the running of the experiment are presently anticipated.

It now appears that a full Pu core rather than a partial Pu core may be preferable for the burnup experiment. Multi-dimensional nuclear calculations for this configuration have been started.

Experiments to measure the critical height of unpoisoned, water reflected, Phoenix-type cores have begun in the CAF, and planning for the PRCF experiments is being continued.

Fabrication of 132 aluminum-clad Al-20 wt% Pu plates for the PRCF is expected to be complete by July 1, 1966, except for sizing of perimeter welds. Plans and schedules are being prepared in the event that fabrication of about 280 more fuel plates is required by October 1, 1966.

#### REACTOR FUELS AND MATERIALS

##### FAST FUELS OXIDES AND NITRIDES

Modification of three existing glove boxes for sodium bonding work has been started.

Improved solid-solution formation of uranium oxide - 20 wt% plutonium oxide powders was obtained after wet-blending the powders with deionized water in an alumina ball mill. Good solid-solution formation after sintering for five hours at 1650 °C in argon - 8% hydrogen was indicated by both x-ray diffraction and alpha autoradiography.

Results of thermal-expansion experiments on PuO<sub>2</sub> and UO<sub>2</sub> - 2 wt% PuO<sub>2</sub> confirm earlier data for stainless steel - PuO<sub>2</sub> cermet and PuO<sub>2</sub> which indicated that large irreversible volume changes are associated with the annealing of pneumatically-impacted materials. Preliminary thermal-expansion coefficients calculated from the cooling curves for UO<sub>2</sub> - 2 wt% PuO<sub>2</sub>:  $11.7 \pm 0.3 \times 10^{-6}/^{\circ}\text{C}$  (20-1550 °C).

Mass spectrometric analyses of radial drillings from UN - 20 wt% PuN irradiated to  $2.4 \times 10^{20}$  f/cc at 2130 w/cm confirmed radiochemical indications of severe plutonium migration. Concentration of PuN varied from 17.8 wt% at the periphery to 22.5 wt% at the mid-radius to 7.9 wt% near the fuel center.



### BASIC SWELLING STUDIES

Two low pressure, controlled temperature capsules are operating successfully at 525 °C and 450 °C, respectively, and a controlled temperature-pressure capsule is operating at 1000 psi and 450 °C. Construction has started on a capsule designed to operate at 450 °C and 5000 psi. Multiple burnups will be obtained by using specimens of different enrichments.

Uranium specimens were recovered from capsules controlled at 700 °C and irradiated to 0.1 and 0.2 at.% B.U., respectively, and from a capsule controlled at 500 °C and irradiated to 0.04 at.% B.U. Density measurements on a high purity uranium specimen and a U+Fe-Al specimen irradiated to 0.2 at.% B.U. at 700 °C revealed only 3% swelling in each of the specimens. This low swelling value and the similar behavior of the two materials corroborate previous data and the evolved concepts concerning the fundamental irradiation behavior of uranium and uranium-base alloys.

### NONDESTRUCTIVE TESTING

Parameter separation capabilities of the eddy current multi-parameter test methods are being extended with development of our channel signal sampling circuitry. Initial tests show that defect signals arising from defects of varying depth may be more accurately distinguished than has been possible with earlier techniques.

A new control system for sinusoidal thermal transducers is being investigated which promises to provide improved control of transducer input power, increasing the accuracy of sample thermal conductivity measurements.

Efforts to construct improved mathematical models of ultrasonic pulses are investigating a time varying mathematical function which includes an exponential damping factor, a hyperbolic sine factor, and a periodic cosine factor. Solutions involve the use of coefficients and arguments which are now being experimentally determined.

### NUCLEAR CERAMICS

Analysis of the radial oxygen distribution in irradiated  $UO_{2.15}$  showed that (as with other  $UO_{2+x}$  specimens) gross migration of oxygen to the center occurred. In the center the O/U ratio after irradiation was 2.40. The derived relationship between the mean oxygen to uranium ratio,  $\overline{O/U}$ , and the heat rating required for center melting is given by

$$\int_{500^{\circ}\text{C}}^{T_m} k dT = - 75.8 (\overline{O/U}) + 221 \text{ watts/cm}$$

Between 500 °C and the "recrystallization temperature" ( $T_{gg}$ ), thermal conductivity was insensitive to mean composition changes for  $2.05 < O/U$





<2.00. A marked decrease in conductivity with increasing O/U was evident for 2.00 <O/U <2.05.

Knoop hardness measurements of pneumatically impacted UO<sub>2</sub> for O/U ratios of 1.90, 1.99, 2.00, 2.02, 2.05, and 2.15 showed<sup>2+x</sup> that the hardness varied almost linearly with increase in O/U from 530 (for O/U = 1.90) to 880 (for O/U = 2.15).

Unique etch-pit distributions were observed in pneumatically-impacted UO<sub>2</sub> single crystals. Impacted pairs of UO<sub>2</sub> single crystals pairs showed a dense fringe of etch pits around the exposed cube surfaces, an intermediate etch-pit population in the interior, and an almost complete lack of etch pits at the interface surfaces.

Improvements in bonding of UO<sub>2</sub> single crystals were observed when an additive compound (Sm<sub>2</sub>O<sub>3</sub>, ThO<sub>2</sub>, or UO<sub>2.08</sub>) was present at the interface.

UO<sub>2</sub> single crystal specimens were prepared, characterized, and sent to a Japanese laboratory as part of the materials and information exchange program. In addition, a rod of Pyroceram 9606 was obtained for use as a thermal conductivity standard.

#### NUCLEAR GRAPHITE

Three pins, each containing 17 samples 0.025 in. dia. x 1.75 in. long, are being fabricated for irradiation at approximately 600 °C. Insertion in the reactor is expected in mid-July or early August.

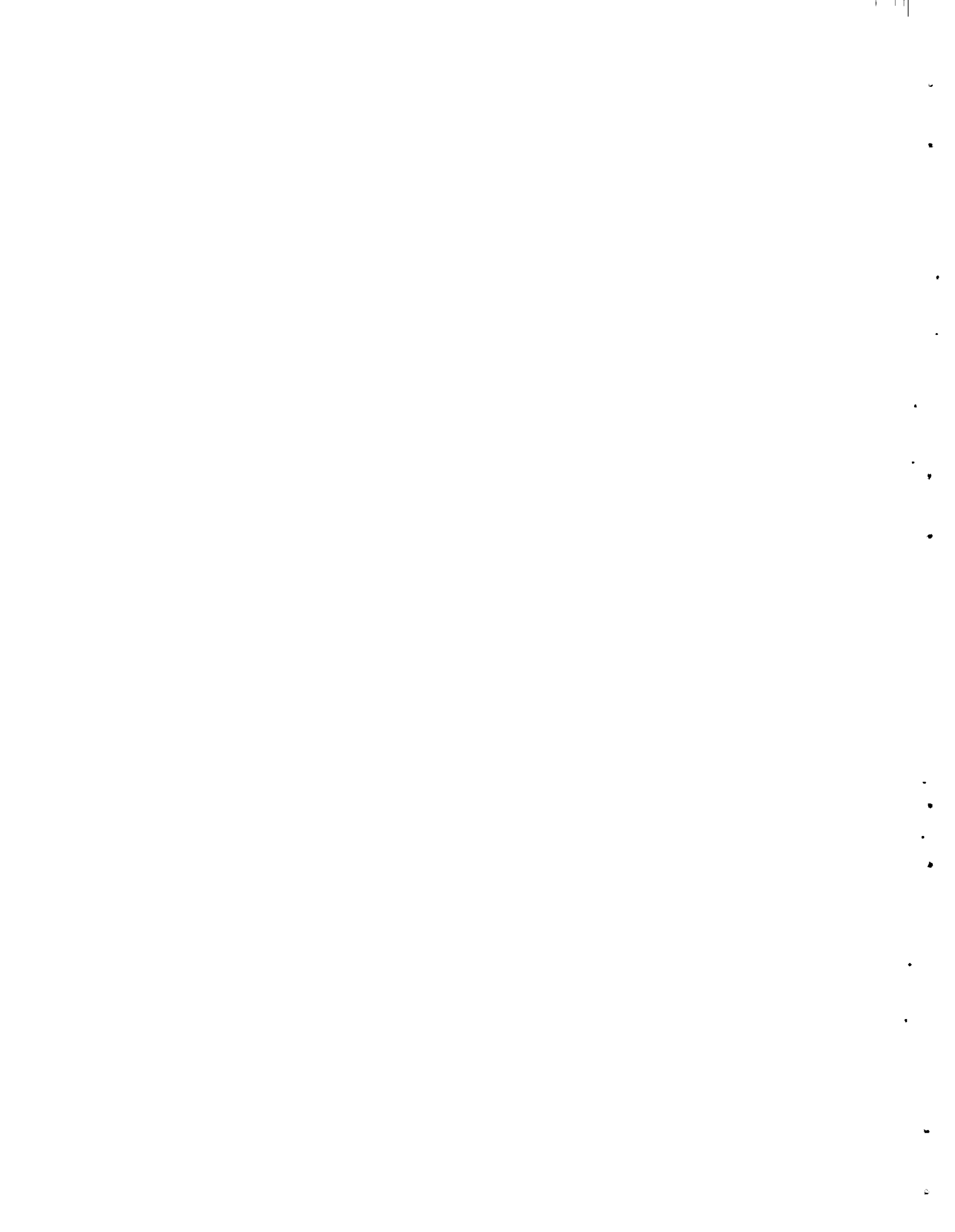
A computer program has been written to calculate values of Young's Modulus and dimensional changes from single crystal values. Preliminary calculations of modulus and of irradiation-induced dimensional changes are compatible with experimental values.

Changes in the sonic modulus occurring upon oxidation of TSX graphite were compared with ultimate tensile and compressive strengths. Samples were oxidized in air at 700 °C to varying extents up to 15% weight loss. The sonic modulus decreases somewhat more rapidly with oxidation than does the ultimate tensile strength which, in turn, decreases more rapidly than ultimate compressive strength.

#### IRRADIATION DAMAGE TO REACTOR METALS

Assembly of a sodium-filled, temperature-controlled capsule containing AISI 316 SS specimens is nearing completion. The test capsule will be charged in ETR Cycle 83.

A refractory metal prototype of the ATR gas loop specimen assembly is ready for insertion in the model loop. The assembly will be examined for changes at the end of each five-day cycle.



The AISI 316 SS order from Allegheny Ludlum has been poured and is being processed to finished stock.

The in-reactor creep test at 840 °C on annealed 304 stainless steel was not started due to heater failure. The capsule will be replaced so that the test may be run.

Construction of the high temperature capsule is continuing. Electrical installations for capsule checkout were started and are to be completed this month.

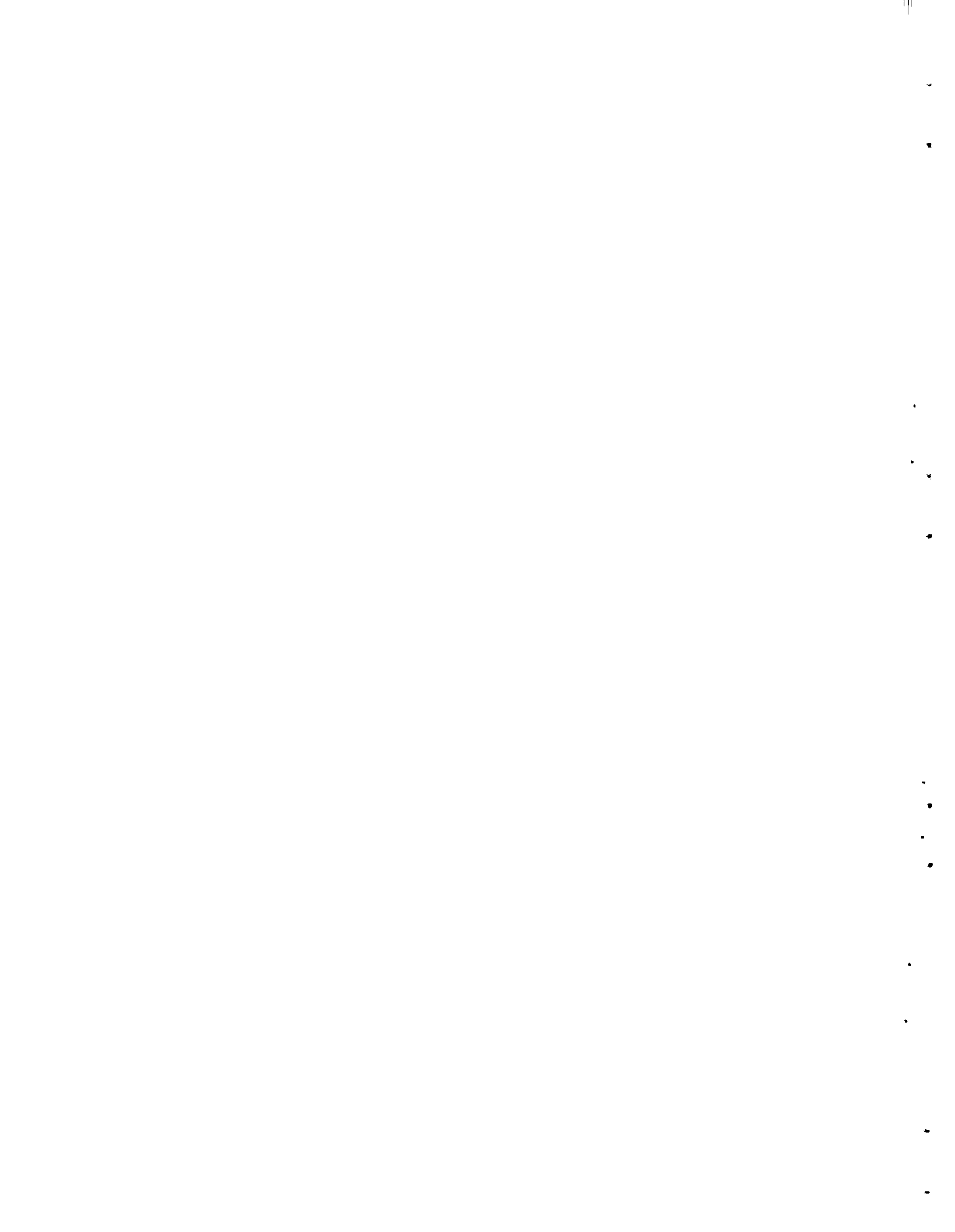
Electron microscopy has been performed or is in progress on AISI 304, 348, 316, and 321 stainless steels. Each material is being characterized in both the fully annealed and cold worked condition. A facility has been completed for preparing highly radioactive bulk specimens for examination in the electron microscope.

Annealed AISI 348 stainless steel has been examined in the electron microscope after irradiation at 60 °C to  $1.0 \times 10^{20}$  nvt (>1 Mev). The same material was given a postirradiation anneal at 450 °C for one hour in vacuum and then examined. Although a large recovery in the mechanical properties occurs after this treatment, the microstructure is apparently changed very little. Only the smaller defect clusters appear to be annihilated at this temperature; the larger clusters seem to be relatively stable. Additional transmission microscopy specimens are being examined after higher irradiation and/or postirradiation annealing temperatures.

Three papers have been written this month. They are: (1) a formal report, "Improved Postirradiation Stress-Rupture Properties of Hastelloy X-280," BNWL-231, by I. S. Levy; (2) a submission to the ANS for presentation at, and publication in the Transactions of the Winter Meeting, "Postirradiation Mechanical Property Improvement in Hastelloy X-280 and Inconel 600," BNWL-SA-724 A, by I. S. Levy; and (3) a submission to Trans. AIME, "Electron Microscopy of Tensile Specimens of Thermomechanically Treated Hastelloy X-280," BNWL-SA-608, by I. S. Levy, B. Mastel, and J. L. Brimhall.

Replica microscopy of stressed sections of irradiated and un-irradiated tensile specimens of Hastelloy X-280 showed that the effect of irradiation was to inhibit precipitation of small matrix precipitates, to enlarge the larger matrix precipitate, and to cause these large precipitates to concentrate around grain boundaries. This evidence reinforces mechanisms suggested last month for mechanical property changes in irradiated Hastelloy X-280.

Metallography of unirradiated Inconel 600 tensile specimens shows that, for the experimental treatment which resulted in the best postirradiation ductility, matrix precipitation is in evidence and grain boundaries are particulate, not continuous, in nature. The standard treatment material, which had poor postirradiation ductility,



showed no matrix precipitate and a continuous grain boundary phase. A mechanism for explaining property improvements similar to that suggested for Hastelloy X-280 is believed to apply.

Stress-rupture tests on unirradiated control specimens of Hastelloy X-280 have commenced. These are being conducted at 1350 °F (730 °C) and 18,000 psi, the 1000-hr rupture stress for standard treated unirradiated material.

Forty-eight tensile and stress-rupture specimens of Inconel X-750, Hastelloy X-280, and Inconel 600 have been discharged after irradiation at 1350 °F (730 °C) to approximately  $1 \times 10^{20}$  nvt (fast).

The fracture toughness ( $K_{Ic}$ ) of normalized A302-B irradiated to  $5 \times 10^{18}$  neutrons/cm<sup>2</sup> at 280 °C in the ETR remains unchanged from the unirradiated condition. The stress intensity factor at arrest ( $K_{Ia}$ ) decreased after irradiation indicating an increase in the rate sensitivity of the material. Specimens irradiated to  $1 \times 10^{19}$  neutrons/cm<sup>2</sup> will be available for testing in the near future.

It has been found that an exposure of five cycles (2820 hr) in the ex-reactor hot water loop at 280 °C increases the hydrogen content of annealed and autoclaved Zircaloy-2 specimens from 10 ppm to 20 ppm. The formation of hydrides due to hydrogen pickup is thought to be the cause of the decrease in fracture toughness of these specimens.

The eddy current device developed by the Electronics Measurement Research Unit for the measurement of instantaneous crack velocities in the DCB specimen has been applied to 7075-T6 aluminum. Crack velocities as high as 750 ft/sec have been observed.

#### ATR GAS LOOP OPERATION AND MAINTENANCE

The ATR model gas loop continued to operate 24 hours per day five days a week. The model heater has successfully logged 683 hours of operation including 21 thermal cycles from room temperature to various operating temperatures. Sixty percent of the time the heater has operated at 2100 °F gas outlet temperature.

Examination of the molybdenum heating elements from a model loop heater is in progress. The material from the outlet end of the heater appears to be more brittle than that from the inlet end.

Iron balls, proposed as a gamma shield in the ATR gas loop filter assembly, have been shown to sinter together at 800 °C in vacuum or in air.

The BNW gas chromatograph was developed further into an automatic model that performed high sensitivity gas analyses on the model gas loop. Impurity detection limits were consistently below 1 ppm, and the unit continued to operate reliably during the last nine months of the fiscal year with essentially no maintenance.



### METALLIC FUELS DEVELOPMENT

In the irradiation of thorium-uranium fuel elements the highest exposure fuel element has now been irradiated to 14,500 MWd/ton.

Radiometallurgy examination is being made of one element irradiated to 11,850 MWd/ton that was intentionally defected and exposed in 300 °C water.

Rod cluster fuel elements containing metallic uranium fuel are being fabricated. Two alloy ingots (350 ppm Fe - 800 ppm Al and 150 ppm Fe - 100 ppm Si) were cast, triple beta heat treated, primary extruded, and assembled as coextrusion billets. The rods will be clad with 0.025 or 0.050 inch of Zr-2 and will contain a central internal void space equal to 10% or more of the fuel volume.

### ENGINEERING DEVELOPMENT

#### NEUTRON FLUX MONITORS

A second twin-lead, dual-chamber assembly was fabricated as the compensating element for the self-powered, boron-11, beta-current concept for neutron flux monitoring.

#### MICROWAVE AND INFRARED DETECTION OF COOLANT IMPURITIES AND MEASUREMENT OF IN-REACTOR TEMPERATURES

Satisfactory operation was achieved with the rotating infrared filter-wheel mechanism for use in measuring moisture content in gases.

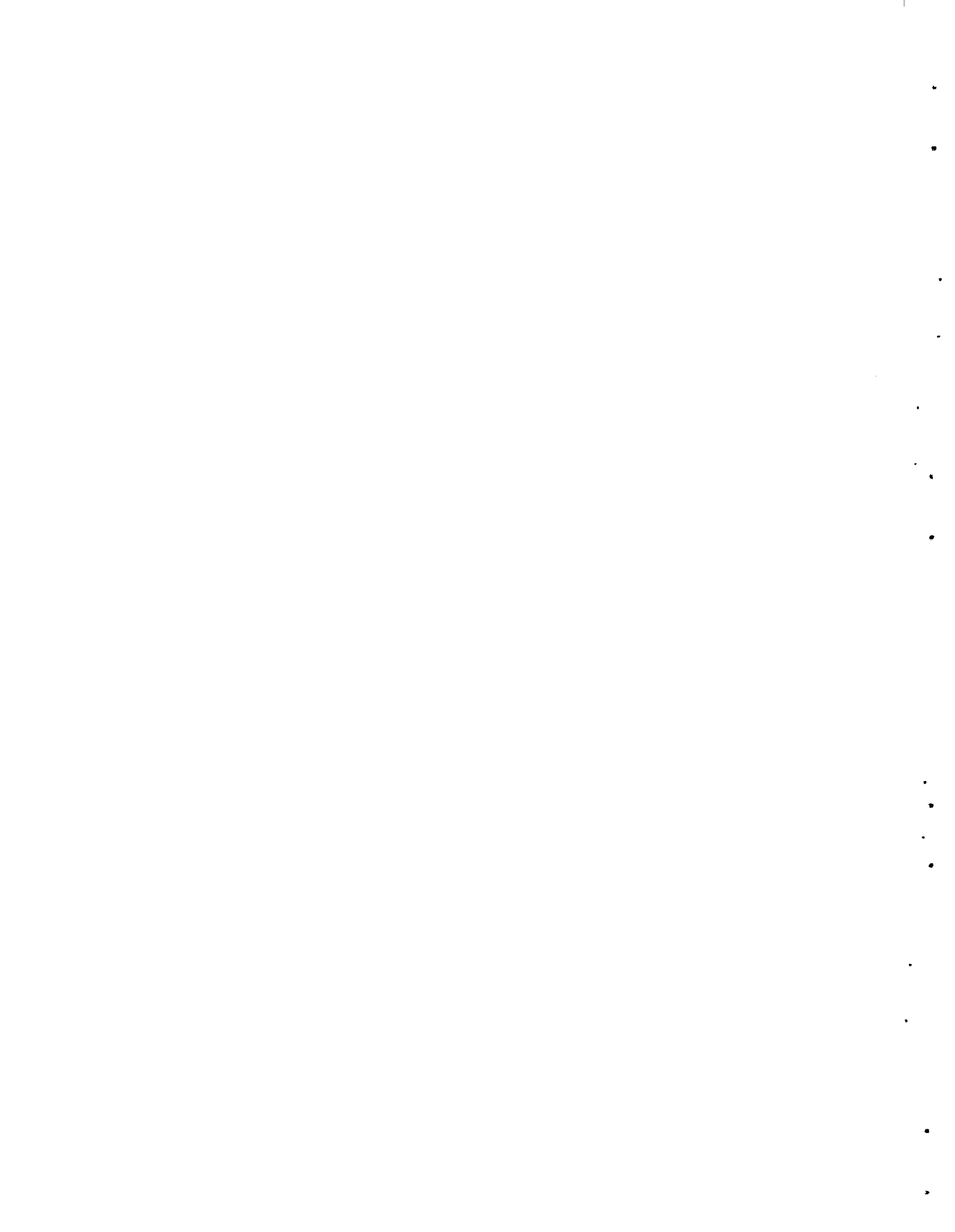
### PLUTONIUM RECYCLE PROGRAM

#### FUELS DEVELOPMENT

A comparison of beta-gamma and alpha autoradiographs of a longitudinal section of a PRTM fuel rod shows that the centrally located dark region on the beta-gamma autoradiograph coincides with the once-molten fuel region whereas the boundary indicated on the alpha autoradiograph lies beyond the once-molten fuel region, thus indicating plutonium diffusion across the liquid-solid interface.

Gamma energy spectra above 50 keV have been obtained from the three Shippingport fuel elements utilizing a lithium-uranium-germanium detector system. The isotopes present appear to be U<sup>237</sup>, Am<sup>241</sup>, and Pu<sup>238</sup> thru Pu<sup>242</sup>.

A prototype stainless steel FERT basket tube with six fuel length spacing ribs was fabricated. Charge-discharge tests in the EDEL-1 test loop are scheduled for July.





Heat transfer studies investigating the ability of various candidate FERTF fuel element baskets to prevent a pressure tube failure if molten fuel is released from the fuel element were extended to include grooved as well as ribbed baskets. Calculations showed that a grooved tube could prevent a zirconium pressure tube failure from such an accident unless one of the grooves were blocked so as to stop coolant flow through it.

The fabrication, assembly, and nondestructive testing of the components for the fuel rod pressure sensing test in PRTR will be completed this month.

A Mark-I-R high power density fuel element with an attached flux wire successfully completed flow testing in the EDEL-1 test loop.

#### FUELS REPROCESSING DEVELOPMENT

A study of the optimum initial size for a reprocessing plant for specific market demands was continued. A computer program to assist in solving this problem has been prepared and is being debugged.

#### REACTOR PHYSICS

Calculations of the efficiency of the  $(\gamma, n)$  reaction in deuterium have been completed for the PRTR using transport theory.

From noise and oscillator measurements in the PRCF it is concluded that the oscillator method should be well suited for transfer function measurements in the PRTR in the presence of extraneous noise signals.

Calculations of power generation in the FERTF of the PRTR have been completed and a contribution to the safeguards report has been prepared.

A paper summarizing the analytical and experimental results of the HPDC experiment in the PRCF has been prepared and submitted for presentation at the 1966 Winter Meeting of the American Nuclear Society.

Determination of boron concentrations in D<sub>2</sub>O is being investigated using reactivity measurements.

A description of the experimental program planned for PRCF with a light water moderated, 2% PuO<sub>2</sub>-UO<sub>2</sub> core was prepared and forwarded to the Commission.

The D<sub>2</sub>O to H<sub>2</sub>O conversion of the PRCF was completed. Using 2 wt% Pu mixed oxide fuel, 1/2" diameter x 36" long in a 0.85" pitch lattice, experiments were completed for a uniform loading with 8% Pu<sup>240</sup> and a mixed loading with 8% Pu<sup>240</sup> in the inner zone and 24% in the outer.



Experiments using 19 fuel elements each containing 108, 124, and 151 grams of Pu were completed in the CAF. The elements are made up of repeating cells of 2 - 1.96" diameter x 0.020" PuAl disks, 2 Al disks and 0.120" of polyethylene. The PuAl is 20 wt% Pu, 8% Pu<sup>240</sup>.

The computer program RETREV was rewritten in Fortran IV (70%) and Sleuth II (30%) for the Univac 1107 computer. The following request options are available: atomic number, mass, cross section type, energy, institution, year, and suppression of printout of the comment section.

In the BNW Master Library the Carbon 12 cross section was modified to include the fast absorption cross section from KFK-120. The aluminum 27 record was modified to include the peak of the 5.9 keV resonance. Chromium and nickel were also updated using the KFK-120 data. The key-punch error in the Pu-239L record was corrected.

The BNL-SRL lattice analysis code HAMMER has been successfully converted for use at this installation on the IBM 7090 or the Univac 1107.

Work was begun this month to reduce the running time of the EXTERMINATOR code on the Univac 1107.

The Rotating-Crystal-Spectrometer (RXS) was used for a single measurement of the double-differential scattering cross section of 0.1 eV energy neutrons from a thin sample of room-temperature D<sub>2</sub>O. The RXS was also used for a measurement of the double-differential scattering cross section of 0.608 eV energy neutrons from room-temperature H<sub>2</sub>O and 0.304- and 0.152-eV energy neutrons from a 0.015" thick sample of solid H<sub>2</sub>O at a temperature of -6 °C.

The triple-axis spectrometer was used to measure the double-differential scattering cross sections of neutrons from H<sub>2</sub>O at 95 °C.

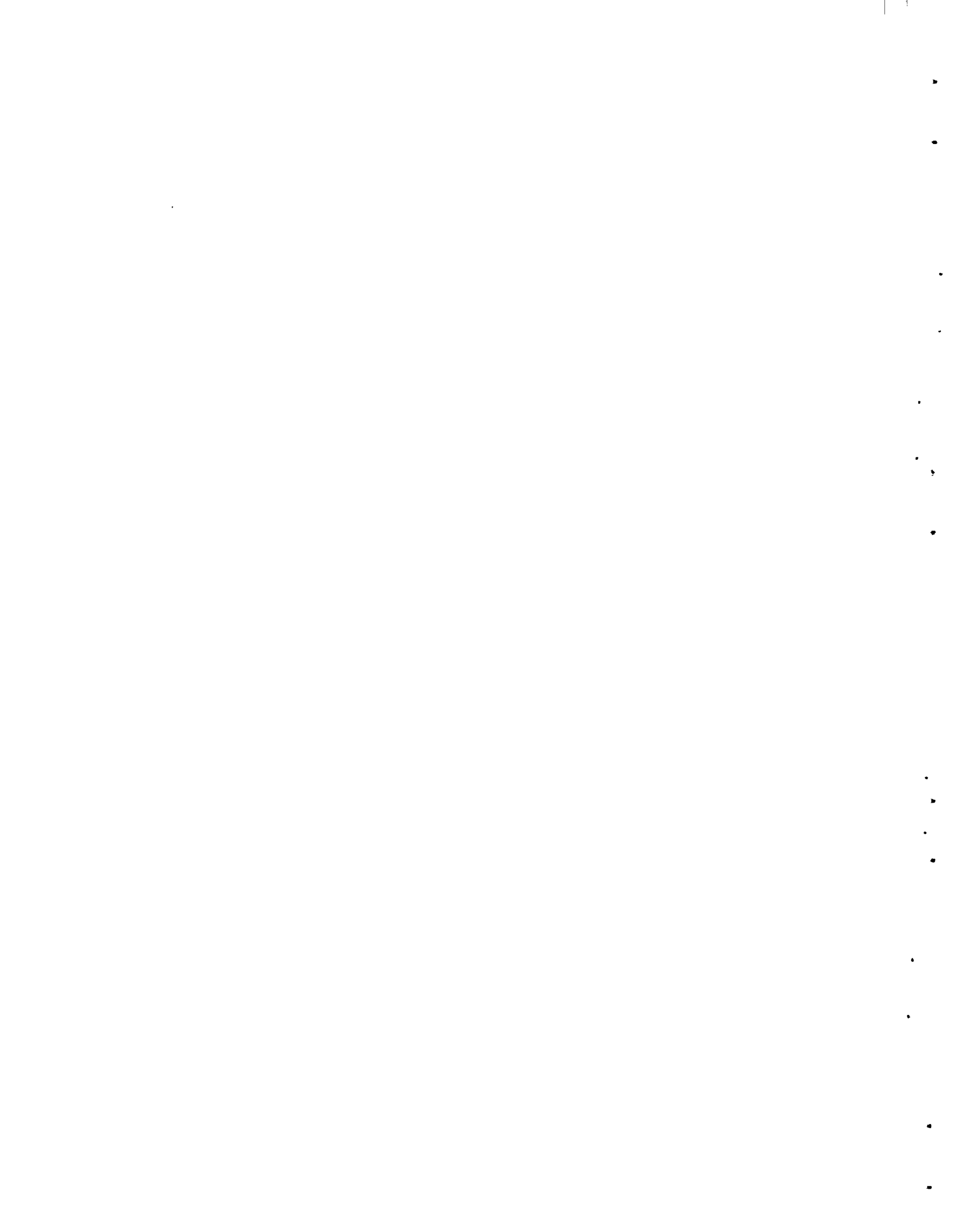
Investigation continued on a method of high-resolution monochromatization using multiple-Bragg diffraction.

An effort was made to reprocess all of the previously obtained fast neutron total cross section data.

At a meeting of the Cross Section Evaluation Working Group, BNW was assigned the responsibility of providing complete sets of evaluated data for several isotopes for the Evaluated Nuclear Data File/B. The isotopes assigned were H<sup>1</sup>, H<sup>2</sup>, Xe<sup>135</sup>, Sm<sup>149</sup>, Eu<sup>151,153</sup>, Dy<sup>164</sup>, Lu<sup>175,176</sup>, and Au<sup>197</sup>. In addition, we plan to provide data for Cu<sup>63</sup> and Cu<sup>65</sup>.

#### REACTOR ENGINEERING DEVELOPMENT

A computer code has been written capable of supplying data on heat transfer limited-moderated and water-cooled reactor cores to facilitate studies of power reactor core designs.



The boric acid test of the PRTR dump valve was completed. The chemical shim test in the Environmental Test Facility has been completed.

Fabrication of the remaining parts of the Shroud Tube Cutter is in progress.

Revisions of the PRTR reflector-moderator systems permitting the use of light water as a reflector are 80% complete.

#### MATERIALS DEVELOPMENT

Experimental difficulties with elastic strain measurements on the inside surface of a PRTR tube specimen have been resolved.

Additional crack propagation tests at prescribed temperatures have been made. The effect of increasing temperature on stress for propagation of a two-inch long simulated crack appears to be minus 48.3 psi (stress)/°C.

A mark on the inside surface of the taper of PRTR tube 5696 was probably caused by contact with a tube alignment mandrel.

Corrosion rates from continuous corrosion probes located in the moderator, reflector, and primary shield system were negligible during the past month.

Laboratory corrosion testing to evaluate potential corrosion problems resulting from a leak in the PRTR bottom primary shield has continued. Aluminum exposed to ammoniated primary shield coolant at pH 10 will have an equilibrium corrosion rate of less than 0.01 mils/month after the protective oxide layer is formed on the aluminum. Further tests to evaluate aluminum corrosion rates in degraded ammoniated coolant are planned.

Pilot plant testing of the PRTR dump valve, shroud tube bellows assembly, and shim rod assembly with borated water has been concluded. Test components are being examined for corrosion effects.

Dissolution rate studies of sintered PuO<sub>2</sub> in H<sub>3</sub>PO<sub>4</sub> have showed that this material is much more difficult to dissolve than PuO<sub>2</sub> fired at 900 °C.

#### CYCLE ANALYSIS

The economically optimum recycle of plutonium in water reactors requires a softer neutron spectrum. The softening of the spectrum may be accomplished by either reducing fuel density, reducing rod size, or adjusting the lattice pitch. Fuel cycle cost improvements are 0.1 to 0.2 mill/kWh<sub>e</sub> depending on the original U<sup>235</sup> enriched lattice.

Although the initial introduction of plutonium recycle in PWR's will cause a greater power distribution problem than U<sup>235</sup> refueling, this problem will vanish after successive refueling with plutonium recycle fuel.



### TEST REACTOR OPERATION

Preparations for starting the batch core critical tests were completed in June. The non-nuclear critical tests which include determining moderator drop rates following a reactor scram were in progress at month end. Accomplishments during the month include flushing primary system and refilling with heavy water, returning core blanket system to helium service, completing installation of the boron addition system, deuterizing and placing in service the cleanup ion exchange units for the primary and moderator systems, and essentially completing the batch core orientation briefings.

Changes to the Operating Safety Limits for PRTR were received from AEC-RLOO substantially as proposed in our April transmittal and were distributed within BNW.

Scope requirements and cost estimates for Phase II of a project to provide improved waste handling capability and control of reactor systems during off-standard situations in the PRTR have been completed.

### EBWR DEMONSTRATION PROGRAM

Analytical correlations of the EBWR experiments in the PRCF have been done using the assumptions of one dimensional diffusion theory and one dimensional transport theory.

### INDUSTRIAL ASSISTANCE

Five hundred of a planned total of 1200 UO<sub>2</sub> - 2 wt% PuO<sub>2</sub> rods were packaged and shipped to Westinghouse.

A purchase order was placed with General Electric Company for design and fabrication of 77 Mark I-R high power density fuel rods containing pelleted UO<sub>2</sub> - PuO<sub>2</sub> fuel.

### ADVANCED SYSTEMS

#### U<sup>233</sup> FUELING OF A FAST COMPACT REACTOR

A rough draft of a formal report analyzing a parameter study of a fast compact lithium-cooled reactor has been written.

### NUCLEAR SAFETY

#### CONTAINMENT SYSTEMS EXPERIMENT

Foundations for the reactor simulator shelter building were completed and building erection started. A test to determine effects of UO<sub>2</sub> cladding material on the behavior of iodine in a laboratory containment vessel showed no difference attributable to the cladding.

Preliminary containment system decontamination experiments have been run using vapor phase cleaning techniques. D.F.'s of two or less





were obtained on painted surfaces. Cleanup efficiencies on stainless steel were higher, ranging up to D.F.'s of 12.

Autoradiographic techniques have shown that several mechanisms are involved in the iodine contamination of painted surfaces in containment systems. These mechanisms are adsorption or deposition of fine particles, possible reaction with the surface, and the deposition of relatively large agglomerates.

#### PRESSURE VESSEL CRACK MONITORING

Continuing investigation of acoustic emissions of stressed piping has revealed that type 304L stainless steel, double cantilever beam specimens show a consistent pattern or maximum acoustic emission activity as formation of a macrocrack is approached; the intensity of emission is markedly reduced once the crack is formed.

A factor of ten improvement in a new high temperature, electrostatic transducer being developed for this application was achieved with use of a self-aligning bearing.

#### RADIOACTIVE RESIDUE PROCESS DEVELOPMENTS

Preliminary experiments were begun on methods for treating the high-volume condensate generated in the WSEP process.

The phosphate glass system was tested successfully for operability and remotability in WSEP.

Corrosion tests indicate 310 stainless steel is preferable to 304L stainless steel as melt pot material of construction for a proposed ORNL Rising Level Glass run in WSEP.

The thermal expansion characteristics of the solid from a proposed WSEP composition showed a very unusual hysteresis behavior.

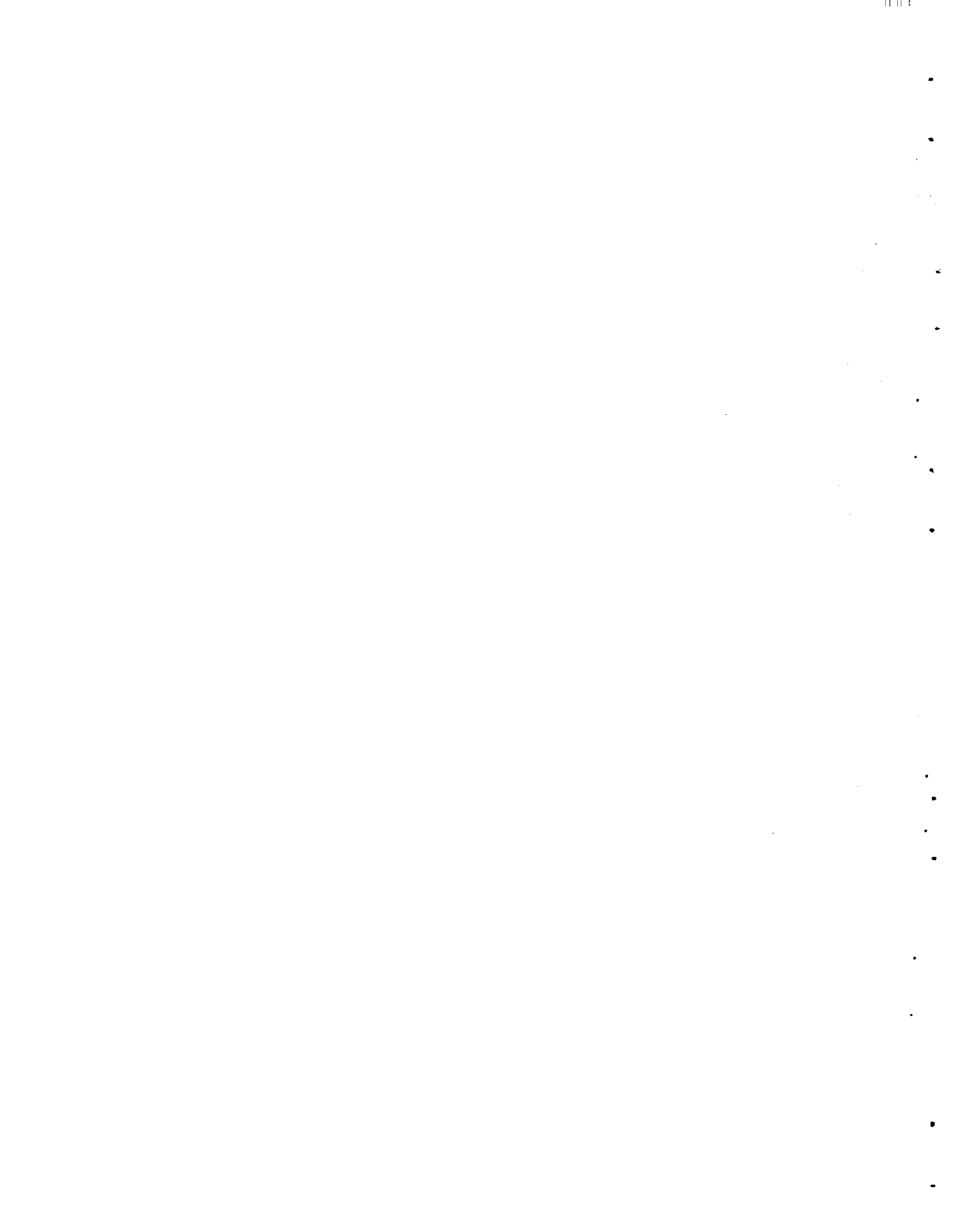
Experiments were started to determine the most effective method for dissolving the mixed hydrous oxide-ferricyanide precipitate remaining after centrifugation of scavenged glass melter condensate in order to permit recycle of the fission products. Hydroxylamine in dilute  $H_2SO_4$  appears most effective.

#### RADIOACTIVE SHIPMENT HAZARDS

Release experiments on samples of simulated high-level waste spiked with actual waste material were completed. The results for cesium appeared to be in fairly close agreement with those predicted by diffusion theory.

#### FISSION PRODUCT AEROSOL CONTAINMENT

Sprays of 37% hydrazine and a combination of 35% hydrazine - 5% ammonium hydroxide removed virtually all of the  $CH_3I$  from an aerosol chamber initially containing  $CH_3I$  - steam atmosphere at 75 °C.



With the present analytical sensitivity of the gas chromatograph-electron capture detector, rate of reaction studies were extended down to concentrations of about 1.6 mg  $\text{CH}_3\text{I}$  per  $\text{m}^3$ .

#### REACTOR SAFETY ANALYSIS AND EVALUATION

Two irradiated A212B subsize-vessel specimens were burst tested. The failure appearances of these specimens indicate that one specimen was tested at a temperature 10 °F (5.5 °C) above the irradiated materials NDT and the other specimen was tested at a temperature 10 °F (5.5 °C) below the irradiated materials NDT.

It has been demonstrated that ultrasonic monitoring techniques to study acoustic emission can be applied successfully to irradiated specimens during failure. The shift in NDT due to the irradiation exposure is seen to correspond to the shift in temperature below which ultrasonic signals are received over a bandwidth of 50 kc to 1 mc.

#### CUSTOMER

##### PHILLIPS PETROLEUM COMPANY

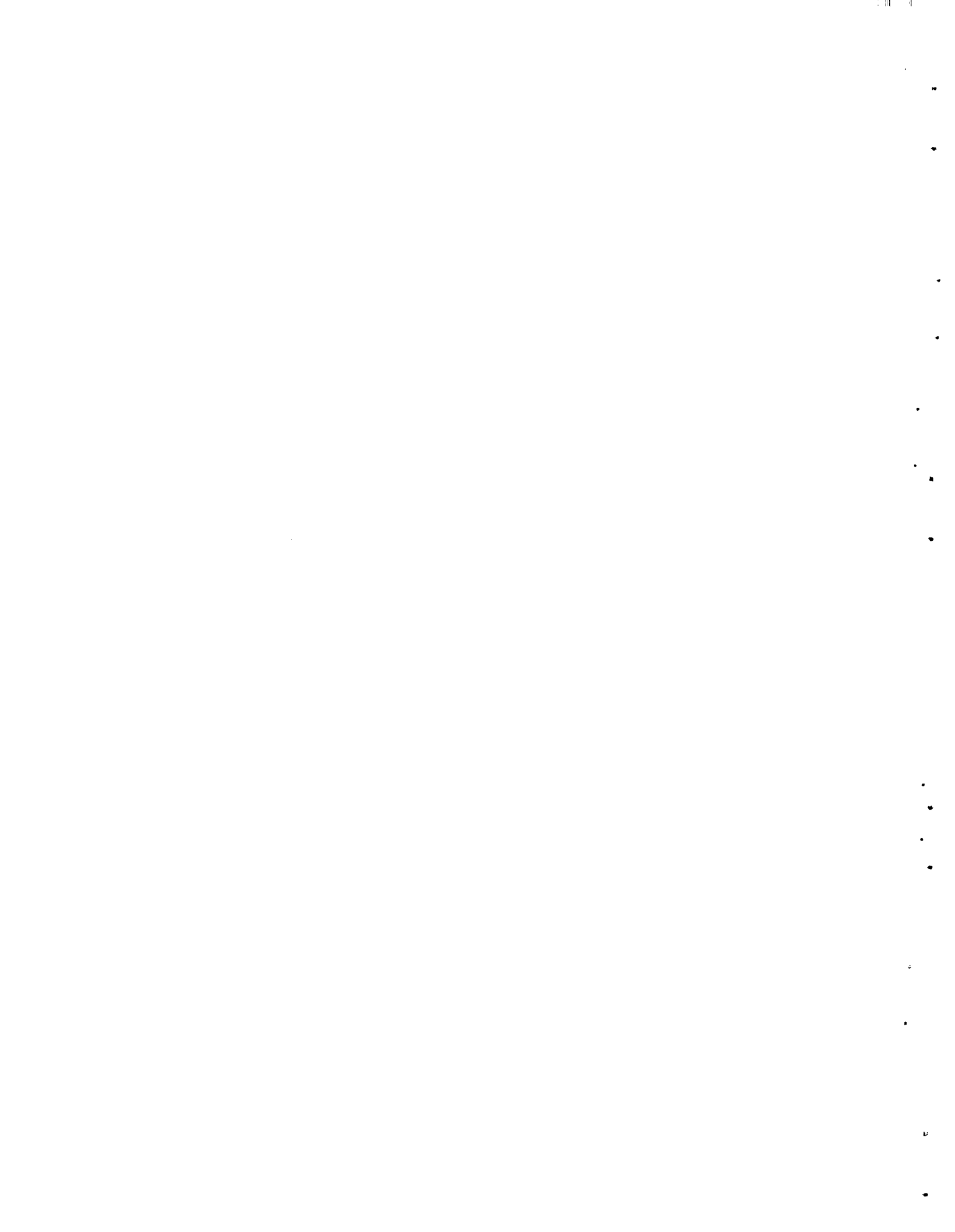
Four capsules, each containing Al-Np alloy of different composition, are being fabricated for resonance integral measurements.

##### GENERAL ATOMIC

Process development and tooling were nearly completed for the fabrication of 12 rods containing  $\text{PuO}_2$ -graphite compacts.

##### U.S. NAVAL RESEARCH LABORATORY

The determination of uncertainties in the differential cross section of the  $\text{Fe}^{54}(\text{n},\text{p})$  reaction and the effects of these uncertainties on the lifetime exposure estimates of the SM-IA pressure vessel have been studied. The analysis indicates that a 35% uncertainty in the estimated safe life of the SM-IA pressure vessel could result from uncertainties in the  $\text{Fe}^{54}(\text{n},\text{p})$  differential cross section.



DIVISION OF REACTOR DEVELOPMENT AND TECHNOLOGY PROGRAMS  
(F. W. Albaugh)

CIVILIAN POWER REACTORS

SPECIFIC FUEL CYCLE ANALYSIS (E. A. Eschbach)

Fast Reactor Economics

Preliminary calculations of the A-C Large Fast Reactor using slab geometry with three core regions, four blanket regions, and one reflector region were completed. These calculations permitted selection of proper enrichments for U<sup>233</sup>, U<sup>235</sup>, or plutonium fissile material in UO<sub>2</sub> or thorium fertile material. Sixty-eight cases have been prepared for processing through ALTHAEA and QUICK, but complete results have not been obtained and no overall analysis has been made at this time.

Fast Utilization Studies

VESTA - Final copies of the report, BNWL-285, "Breeding Isn't Everything - The Economics of Uranium Conservation," are now being cleared for general distribution in August.

DAEDALUS - The code to translate MELEAGER burnup data into a linear programming problem has been written. The code is being debugged with sample data from the Indian Point Reactor Simulation. The next steps are the use of the 1107 LP codes to solve the problem and the use of data from two reactors to study their interactions in a static model. The time element will then be added to produce a dynamic simulation of two interacting reactors in an expanding economy.

CONCEPTUAL REACTOR DESIGN STUDIES (J. C. Fox)

Nuclear Electric Plant Capital Costs vs. Site Location

Estimated site preparation costs as influenced by local siting factors are essentially complete, and order of magnitude costs for special facilities which may be required at the various sites are being developed. The site preparation costs at most sites, dealing primarily with land clearing, grading and drainage charges, are based on an estimated 800-foot square level area requirement for the 1000 MWe reference reactor plant. The plant location is assumed to be adjacent existing facilities at each site.

Cooling towers, which may be required at sites using river cooling water, and marine lines at ocean and lakeside sites are included in the special facility cost estimates. Marine line costs are based on an estimated requirement for 16-foot diameter, reinforced



concrete pipes with 2600-foot discharge and 3200-foot intake line lengths. Cooling tower costs will be based on an induced draft re-circulating coolant installation.

Other cost variables, consistent in accuracy and value with the intent of the study, have been reasonably well defined with the exception of land costs and a draft of the study report is being prepared.

#### Fast Reactor Fuel Cycle Calculations

A comment issue report, "Comparison of U<sup>235</sup> and Plutonium Fueling for a Fast Oxide Breeder Reactor," by J. J. Regimbal, D. E. Deonigi, R. H. Holeman, and J. H. Nail, Jr., June 29, 1966, has been prepared.

An informal report covering neutronics and mass balance calculations for a fast spectrum carbide breeder reactor is being assembled.

#### Nitride Fuel Cycle Studies

Work is continuing on the draft of a document describing the technical and economic analysis of a fast breeder power reactor fuel cycle utilizing uranium and plutonium nitrides as fuels. Efforts will be made to complete this document for publication as soon as possible.

#### USAEC-AECL COOPERATIVE PROGRAM (J. J. Cadwell)

##### In-Reactor Corrosion of Zirconium Alloys

The status of zirconium alloy specimens exposed in the G-7 loop of the Engineering Test Reactor under the cooperative USAEC-AECL program is as follows:

<u>Quadrants</u>	<u>Exposure, days</u>	<u>Status</u>
205, 206 plus out-of-flux specimens	25.5	Weight gain and hydrogen analyses complete; metallography complete.
217 <sup>(a)</sup>	37.3	Analysis under way at BNW.
210, 211, 214, plus out-of-flux specimens	77.4	Enroute to BNW from NRTS, Idaho. Analysis is under way on out-of-flux specimens
233, 234, plus out-of-flux specimens	8 ETR Cycles 150 days	Charged about 6-1-66; to be discharged in May 1967.

(a) This is a reference quadrant containing specimens from the Irradiation Damage to Reactor Materials and USAEC-AECL programs (titanium, niobium, and niobium-1 wt% Zr); contains 30 specimens.





Each of the above quadrants contains 36 specimens except as noted as noted for Quadrant 217; six zirconium alloys are included in the test. The quadrants are exposed in the G-7 loop in pH-10  $\text{NH}_4\text{OH}$  at 270 - 280 °C.

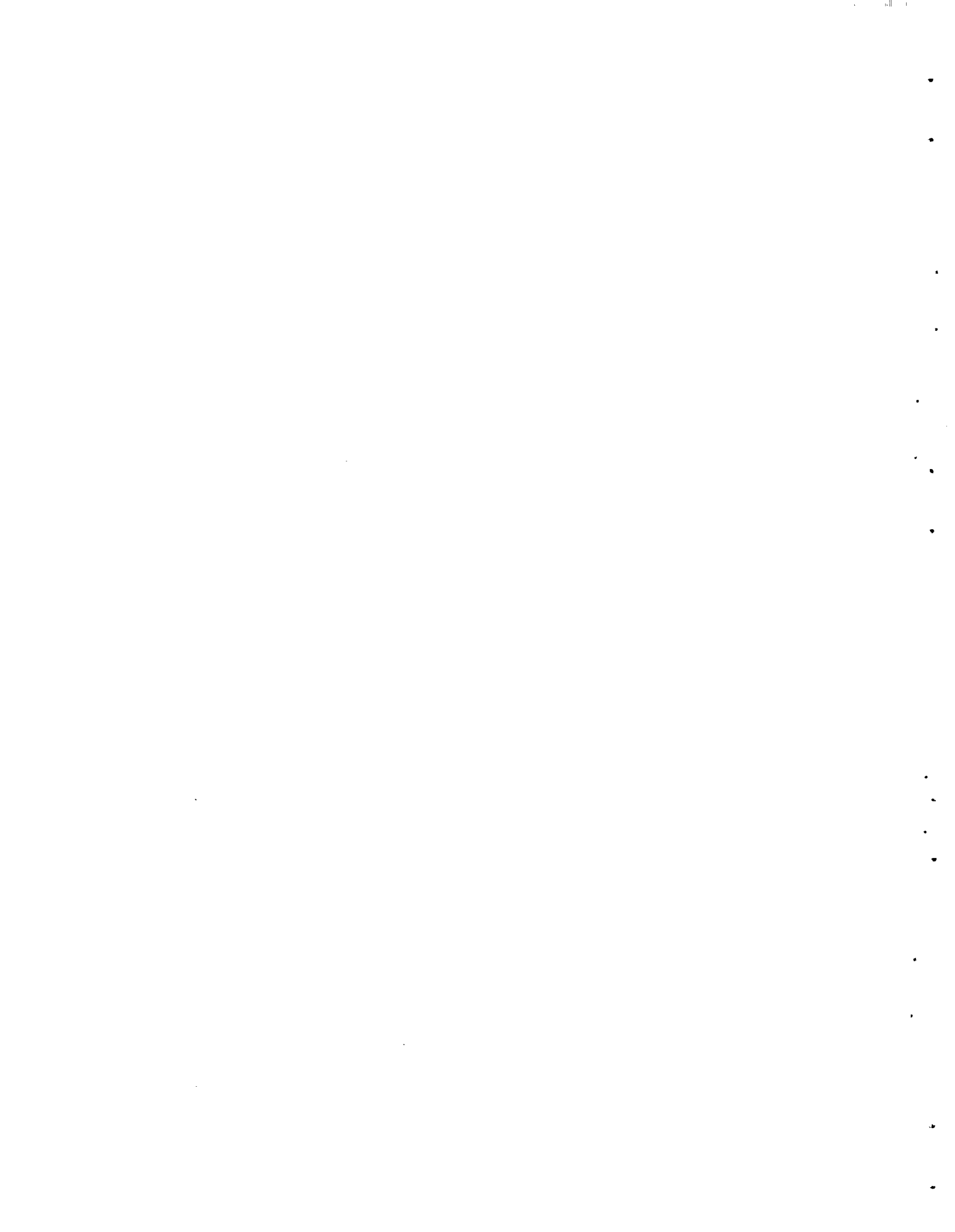
The table which follows summarizes in-flux and out-of-flux hydrogen pickups for zirconium alloy specimens in the Cycle 75/76 exposure. Hydrogen pickups are high for VALLOY-S, intermediate for Zircaloy-2, Zircaloy-4 and preautoclaved VALLOY, and low for VALLOY and specimens containing niobium. Preautoclaving increased the in-flux hydrogen pickup for Zircaloy-2, Zircaloy-4 and VALLOY. In-flux and out-of-flux hydrogen pickups in terms of ppm did not differ markedly, except for prefilmed VALLOY, which showed lower pickups out-of-flux. Two out-of-flux preautoclaved Zircaloy-2 specimens showed exceptionally high percentage pickups, even taking into account hydrogen introduced in autoclaving. There does not appear to be a significant difference in hydrogen pickup at the two out-of-flux positions.

#### Cross-Flow Mixing Between Parallel Flow Channels During Boiling

Test section fabrication and analytical calculations are continuing in the study to determine values of cross-channel mixing during two-phase flow in rod bundle fuel elements. The purpose of this study is to obtain a method of predicting local flow and enthalpy conditions in each sub-channel of rod bundle fuel elements. This information will provide a more accurate prediction of boiling burnout conditions.

Assembly of the electrically heated test section that will be used to study both turbulent mixing and flow diversion in two interconnected channels was completed. This test section simulates the type of flow channel configuration that would be formed by a channel in a square pitch rod array located adjacent to a channel in a triangular pitch rod array as in a 19-rod bundle. Installation of this test section in the experimental facility is presently in progress. Fabrication of a second test section, which will be used to study only turbulent mixing during two-phase flow, is about 25% complete. This test section simulates the type of flow channel configuration that would be formed by two adjacent channels in a square pitch rod array.

Efforts were continued to extend computer calculations which apply numerical methods of solving parallel channel mixing equations to an arbitrary multirod array. For two continuously connected parallel channels, these methods have produced stable solutions with and without boiling, and comparisons of the results of the computer program for the nonboiling case with exact mathematical solutions have revealed adequate agreement. Attempts to obtain stable solutions for the more complex multichannel systems have been unsuccessful so far. Additional calculations will have to be performed before a conclusion can be made regarding the adequacy of extending this technique to such systems.



SUMMARY OF HYDROGEN ANALYSES  
ON ZIRCONIUM ALLOYS EXPOSED IN ETR CYCLES 75/76

Exposure: 25.5 days, 270-280°C,  $2.1 \times 10^{20}$  nvt, fast

Alloy		In-Flux		Out-of-Flux <sup>(b)</sup>			
		Hydrogen Pickup ppm <sup>(a)</sup>	% Corrosion Hydrogen	Hydrogen Pickup ppm	% Corrosion Hydrogen		
Zry-2	Annealed, etched	10	30	(12)			(31)
Zry-2	Annealed, preauto-claved	23	56	16 (22)	130		(175)
Zry-2	80% Cold Work, etched	20	36	21 (18)	64		(46)
Zry-4	Annealed, etched	11	15	5 (8)	9		(14)
Zry-4	Annealed, preauto-claved	19	31	11	58		
VALLOY <sup>(c)</sup>	Annealed, etched	4 <sup>(d)</sup>	12	(2)			(5)
VALLOY	Annealed, preauto-claved	35 <sup>(d)</sup>	9	2 (1)	8		(4)
VALLOY-S <sup>(c)</sup>	Annealed, etched	127	134				
VALLOY-S	Annealed, preauto-claved	86	122	(103)			(150)
Zr-2.5 Nb	Quenched 30% CW aged, etched	10	26	6 (4)	11		(8)
Zr-2.5 Nb	Quenched 30% CW, aged, preautoclaved	6 <sup>(d)</sup>	24	(<0)			(-)
Zr-2.5 Nb	Quenched, 20% CW, etched	2	4	5 (2)	11		(5)
Zr-2.5 Nb	Quenched 20% CW, aged, preautoclaved	2	9	(<0)			(-)
Zr-2.5 Nb	Annealed, wo% CW, etched	2	6	(1)			(3)
Zr-2.5 Nb	Annealed, 20% CW, pre-autoclaved	4	12	2 (1)	6		(2)
Zr-3 Nb-1 Sn	Annealed, etched	3	5	2 (4)	4		(9)
Zr-3 Nb-1 Sn	Annealed, preautoclaved	3	20				
Zr-3 Nb-1 Sn	Quenched, aged, etched			4 (5)	8		(10)

- (a) ppm hydrogen is calculated on the basis of the following sample thicknesses: Zry-2, VALLOY and VALLOY-S, 50 mils; Zr-3 Nb-1 Sn, Zr-2.5 Nb, 40 mils; Zr-4, 30 mils.
- (b) Data are reported separately for two out-of-flux positions,  $\sim 1$  sec and  $\sim 1$  min (water transport times) from the flux. The data at the 1 sec position are reported in parentheses.
- (c) Exposure  $3.0 \times 10^{19}$  nvt, fast.
- (d) Adjusted from value reported in April after recheck of hydrogen blank values.



### Hydraulic and Nuclear Stability in Parallel Flow Channel Systems

Debugging of the hydrodynamic model being used for the analog computer study of the BLW-250 nuclear and hydraulic stability was continued. Modifications to the analog program were made to correct errors in transient response to a step power change. Preliminary calculations using these modifications for a single channel with a constant pressure drop have given the instability threshold power level and frequency of flow oscillations which are in reasonable agreement with AECL digital computer calculations using HYDNA.

Modifications to the digital computer code, HFN, have been made that allow calculations of parameters required for a 2-node kinetics model of a reactor based on coupled reactor theory. The modified version is currently being checked by comparison with experimental data obtained from the 2-zone (UO<sub>2</sub> and PuAl) loading in the PRTR. Initial results indicate inadequacy in the methods used to calculate coupling coefficients and further analytical work is in progress. Successful development of this model will permit an extension to the range of stability problems that can be studied under the present program. For example, this model will allow studies at either high or low power levels where the boiling lengths become very long or very short, respectively. The present 4-node model, derived using a finite difference approximation for derivatives of the neutron flux, will not adequately represent the kinetic behavior of the reactor under such extreme conditions.

### Boiling Water Reactor Stability Study

Debugging of the hydrodynamic model being used for the analog computer study of the BLW-250 nuclear and hydraulic stability was continued. Modifications to the analogue program were made to correct errors in transient response to a step power change. Preliminary calculations using these modifications for a single channel with a constant pressure drop have given the instability threshold power level and frequency of flow oscillations which show reasonable agreement with values from digital computer calculations using HYDNA.

### Evaluation of Zr-2.5 wt% Nb Pressure Tubing

The general objective of this program is to evaluate Zr-2.5 wt% Nb alloy tubing as a pressure tube material with reference to tests and reactor experience that has been obtained on Zr-2 pressure tubes.

For crack propagation tests, several Zr-2 tubular test pieces have been prepared with the milled slots placed at angles ranging up to about 60° between the direction of the slot and the tube axis. One test specimen with a 2-inch long slot orientated at 45° from the tube axis failed at about the same hoop stress as a test specimen with a 1-1/2-inch long slot orientated parallel to the tube axis. The crack propagated at an angle with the tube axis and stopped near the test



piece end fitting so that both ends of the crack lay in a single plane parallel with the tube axis.

The static creep test of Zr - 2.5 wt% Nb specimen stresses at 70,000 psi hoop stress failed in 1453 hours. The uniform strain was about 2-1/2%. Another test at 40,000 psi hoop stress has been started. Further testing of the 350 °C flow loop continued with flow through the test assembly being varied from about 10 gpm to about 30 gpm. Over the range of flow rates tested so far, the pressure fluctuations in the system even with pressure snubbers installed is substantially greater than can be tolerated for precise measurements of creep deformations.

### APPLIED AND REACTOR PHYSICS

#### PLUTONIUM CRITICALITY STUDIES (E. D. Clayton)

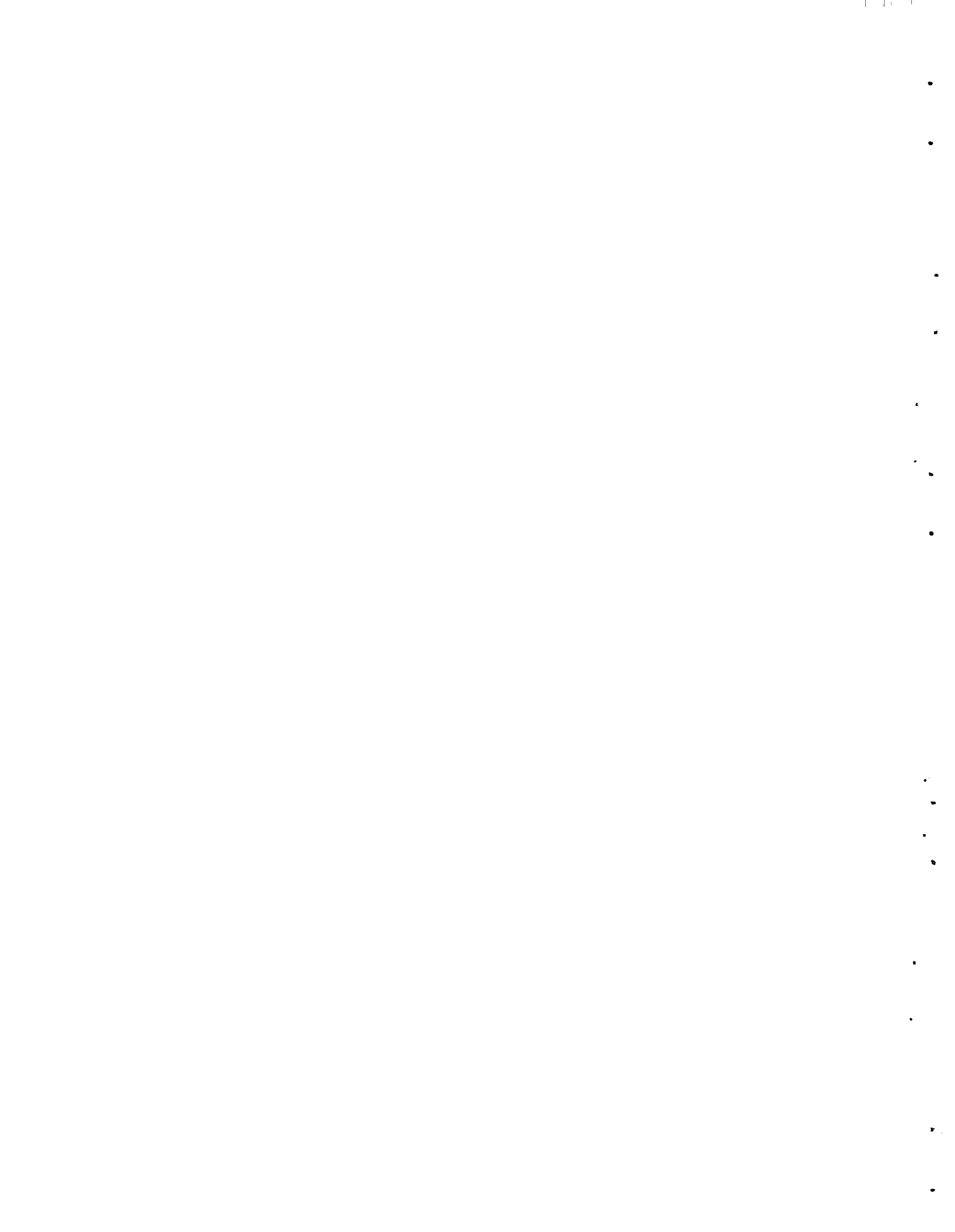
##### Basic Criticality Experiments With Plutonium Nitrate Solutions in Slab Geometry

Criticality experiments were continued for determining critical thicknesses of bare and water reflected "infinite" slabs of plutonium nitrate solutions. The criticality vessel for these experiments consists of an expandable slab tank with height and length of 42 in.; the vessel thickness may be adjusted throughout the range of 3 - 9 in.

In the initial experiments reported last month the vessel was unreflected. In order to effect a direct comparison between bare and reflected critical thicknesses, the reflector tank was installed and a series of experiments performed with the vessel fully reflected with water. The same plutonium nitrate solution was used in each case; the Pu concentration was ~60 g Pu/l with an acid molarity of ~2. Measurements were made over a thickness range of 4.5 - 6.5 in. For a water reflected critical thickness of 5 in., the correction to an "infinite" slab reduces the thickness by about 0.4 in. The sides of the vessel are of 0.062 in. stainless steel reinforced with a lattice framework for rigidity. As in the case of the unreflected vessel, the critical height was determined as a function of slab thickness. For a thickness of 6.3 in., adding a water reflector reduced the critical height of the 42 in. long vessel from 38.3 in. to 11.3 in. The reflector savings is about 2.3 cm. The results of a complete chemical analysis of the Pu solution have not yet been received. The experiments, and interpretation of data, are proceeding. From the data to be obtained, it will be possible to more accurately specify critical thicknesses of slab tanks and to determine "safe" values for criticality control.

##### University of Washington - Battelle-Northwest Cooperative Research Program

Work has begun on a cooperative research program between the University of Washington and Battelle-Northwest. The work is being partly funded by a grant to the University's Department of Nuclear Engineering from the National Science Foundation. The research





proposal presents a plan whereby the experimental facilities of the Plutonium Critical Mass Laboratory may be used on a part-time basis by faculty and students of the University of Washington in carrying out a number of important conjoint research projects that will also serve as thesis research. The first areas of research involve neutron spectrum studies in undermoderated plutonium assemblies, pulsed neutron source experiments, and measurements of reactor noise.

#### HIGH TEMPERATURE REACTOR LATTICE PHYSICS STUDIES (R. E. Heineman)

##### Reactor Construction

The insulation between the reactor and shell has been completely installed. The AEC has accepted the job from the subcontractor. The reactor room has been cleaned and a temporary air lock constructed in front of the shell prior to installing the reactor graphite. The graphite lintel bars for layers 5 and 23 of the reactor were received from the vendor. Mockup of the reactor stack was resumed, and 75% of the lay-up has been completed.

An engineering review of certain systems and parts of the HTLTR is being made by Battelle engineers. The study includes the primary coolant loop, the structural floor loading beneath the reactor shell and in the reactor hall, and the electrical bus bar system for the core heaters. Preliminary results have been compiled and are being reviewed.

##### Reactor Mockup and Materials

The report which documents the results obtained from Mockup Run Number 4 is approximately 85% complete.

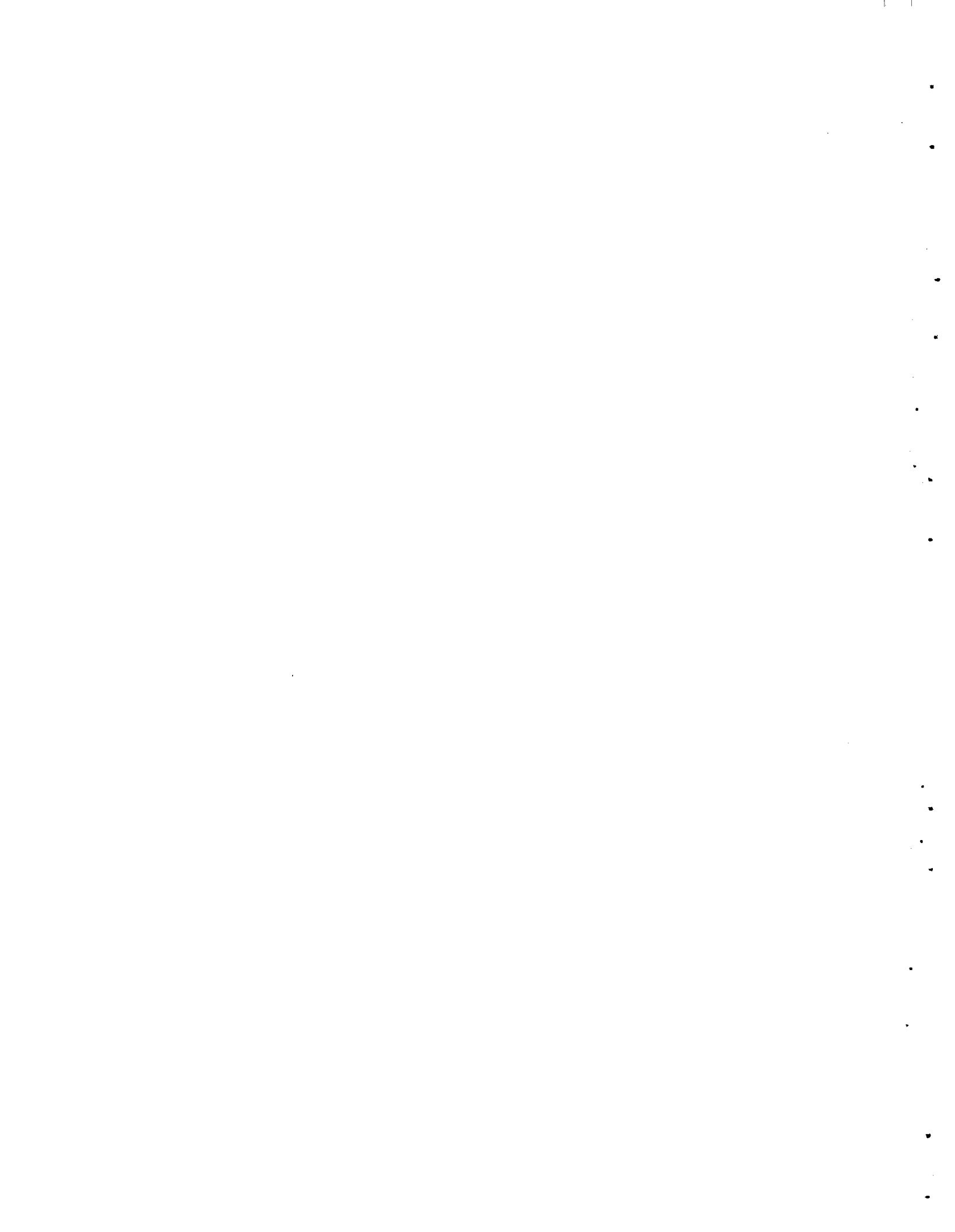
The graphite to copper electrical connection at the bus-bar was removed and inspected. Both the graphite and copper appeared to be in excellent condition.

A contract was awarded for the co-precipitated 4%  $Gd_2O_3$  - 4%  $Eu_2O_3$ -Ni plates to be used in the blades of the HTLTR safety rod. Delivery, scheduled for the last week in August, is compatible with the schedule for the fabrication of the safety rods.

More than three-fourths of the ceramic driver fuel elements have been shipped by the vendor. The graphite cladding is due in July.

##### Reactor Equipment

Discussions were held with the Architect-Engineer to further explain the criteria for the moisture removal system. The procurement specification has been issued by the Architect-Engineer.



The experimental programs require that reactor cells, fuel trains, and test samples be positioned, oscillated, and replaced during HTLTR operation. The systems to accomplish these functions are known as the HTLTR Oscillators. The oscillator development has been assigned to Battelle-Northwest.

A decision to use an electro-hydraulic servo driver system was made, and bids on these systems are due on July 6, 1966.

Fabrication status of subassemblies is as follows: Key, 75%; Carriage, 25%; Oscillator mechanism, 27%; Valves, 63%; and Drive, 18%. Late delivery of purchased components halted carriage fabrication for most of this month.

Design of the cold test mockup is complete and fabrication is about 40% complete. All components for this mockup will be delivered this month. Design for hot test modification and equipment has been initiated.

Details of the electronic interface between the computer, PMACS, and the oscillator were finalized, design of a computer simulator for oscillator testing was completed, and parts for the simulator ordered.

A report describing the selection of the drive system was started.

A motor-generator set has been obtained from an excess list as a backup power source for the instrumentation system.

### Programmed Measurement and Control System

#### Acceptance Tests and Modifications

The acceptance test for the Programmed Measurement and Control System (PMACS) has been signed with the exception of the alpha-numeric display portion of the system. It was discovered that the design of the character generator in the alpha-numeric display will not allow continuous operation of some characters. The vendor was contacted about this problem, and they sent replacement transistors and heat sinks. Since the replacement transistors were found to be inadequate, the vendor requested that the character generator be shipped back to their plant for rebuilding. Other portions of the system that had held up acceptance were resolved as follows:

Excessive noise was present on the x-y drive lines of the analog display. RC Filters were installed at the oscilloscope end of the x and y drive lines from the digital-to-analog converter, reducing the noise at the scope to an acceptable level.

A weak wiper arm on one section of the Safety Circuit By-Pass Switch caused intermittent failure. Installation of a new switch has been recommended.

11  
11  
11  
11

•  
•  
•

•  
•  
•

•  
•

•  
•

A faulty mercury wetted relay was replaced in the precision resistance temperature detector (RTD) ranging logic. Precision RTD noise is now only 3 analog-to-digital channels of scatter with an occasional count appearing in a fourth channel. The resolution supplied (0.014 °C) has been accepted, although 0.01 °C resolution is required by the specification.

A Dectape drive motor was rebuilt. A Teletype shaft froze because of lack of lubricant; a routine maintenance procedure will be set up to prevent further failures.

A drive system was assembled for the small backup analog display tube which has been added. The instruments in the panels in the control room were rearranged according to systems. The necessary changes to the several drawings involved were forwarded to the Architect-Engineer for consideration.

#### System Reliability

A data-gathering technique has been developed to record operating, maintenance and failure experience with the control and safety systems. It will be reviewed with the reactor operations group and implemented. Many groups will be interested in how well the systems perform. A careful recording of experiences with the systems will be helpful for prospective users of similar equipment for both AEC and private reactor installations, and safeguards and regulatory organizations of the AEC.

#### Programming

Debugging was completed on the MICRO routine, and one more portion of the main supervisory program. This portion keeps track of all tape requests from the queue table and selects the tape units at the correct time. Debugging was about 80% completed on DISPLAY, the demand display routine for the alpha-numeric TV. This program will, upon receipt of various simple keyboard requests, display such items as gas temperatures.

Programming has been started on two other routines:

1. Limit, a program which periodically scans the current value table containing all analog inputs, checks for out of limit points and display their location and value.
2. Logi, a program which is controlled by operator demand and when called will type out all of the current analog input values, both in the raw counts and engineering units. In addition, an alpha-numeric identification of each channel will be typed along with a heading giving the time of day.



Programming continued on the reactor flux-to-level and period data.

Transient temperature studies of the HTLTR show that there are two sets of time constants. The response at a point close to the heat source is relatively fast and represents the time to achieve an equilibrium temperature distribution. A much longer time constant is dominant after equilibrium. This results from a change in temperature of the total mass of graphite.

The local transient response is still not well defined. Because of the amount of interaction among the heaters and thermocouples and the large thermal time constants, a feedback control alone may be too slow to achieve a uniform temperature in a reasonable time. The TIGER V code has been used to obtain transient temperature data. A few more runs will be made to try to define the shorter time constants, since the longer one can be considered as resulting from a pure integration. The ultimate method will probably require a combination of feedback and feedforward control.

### Reactor Operations

A formalized training course has been instituted on PMACS operation and programming. This course is in preparation for detailed writing of the Operating Procedures for the individual experimental operations.

### Reactor Physics Program

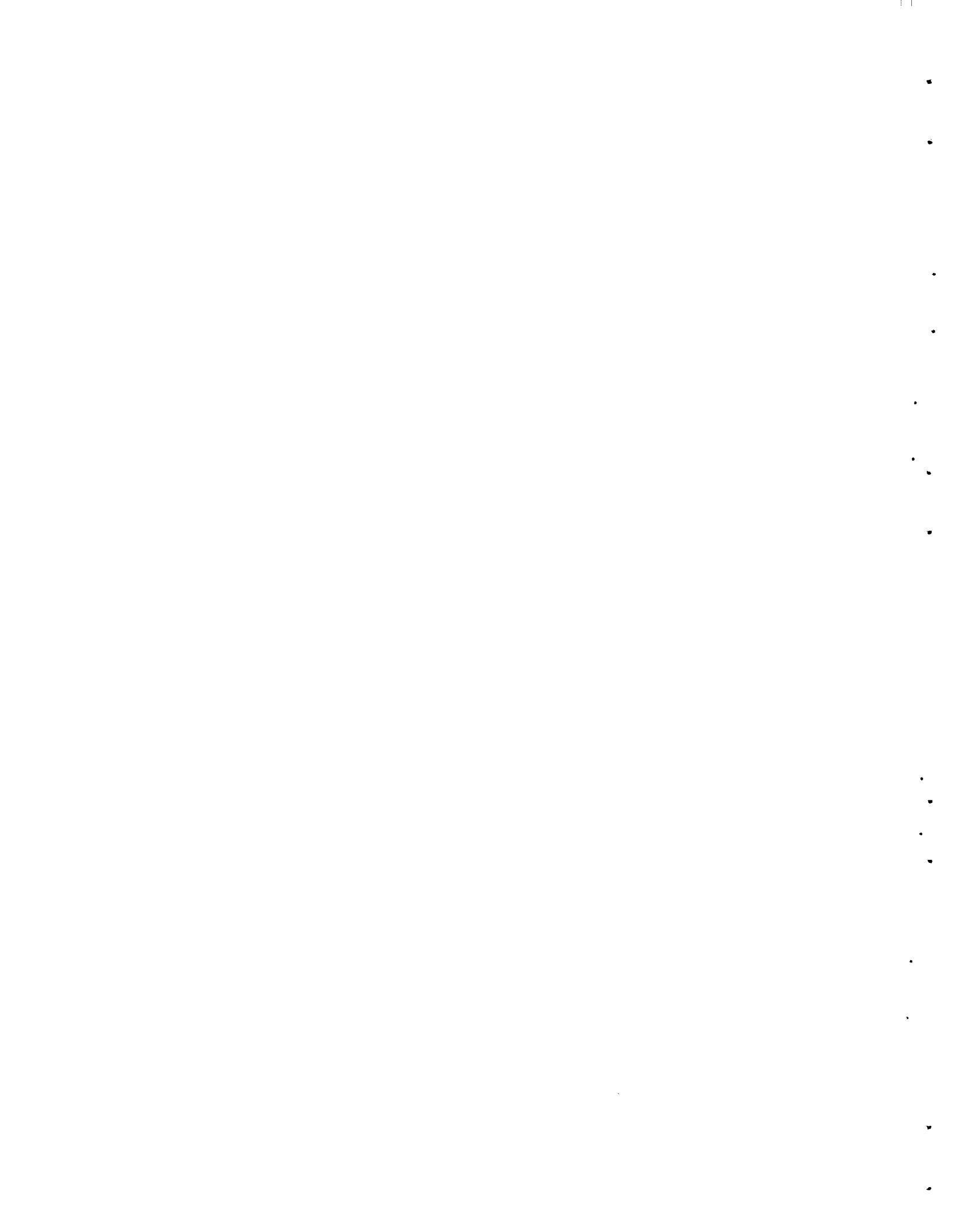
#### Experimental Program

Work has started on the design of the mechanical system for coupling the ends of the oscillator rams to the various parts in the experimental lattice that have to be inserted into, extracted from, and moved within the reactor. The coupler is required to operate in the reactor atmosphere at temperatures up to 1000 °C and to adapt the normal motions of the oscillator--a longitudinal displacement controlled by PMACS, or an axial rotation which is manual--to move the parts as required or switch the point of application of the ram from one part to another.

Discussions have been held to define the work needed to design the fuel element heaters to obtain fuel temperature coefficients. The first heater will be a variation of one which has been successfully used previously up to 950 °C.

The cross section library for THERMOS calculations containing the isotopes and mixtures of interest to HTLTR experiments is now complete. All cross sections are from the BNW Master Library.

The library contains, as a function of temperature, cross sections for natural boron, carbon, nickel, copper, cadmium, samarium, europium, gadolinium, lutetium, and gold. It also contains the isotopes  $N^{14}$ ,  $O^{16}$ ,  $Al^{27}$ ,  $Th^{232}$ ,  $U^{233}$ ,  $U^{234}$ ,  $U^{235}$ ,  $U^{238}$ ,  $Pu^{239}$ ,  $Pu^{240}$ ,  $Pu^{241}$ ,  $Pu^{242}$ , Leonard's cross sectional values for  $Pu^{239}$  and Sher's cross sectional





values for Pu<sup>239</sup>. Park's scattering kernels for graphite at various temperatures are also included.

The method used to identify each of the above isotopes and mixtures is as follows: the first ident number (ID) is derived in the usual THERMOS notation, i.e., isotope A and Z. For example, <sup>92</sup>U<sup>235</sup> is identified as 23592.

The second THERMOS ident number (IDA) utilizes the usual THERMOS notation along with some additional notation to specify the desired temperature. The usual THERMOS notation for the second ident number is:

<u>IDA</u>	<u>Description</u>
1	$\sigma_a$
2	$\sigma_f$
3	$\sigma_{act}$
4	$\sigma_s$
5	D
10	Mixture or Alloy
50-99	Special Kernels

The additional notation that is used with this particular library is:

11	$\sigma_a$ - fuel isotope with no resonance parameter table on BNW Master Library
12	$\sigma_f$ - same as above
21	$\sigma_a$ - Leonard's data for Pu <sup>239</sup>
22	$\sigma_f$ - Leonard's data for Pu <sup>239</sup>
60	Park's graphite kernel

The complete second ident number is obtained by adding the desired temperature ident (see below) to the proper IDA. Thus, to obtain cross sections at 828 °K using Sher's values for Pu<sup>239</sup>, the two ident numbers are 24994 801.

<u>Temp. (°K)</u>	<u>Ident Temp.</u>
100	100
293.6	300
698	700
828	800
873	900
1273	1300
1500	1500
2000	2000



Tape U9369 contains the library described above and is used on the UNIVAC 1107 computer with the version of the THERMOS code that utilizes 30 energy groups.

Calculations of reactivity worths of cells and poison materials using THERMOS and HRG were continued. This work is preliminary to using unpoisoned lattice cells in the HTLTR measurements of excess neutron production as a function of temperature. The calculations referred to in earlier monthly reports are being used to document the program of measuring Maxwellian cross sections and  $\eta$  values to high temperatures.

Two dimensional diffusion theory calculations have been used to estimate the effect of cylindricizing the cubic graphite stack of the actual reactor.

### Learning Loops

Work is being done on real-time processing of experimental data to obtain values of reactor parameters. Two machine programs have been formulated and made operational on the PDP-7 computer coupled to the HTLTR. The first learning loop (BNW program Learn-I) predicts critical fuel loading by observing counts, time, shim control, and fuel loading during an approach to criticality. The second learning loop (BNW program Learn-II) observes counts and time, and calculates the asymptotic period and reactivity of the reactor.

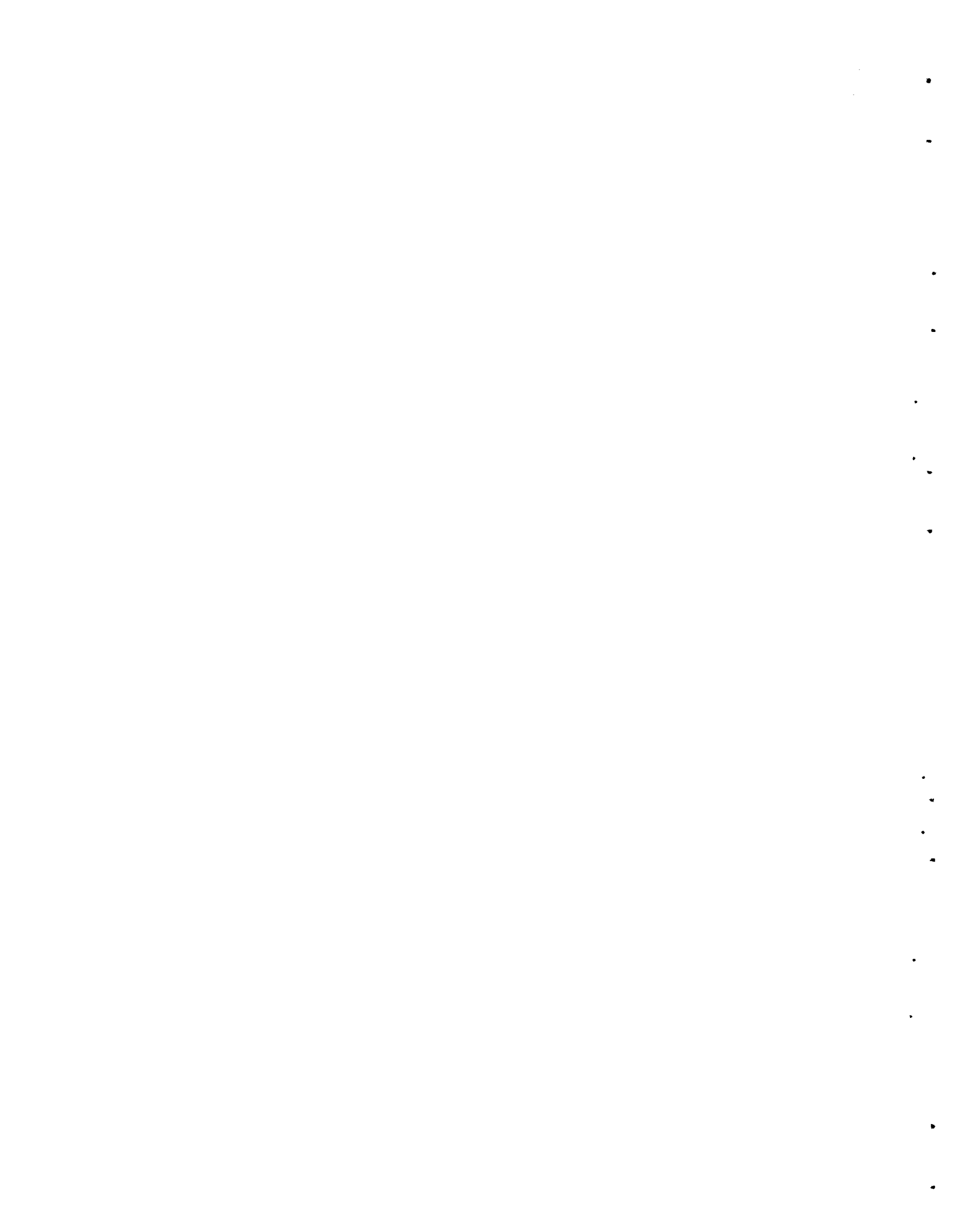
Both programs were formulated in pure Fortran language, to provide freedom from obsolescence and to enhance the likelihood of achieving satisfactory chain-linkage coupling to the PMACS control program being developed. Trial runs, based upon simulating realistic observations by feeding in actual measurements made on the Physical Constants Test Reactor, now total well over 50 hours of generally satisfactory program and computer operation. Conversion of asymptotic period to reactivity shows solid agreement with the 5-figure period-to-reactivity PCTR tables (HW-73457) over the full operational range. Critical fuel loading predictions show satisfactory reliability until just after the last fuel element is loaded. Then the analysis switches to prediction of critical shim position. Further refinement of the learning logic still is needed to span this terminal phase of the approach to criticality.

### PHOENIX FUEL REACTOR PROGRAM (P. L. Hofmann)

#### MTR-Phoenix Experiment

##### Nuclear Design Calculations

Multidimensional analysis of both the partial Pu core and the full Pu core for the MTR-Phoenix burnup experiment were continued during the past month. The work on the partial Pu core is primarily a methods development effort aimed at synthesizing a 3-D power map from 2-D calculations. The partial Pu core was selected for this work because of the extensive analysis already carried out for this core configuration.



A 4 energy group 2-D splice has been compared to a 2 group 3-D calculation. In the following table the calculations for the same control rod position and the same set of basic cross section data are compared.

<u>Calc. Model</u>	<u>k<sub>eff</sub></u>	<u>Pk-to-Avg. Power Density</u>	<u>Allowable Power Level</u>
4 group 2-D splice	0.994	5.62	19.0 MW
2 group 3-D	1.046	5.40	19.5 MW

At present a 2 group 2-D splice calculation is being carried out in an attempt to separate the 2 group vs 4 group effects from the 2-D splice vs 3-D calculation effects. The necessity for introducing 2 group calculations comes about because the 3-D code, WHIRLAWAY, is limited to 2 energy groups. Our standard analysis methods make use of 4 energy groups.

A new code, POWER WRITER, makes it now possible to get power distributions directly out of WHIRLAWAY. This code edits the flux maps from WHIRLAWAY and constructs power maps directly.

Since it now appears that a full Pu core rather than a partial core may be used for the burnup experiment, a major portion of the design effort is being concentrated on obtaining data for the full Pu MTR-Phoenix core. Three-D calculations are being carried out for various positions of the control rods operated as a bank, and for certain groups of rods full in or full out. To date, only three calculations have been completed, and the results are shown in the following table.

<u>Rod Position*</u>	<u>k<sub>eff</sub></u>	<u>Pk-to-Avg. Power Density</u>	<u>Allowable Power Level</u>
45.2 cm	1.058	4.14	25.2 MW
50.8 cm	1.033	4.25	24.5 MW
57.6 cm	0.996	4.46	23.4 MW

\*cm from top of fixed fuel to top of rod follower fuel.

Leonard's Pu<sup>239</sup> cross sections have been used in the above calculations as a matter of convenience. If the more up to date Sher data are used with its resulting 3% loss in reactivity, the effect on allowable power from a change in critical rod position is rather small. The above results were obtained without the use of flux suppressors or graduated fuel compositions.

#### CAF-Phoenix Experiments

Experiments to measure the critical height of unpoisoned, water-reflected, Phoenix-type cores have begun in the Critical Approach Facility. The core height is adjusted by adding fuel discs and polyethylene spacers to the fuel element cans. Adding fuel to 19 cans and

4

5

6

7

8

9

10

11

12

13

14

15

16

17

18

decontaminating them required two days, which was much faster than anticipated. Critical approaches were completed in the radial direction for four different fuel heights using 19 fuel elements.

#### PRCF-Phoenix Experiments

Planning for a critical experiment which will be conducted in the Plutonium Recycle Critical Facility (PRCF) and which will use fuel elements of the MTR geometry continued during the month. Drawings describing the PRCF experimental arrangement have been prepared and circulated for comments. Fabrication of 132 fuel plates are expected to be completed in July. Additional high exposure plutonium has been requested for an additional 26<sup>4</sup> plates to increase the size of the core from 9 elements to 27 elements. An order has been placed for standard MTR fuel element end fittings and cadmium shim assemblies for use in the PRCF experiment.

#### Fuel Fabrication for PRCF

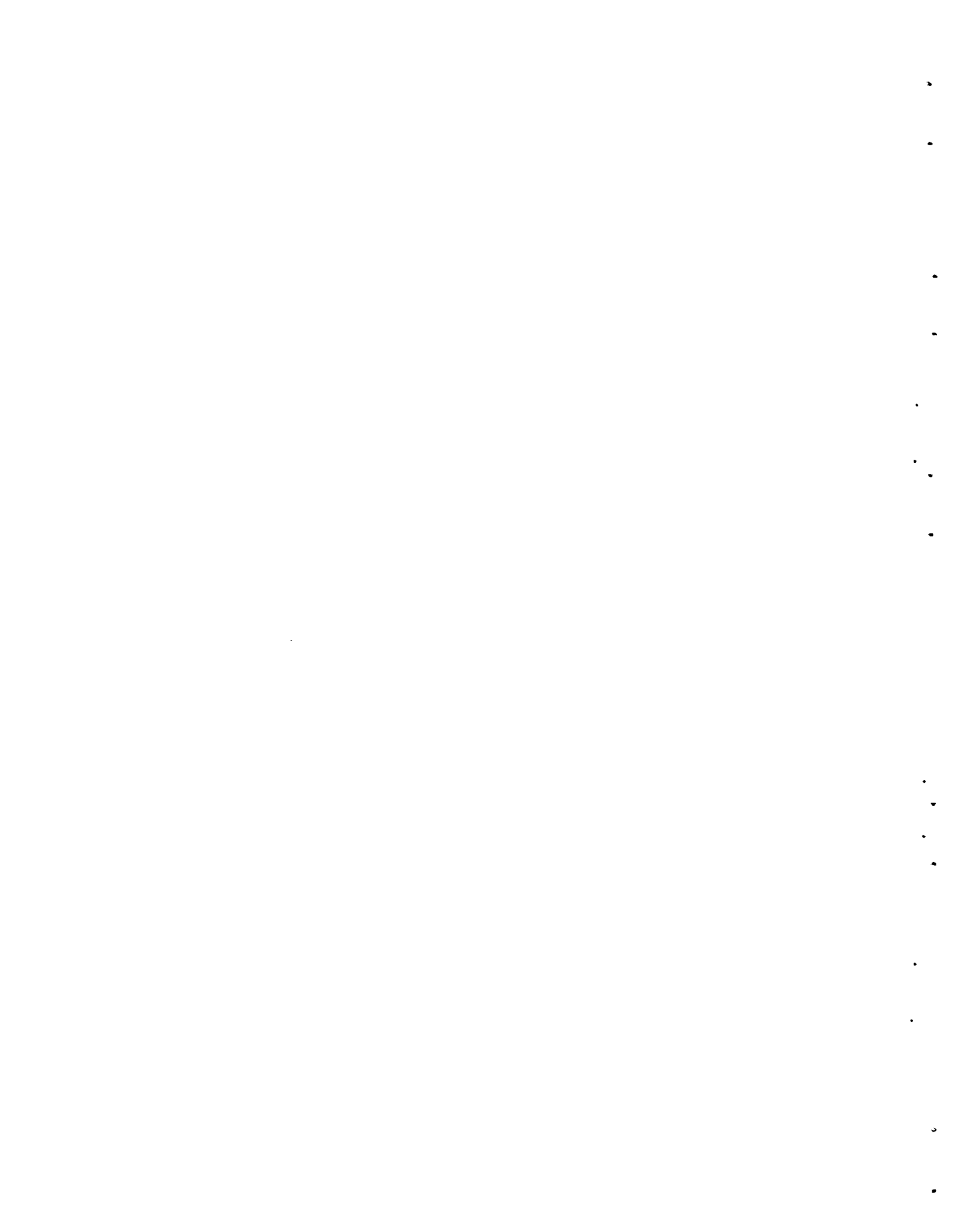
All of the 132, Al - 20 wt% Pu alloy, fuel plates are scheduled to be clad with 0.020-inch thick aluminum by July 1, 1966. Final dimensional sizing of the perimeter weld will not have been completed because the equipment for doing this will not be in operation until the first part of July. Because of the shortage of high exposure Pu, fabrication of 12, Al - 10 wt% Pu alloy, fuel plates is being delayed until July. At that time it is expected to be known whether the PRCF Phoenix experiment will utilize the presently planned partial core load or a full core load of Al - Pu fuel plates. For the latter case, a preliminary estimate of fabrication was drafted, taking into account the availability of high exposure plutonium. The estimate indicated that the small quantity of high exposure plutonium available makes it very difficult to fabricate required additional PRCF fuel plates by October 1, 1966. A target completion date of December 15, 1966, could probably be met.

#### Planning of the MTR Burnup Experiment

A meeting was held with personnel from the MTR at the National Reactor Test Site to discuss the Phoenix Experiment in the MTR. No major problems are anticipated in carrying out the various proposed measurements, except that the use of in-core flux monitors will be virtually impossible due to the difficulty of stringing cables through the structures above the core. It was also pointed out that the determination of rod-free criticality will probably be limited to the beginning and end of the burnup cycle. Intermediate points are difficult to obtain because of the lack of storage facilities for the irradiated fuel.

#### Phoenix Fuel Applications Study

A study is under way to investigate the performance of Phoenix fuels for power reactor applications in the 200 - 300 Mw(t) range. Several fuel types and designs will be analyzed in a number of different core configurations.





Of primary interest is a comparison of pin and plate type fuel elements from both a physics and engineering standpoint, since the pin geometry is customary in power reactors, whereas plate geometry will be used in the MTR experiment. Nuclear calculations having different metal-to-water ratios, pin sizes, and fuel compositions have started. The design analysis to establish the thermal hydraulic limits and heat transfer capabilities of these cores is in progress.

### REACTOR FUELS AND MATERIALS

#### FAST FUELS OXIDES AND NITRIDES (W. E. Roake)

##### Thermal Expansion Studies

Results of thermal-expansion experiments on  $\text{PuO}_2$  and  $\text{UO}_2 - 2 \text{ wt}\%$   $\text{PuO}_2$  confirm earlier data for stainless steel -  $\text{PuO}_2$  cermets and  $\text{PuO}_2$ , which indicated that large irreversible volume changes are associated with the annealing of pneumatically-impacted materials.

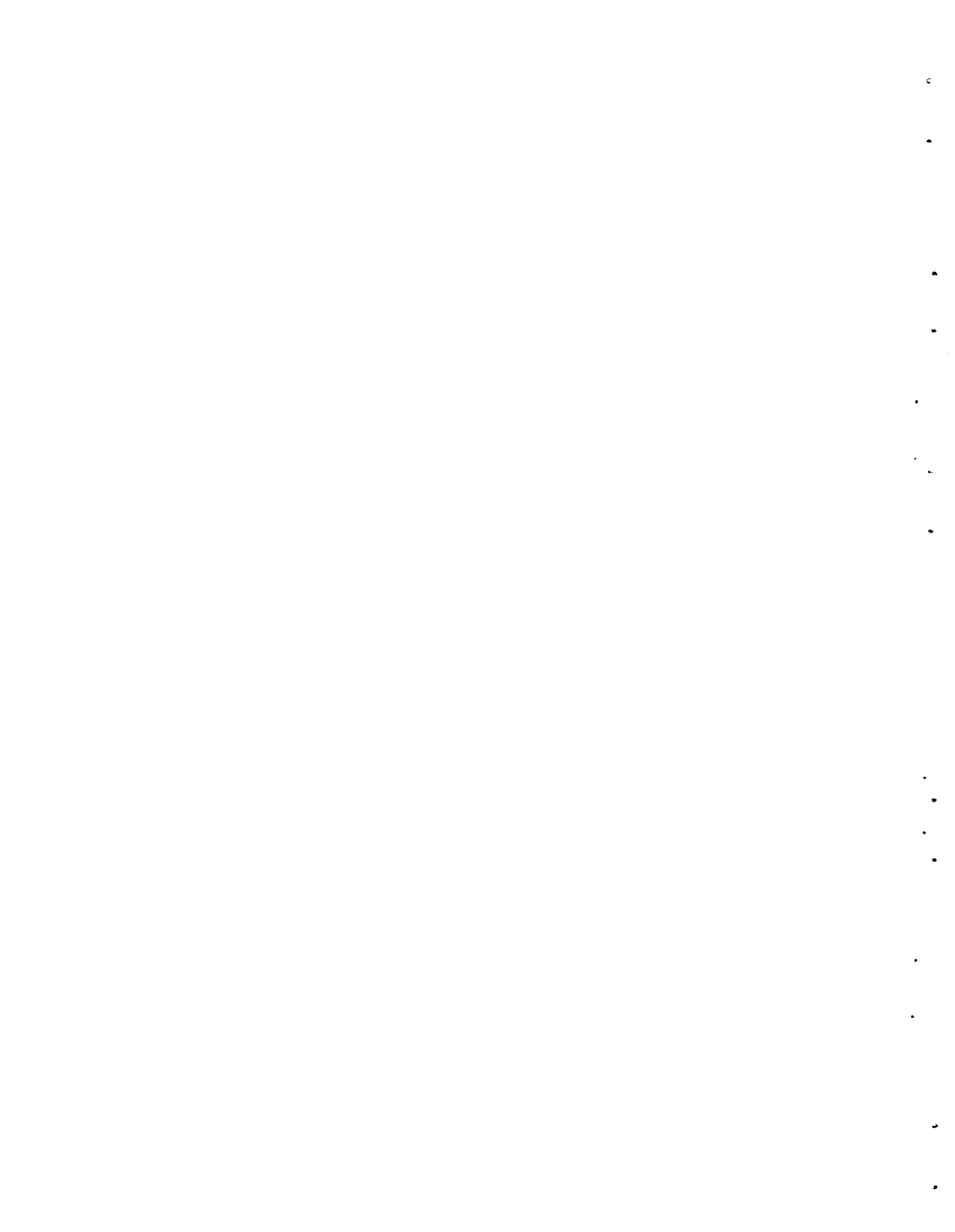
One heating cycle was completed on a pneumatically-impacted  $\text{PuO}_2$  specimen. A contraction of 0.81% occurred between 1015 and 1220 °C, followed by a 1.48% expansion between 1220 and 1385 °C. Above 1400 °C, the rate of reaction between  $\text{PuO}_2$  and the tungsten sample holder was sufficiently large to mask thermal expansion. A coefficient of  $13.1 \times 10^{-6}/^\circ\text{C}$  (200 - 1400 °C) for  $\text{PuO}_2$  was estimated from the cooling portion of the cycle.

Four thermal expansion heating and cooling cycles to 1550 °C were completed on a pneumatically-impacted  $\text{UO}_2 - 2 \text{ wt}\%$   $\text{PuO}_2$  specimen. The first continuous cycle (3.5°C/min) showed a large and rapid volume increase beginning at 1000 °C, which was essentially complete at 1550 °C. The cooling leg of the cycle and three additional cycles showed no further irreversible changes. The net expansion after the first cycle was 1.46%, and the average reversible expansion coefficient was  $11.7 \pm 0.3 \times 10^{-6}/^\circ\text{C}$  (20 - 1550 °C).

In contrast to the  $\text{UO}_2 - 2 \text{ wt}\%$   $\text{PuO}_2$  sample, which exhibited only pronounced grain growth after four cycles, the  $\text{PuO}_2$  sample exhibited large open cracks penetrating up to 90% of the sample diameter after one cycle. This crack formation may account for the apparent contraction of  $\text{PuO}_2$ .

#### Irradiation Performance of Fast Reactor Fuel Candidates - UN - 20 wt% PuN

Mass spectrometric analyses of radial drillings from UN - 20 wt% PuN irradiated to  $2.4 \times 10^{20}$  f/cc at 2130 w/cm confirmed radiochemical indications of severe plutonium migration. Concentration of PuN varied from 17.8 wt% at the periphery to 22.5 wt% at the mid-radius to 7.9 wt% near the fuel center.



### Preparation of Hypostoichiometric Mixed Plutonium-Uranium Oxides

Improved solid-solution formation of uranium oxide - 20 wt% plutonium oxide powders was obtained after wet-blending the powders with deionized water in an alumina ball mill. Good solid-solution formation after sintering for five hours at 1650 °C in argon - 8% hydrogen was indicated by both x-ray diffraction and alpha autoradiography.

### Sodium Bonding Hoods

Modification of three individual sections of a glove box previously used for a swage was started. The modified hoods will be used to house equipment for sodium bonding fuel to cladding in a high purity inert atmosphere. The completed hoods will consist of one individual nine-foot-long hood and one nine-foot-long hood connected to one six-foot-long by eight and one-half-foot tall hood.

Installation of the modified hoods is expected to be completed by the middle of July.

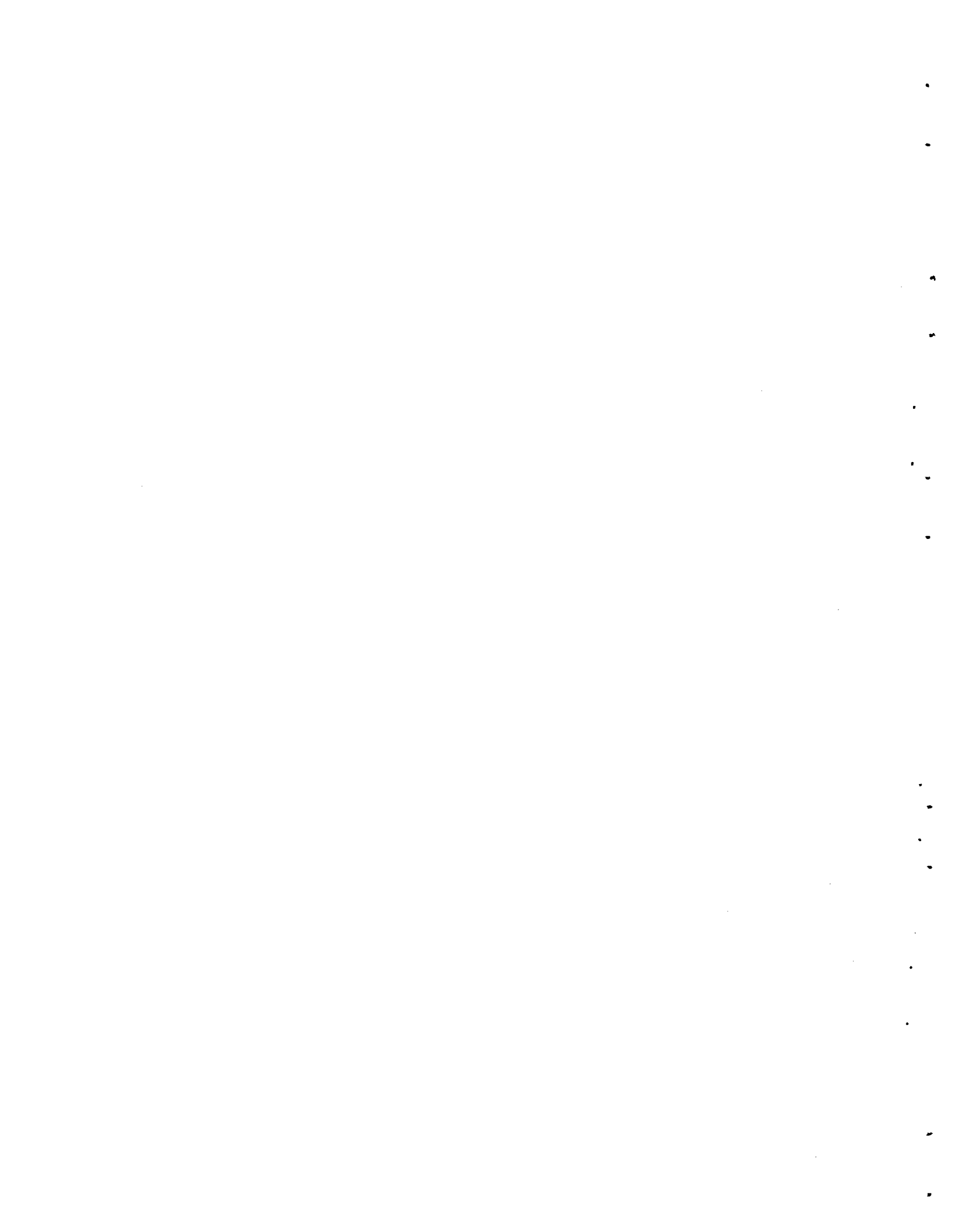
### BASIC SWELLING STUDIES (G. A. Last)

The purpose of this program is to characterize fissionable materials and understand their behavior during irradiation. The theories developed provide a basis for the engineering exploitation of metallic fuel materials in advanced reactor applications. Specimens under study at the present time include uranium with and without dilute alloy additions and thorium-uranium alloys.

### Irradiation Program

A tandem assembly of two capsules continues to operate successfully. One of the capsules is controlled at 250 °C and 1000 psi; the other is a low pressure (~30 psi) capsule controlled at 525 °C. The goal exposures are 0.75 at.% B.U., and 0.4 at.% B.U., respectively. Another controlled temperature, low pressure (~30 psi) capsule is now being controlled at 450 °C toward a goal exposure of 0.3 at.% B.U. This capsule had been designed to operate at 450 °C, but this temperature could not be maintained due to insufficient heat transfer. The control temperature was increased to 625 °C which was maintained while the reactor was up. A lower control temperature of 525 °C was necessary during periods of reactor down time. These temperatures were used for approximately three weeks. Due to an undetermined cause, the heat transfer increased to a point such that control at the original design temperature of 450 °C is now possible. These capsules will provide data needed to evaluate the effects of temperature, pressure, burnup, burnup rate, and minor alloying additives on the irradiation behavior of uranium.

Construction has started on a controlled temperature (450 °C) - pressure (5000 psi) capsule which will operate toward a goal exposure of 0.2 at.% B.U. in the natural specimens. The capsule contains 12 specimens representing six materials in two metallurgical conditions (as



extruded and beta quenched). Six of the specimens are high purity uranium (natural, 1.44% U<sup>235</sup>, and 2.88% U<sup>235</sup>); two are U+Fe-Si, and four are U+Fe-Al (natural and 1.47% U<sup>235</sup>) alloy. The three levels of U<sup>235</sup> will provide three different burnups within approximately the same environment which will enhance the evaluation of the effects of burnup and burnup rate. This capsule will also provide information on the effects of high pressure (5000 psi) and minor alloying additives on the behavior of uranium irradiated at 450 °C.

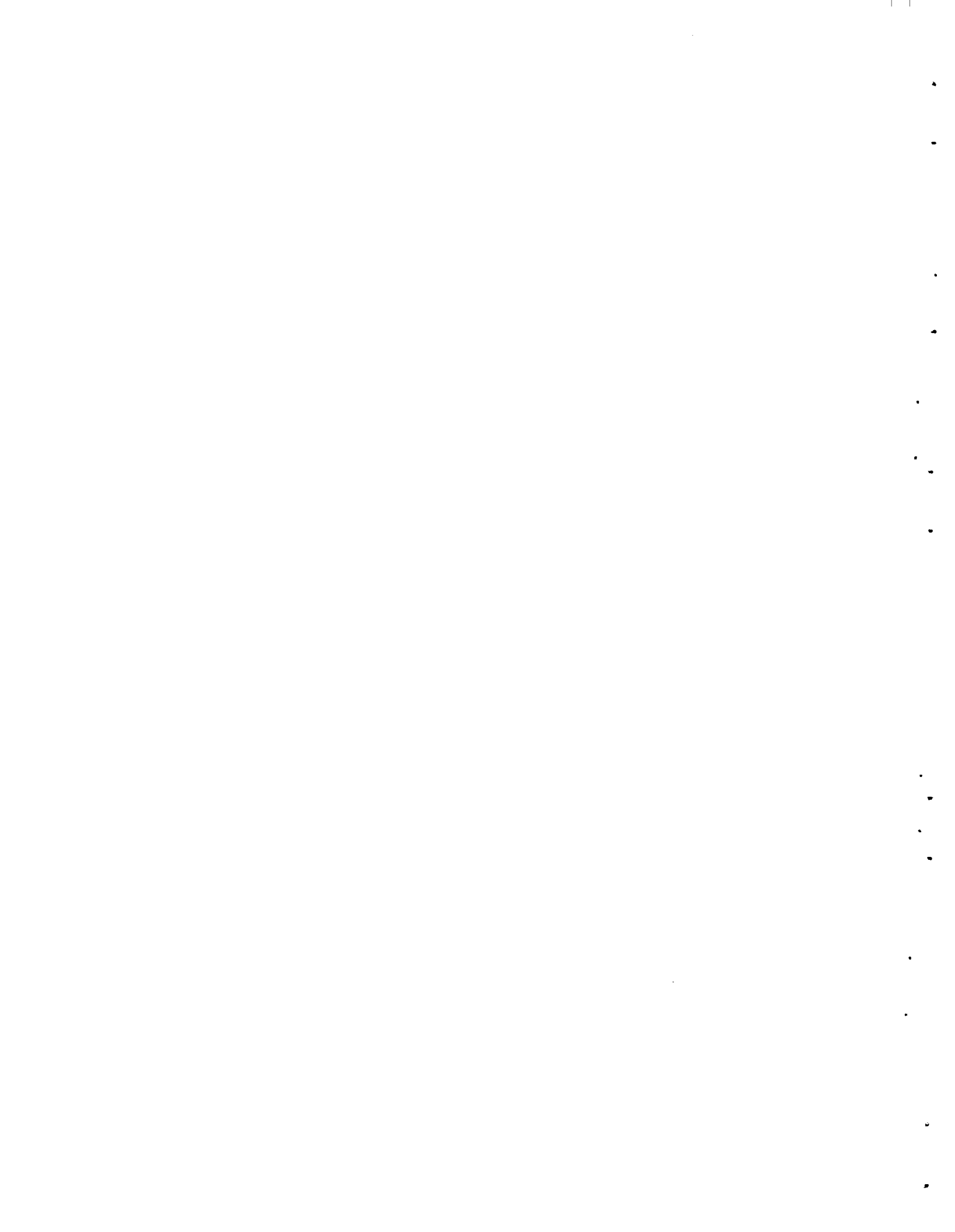
#### Postirradiation Examination

Three controlled temperature capsules were opened in Radio-metallurgy and the specimens were recovered for density measurements and metallographic analyses. Capsule 25, containing high purity uranium specimens enriched to 1.44 wt% U<sup>235</sup>, was controlled at 500 °C and was irradiated to 0.04 at.% B.U. Capsules 33 and 34 were both controlled at 700 °C (beta phase) and were irradiated to 0.10 and 0.20 at.% B.U., respectively. The specimens were high-purity natural uranium, U+Fe-Si alloy, and U+Fe-Al alloy.

Most of the specimens from Capsules 33 and 34 appeared visually to be in excellent condition with little or no warping, surface roughening or cracking being observed. Density measurements on a high-purity uranium specimen and a U+Fe-Al alloy specimen (400 ppm Fe, 640 ppm Al, 85 ppm Si, 500 ppm C) irradiated at 700 °C to 0.2 at.% B.U., revealed only three percent swelling or a value of 15 percent swelling per atom percent burnup. This is presumably due to fission gas porosity, but some internal cracking and tearing may have also occurred as these samples were cycled several times through the alpha-beta transformation. Metallographic examination will define the source of the measured swelling. It is noteworthy that the swelling was so small and that the alloy specimen exhibited the same behavior as the high purity uranium. These observations tend to corroborate the concepts that have been developed with previous irradiations at lower temperatures (alpha phase) and with lower burnup (0.05%) irradiations at 700 °C (beta phase). The densities of the remaining specimens will be measured shortly and metallographic examination will be initiated.

Some of the specimens from Capsule 25 showed severe distortion while others had not changed appreciably in external appearance. The specimens that had large original grain sizes and operated at about 450 °C were, in general, those that exhibited distortion. Density values are being determined and selected specimens will be examined metallographically.

Optical microscope examination of postirradiation annealed specimens of Th-1 and 5 wt% U (1.5 at.% B.U.) indicates the presence of grain boundary porosity. Replicas were prepared from the surfaces for examination in the electron microscope.



Equipment is being modified to permit the postirradiation annealing of uranium specimens to pressures of 15,000 psi and to temperatures of 900 °C. The experiments to be conducted are designed to yield information concerning the swelling behavior of uranium, the healing of microtears formed in uranium irradiated in the 400 - 600 °C temperature range, and the diffusion of fission gases across a U-U interface and a U-Zr 2 interface.

#### NONDESTRUCTIVE TESTING (J. C. Spanner)

##### Electromagnetic Testing

The four channel signal sampling circuit fabricated for use with the multiparameter eddy current tubing tester was checked and test specimen cross section displays were obtained. The displays obtained are similar to those obtained without the new sampling circuits, and first results show that some of the desired increase in the parameter separating capability of the equipment is being obtained. For example, it is now possible to discriminate against signals due to a drilled hole having a particular depth. These capabilities were not possible in the previous arrangement. Further tests are in progress to more fully evaluate the new technique.

Design data are being obtained for the prototype tubing tester which will use the multiparameter concepts developed to date. The new tester will have two channel readout, like the Hanford Model 1004 tubing tester, and the multiparameter concept will be applied to greatly reduce the effect of test probe wobble. Laboratory tests, using the developmental multiparameter eddy current test equipment operating at two frequencies, show that a large reduction in probe wobble effects can be obtained. The new test will have four-dimensional capability so it is expected that it will be capable of indicating the location of flaws (either inner wall or outer wall), discriminate against probe wobble signals in both output channels, and either readout another parameter or give a more refined discrimination against probe wobble signals.

##### Infrared and Thermal Research

A new control system for the sinusoidal thermal transducer driver has been developed. Tests showed that much better control of the transducer power input is obtained over a wider range with the new system. In addition, the new system is less noisy, which should make possible more accurate measurements of the power input to the transducer.

An experimental high sensitivity solid state temperature measuring detector has been installed in the transducer, and tests are being conducted to determine whether or not improved accuracy in temperature measurement has actually been attained. Modifications were made to lower the characteristic impedance of the present thermal transducer, and subsequent testing shows that the frequency response of the





transducer has been increased and that greater power inputs are now possible. This is expected to improve the signal-to-noise ratio for thermal impedance measurements made on highly conductive samples with the transducer.

One of the goals of the present work is to develop an instrument for rapidly measuring the high and low temperature thermal properties of materials. If successful, these measurements will require no special shaping of samples except for grinding a flat surface on one side. The samples would merely be placed on a support in which a thermal transducer was mounted. Such a rapid thermal property measurement method would mean that thermal properties of many materials, not listed for a wide range of temperatures, could be economically measured and information not presently available in the literature could be published. Present emphasis is on metals and other good conductors since much of the interest in nuclear high temperature applications is oriented in that direction.

#### Fundamental Ultrasonic Studies

Research continued on a program to provide an improved understanding of ultrasonic propagation phenomena. In previous ultrasonic pulse studies, the pulse frequency spectra appeared to be poorly represented by Fourier series approximations using existing digital computer programs which convert time varying data into the frequency domain. Since this transformation is essential to ultrasonic pulse propagation studies, a new approach to the problem was undertaken.

As an initial trial, attempts were made to represent the signals by a time varying function which includes an exponential damping factor, a hyperbolic sine factor, and a periodic cosine factor. Solutions involve the determination of coefficients and arguments which establish good agreement with experimentally observed signals. A trial and error procedure is necessary in order to find suitable values for the unknown parameters, and such a procedure requires some estimate of the parameters involved. Starting values are critical and so far methods to obtain suitable estimates have not been successful.

Concurrently, the one sided Fourier transform was coded in preparation for use with the new time varying function. Testing of this program has been held up by the aforementioned difficulties. The present studies have been designed to be compatible with previous analysis of ultrasonic wave propagation, and when debugged, the analysis should easily be incorporated in the main program.

In the general study of attenuating acoustic waves, expressions for the reflection and transmission factors in the presence of attenuation have been derived and programmed. There are also studies by others in the field of acoustic wave behavior which provide theoretical expressions for the scattering of ultrasonic waves by polycrystalline metals. Since scattering is the most predominate contribution to



attenuation in the MHz frequency range, Rayleigh and stochastic scattering values given by the aforementioned expressions are being calculated for a variety of metals and conditions. These scattering values are then being used to calculate reflection and transmission factors having a range of frequencies. The resulting division of amplitudes between reflected and refracted waves should provide information which will cover typical conditions encountered in practice.

### NUCLEAR CERAMICS (R. E. Nightingale)

#### Stoichiometry Effects on Irradiation Behavior of UO<sub>2</sub>

Analysis of the radial oxygen distribution in irradiated UO<sub>2.15</sub> (the last of six specimens with O/U's of 1.90, 1.99, 2.00, 2.02, 2.05, and 2.15 to be studied) showed that, as with other UO<sub>2+x</sub> specimens, gross migration of oxygen to the center occurred. In the center the O/U ratio after irradiation was 2.40. The data are being analyzed in an attempt to compute partition functions for oxygen concentration in the melt in equilibrium with the solid for the various mean oxygen pressures represented in the experiment.

Correlation of heat-transfer parameters with mean fuel composition was completed. The principal result was the relationship between the average oxygen to uranium ratio,  $\overline{O/U}$ , and the heat rating required for center melting. This can be linearly expressed as:

$$\int_{500 \text{ }^{\circ}\text{C}}^{T_m} k \, dT = - 75.8 (\overline{O/U}) + 221 \text{ watts/cm}$$

where  $T_m$  = melting temperature  
and  $k$  = thermal conductivity.

Between 500 °C and the "recrystallization temperature" ( $T_{gg}$ ), thermal conductivity was insensitive to mean composition changes for  $2.05 < \overline{O/U} < 2.00$ ; a marked decrease in conductivity with increasing O/U was evident for  $2.00 < \overline{O/U} < 2.05$ . This trend is reasonable because:

- (1) For  $\overline{O/U} < 2.00$ , much of the excess uranium exists as second-phase inclusions which contribute little toward altering thermal conductivity.
- (2) For  $\overline{O/U} < 2.00$ , the excess oxygen is in solution and acts as phonon scattering centers which strongly reduce the lattice conductivity.
- (3) For very high O/U (i.e., above 2.05) it is reasonable to expect precipitation of U<sub>4</sub>O<sub>9</sub> or some other, higher oxide phase so that as composition varies, the matrix changes only in the proportion of the two phases present without significant change in composition within a particular phase. As with UO<sub>2-x</sub>, then, the



thermal conductivity should be relatively unaffected by small compositional changes within the two-phase region.

The conductivity between  $T_{gg}$  and melting reached a minimum near  $O/U = 2$ ; it rose more rapidly as a function of stoichiometry for  $O/U > 2$  than for  $O/U < 2$ . It thus appears that the addition of oxygen decreases the low-temperature thermal conductivity and increases the high-temperature conductivity. The uniform decrease in heat rating required for center melting reflects principally the decrease in  $UO_{2+x}$  melting temperature with increasing  $O/U$  ratio.

#### Stoichiometry Effects on $UO_2$ Hardness

Knoop hardness measurements of pneumatically-impacted  $UO_{2+x}$  for  $O/U$  ratios of 1.90, 1.99, 2.00, 2.02, 2.05, and 2.15 showed that the hardness varied almost linearly with increase in  $O/U$  from 530 (for  $O/U = 1.90$ ) to 880 (for  $O/U = 2.15$ ). Specimens were prepared by blending  $UO_2$  powder with  $U_4O_9$  or  $U$  powders and compacting the mixtures at 1200 °C and 250,000 psi. Compacts with  $O/U > 2$  were partially homogenized but contained small  $U_4O_9$  inclusions that precipitated on cooling. For  $O/U < 2$ , all the excess uranium was present as 10-20  $\mu$  metal inclusions.

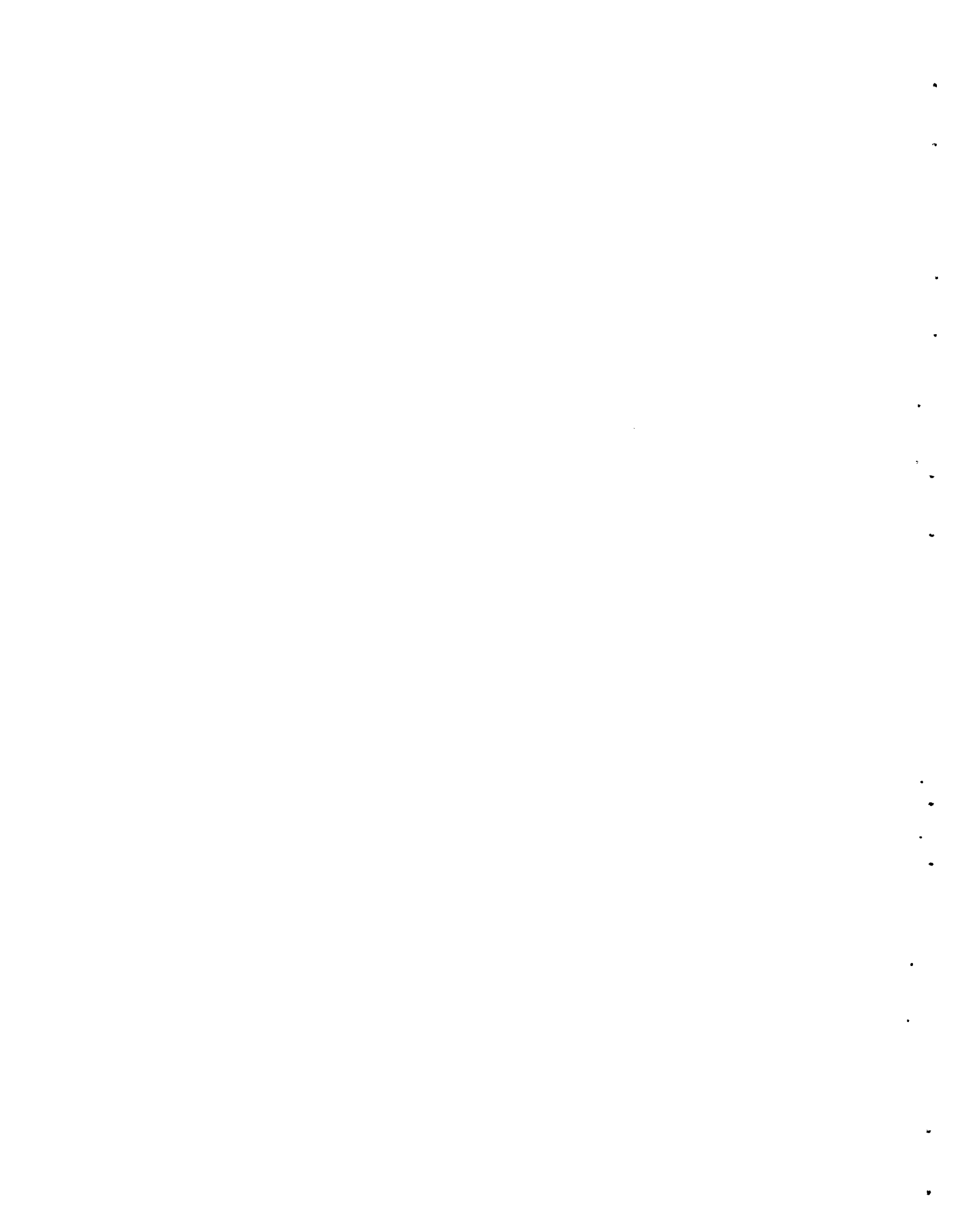
For  $O/U$ 's  $> 2$  this behavior seems reasonable in terms of dislocation pinning by dissolved oxygen ions. The low hardnesses for  $O/U$ 's  $< 2$  probably result from the presence of the soft uranium inclusions which are present in such quantities as to be unavoidable in placement of the indenter.

#### Recovery and Recrystallization in Pneumatically-Impacted Ceramics

Recent thermal expansion and thermal diffusivity measurements on  $UO_2$ ,  $PuO_2$ , and their solid solutions indicate that irreversible structural changes occur during post-impaction annealing. To explain these effects and to relate them to the general phenomena of recovery and recrystallization after mechanical working, differential thermal analysis (DTA), measurements were initiated to investigate the presence and release of stored energy. Several DTA runs to 1420 °C were made on pneumatically-impacted  $UO_2$  powder. The sensitivity of the DTA apparatus was not sufficient to detect heat effects. Additional experiments are currently in progress using solid DTA samples and a modified sample holder in an attempt to improve the sensitivity of the instrument.

#### Mechanism of Pneumatic-Impaction Bonding

Unique etch-pit distributions were observed in pneumatically-impacted  $UO_2$  single crystals. Impacted pairs of  $UO_2$  single crystals showed a dense "fringe" of etch pits around the exposed cube surfaces, an intermediate etch-pit population in the interior, and an almost complete lack of etch pits at the interface surfaces. Differences in polycrystal plastic deformation suggest that pressure is not being transmitted to areas located between the single-crystal cubes. The



relationships between these etch pits and accompanying plastic deformation, bond character, and apparent pressure distribution around and within the specimens is being investigated.

Improvements in bonding of  $UO_2$  single crystals were observed when an additive compound ( $Sm_2O_3$ ,  $ThO_2$  or  $UO_2.08$ ) was present at the interface. This may be due to the introduction of excess oxygen leading to a defect crystal structure, enhanced inter-crystal diffusion, or reaction with the oxygen or metallic component, to improved plasticity, or to other factors.

#### Materials for Basic Research

Eight large  $UO_2$  single crystals, weighing 235 grams, were selected, prepared, and sent to the Engineering and Research Laboratory, Mitsubishi Atomic Power Industries, Inc., Japan, for use in elastic modulus and internal friction studies. Crystal specimens will be prepared in Japan to the required lengths of 13 to 28 mm with several specimen orientations. Representative samples of the crystals were characterized for stoichiometry and purity.

A 50 x 356 mm rod of Pyroceram 9606 was obtained from the National Bureau of Standards for use as a thermal conductivity standard. The material is similar to the Pyroceram 9606 standard being proposed by N.B.S.

#### NUCLEAR GRAPHITE (R. E. Nightingale)

##### Irradiation of Nuclear Graphite

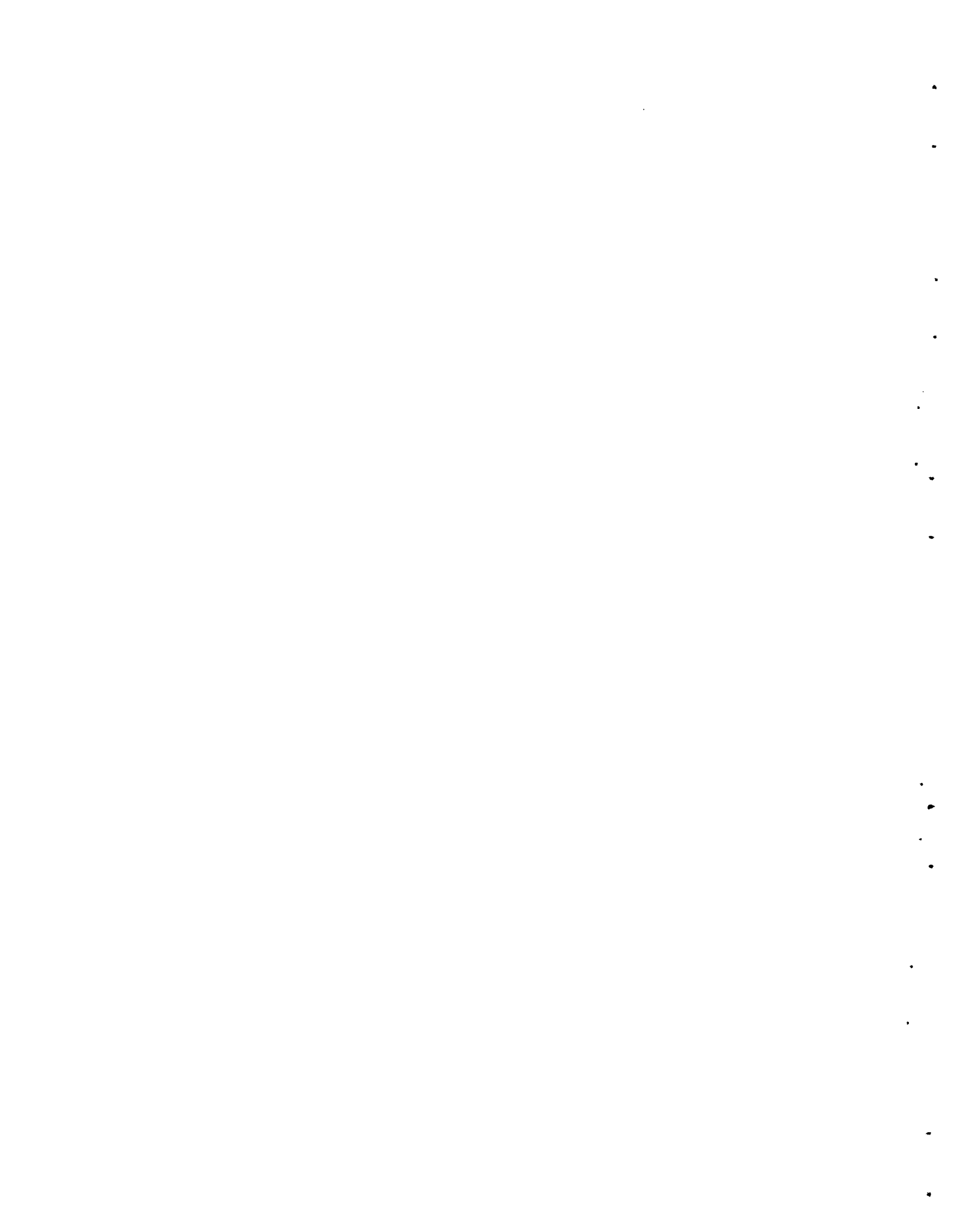
The graphite capsule, H-3-12, presently in the GETR is in the final cycle of irradiation and is scheduled for removal during the week of July 3rd. At that time the maximum neutron exposure will be approximately  $2.2 \times 10^{22}$  nvt,  $E > 0.18$  MeV.

##### Irradiations of "Dimensionally-Stable" Graphites

The second capsule, H-3-23, in the present series for the irradiation of "dimensionally-stable" graphites has successfully completed the first cycle of irradiation. One thermocouple has failed, and the one with the scraped insulation operates intermittently. The binary gas system is functioning very well.

##### Graphite Irradiations in EBR-II

Immediate plans for irradiations in EBR-II are for the insertion of three pins in the reactor in mid-July. Each pin contains 17 graphite samples 0.250" dia. x 1.75" long. Two of the pins, scheduled for a six-month irradiation residence will get an exposure of about  $10^{22}$  nvt ( $E > 0.18$  MeV). The third pin will receive approximately half this dose. The irradiation temperature of all three capsules should be approximately 600 °C.





Nine additional pins are also being assembled for future tests in the reactor. These pins will be installed in the reactor on a space-available basis.

#### Averaging Techniques in Polycrystalline Graphite

A computer program has been written to be used in calculating the polycrystalline values of Young's Modulus and dimensional changes from single-crystal values. Preliminary calculations indicate that a constant stress model taking into account c-axis accommodation gives values of Young's Moduli which are in good agreement with the experimental values. An irradiation model has also been proposed. The basis of the proposed model is that irradiation will change the amount of accommodation in polycrystalline graphite. Such changes are accounted for by varying the probability that a crystallite of given orientation will contribute to the overall properties of the graphite. Thus far, the calculated overall changes of length and elastic moduli are compatible with the experimental values.

#### Irradiation of NCC Pyrolytic and Single-Crystal Graphite

A capsule designed to irradiate samples at 50 °C was tested in the Snout Facility in KW Reactor. Capsule temperatures ran significantly higher than desired, evidently due to an underestimate of the gamma heating. A new capsule designed to allow for the greater heat generation has been fabricated and will be tested.

The four sets of samples for the irradiations have been received from Union Carbide. Goal exposures for the tests are 2, 5, 10, and 20 x 10<sup>17</sup> nvt (E > 0.18 MeV).

#### The Effect of Oxidation on the Sonic Modulus of TSX Graphite

To compare changes in the sonic modulus occurring upon oxidation with changes in the ultimate tensile and compressive strengths, a series of parallel samples of TSX graphite was oxidized in air at 700 °C to varying extents up to about 15% weight loss. Measurements of sonic moduli were made both before and after oxidation. The mechanical measurements were then performed on the oxidized as well as a few unoxidized samples. It has been found that the variation with oxidation of all three properties follows a relationship of the form

$$P/P_0 = A(W/W_0)^B \quad (1)$$

where P = the property under consideration  
 P<sub>0</sub> = the initial value of this property  
 W = the weight of sample remaining  
 W<sub>0</sub> = the initial sample weight

and A and B are constants. Because of the variation in the initial density within the series of samples, it was first necessary to obtain values of P<sub>0</sub> for the oxidized samples by correcting the values obtained



on the unoxidized samples to the proper initial density, P, by means of the equation

$$\log P = m \log \rho + b \quad (2)$$

This equation is identical in form to equation (1). The values of A and B in equation (1) were obtained by the "least squares" method and are compared in the following table with some values for PGA graphite published by Rounthwaite et al.\*

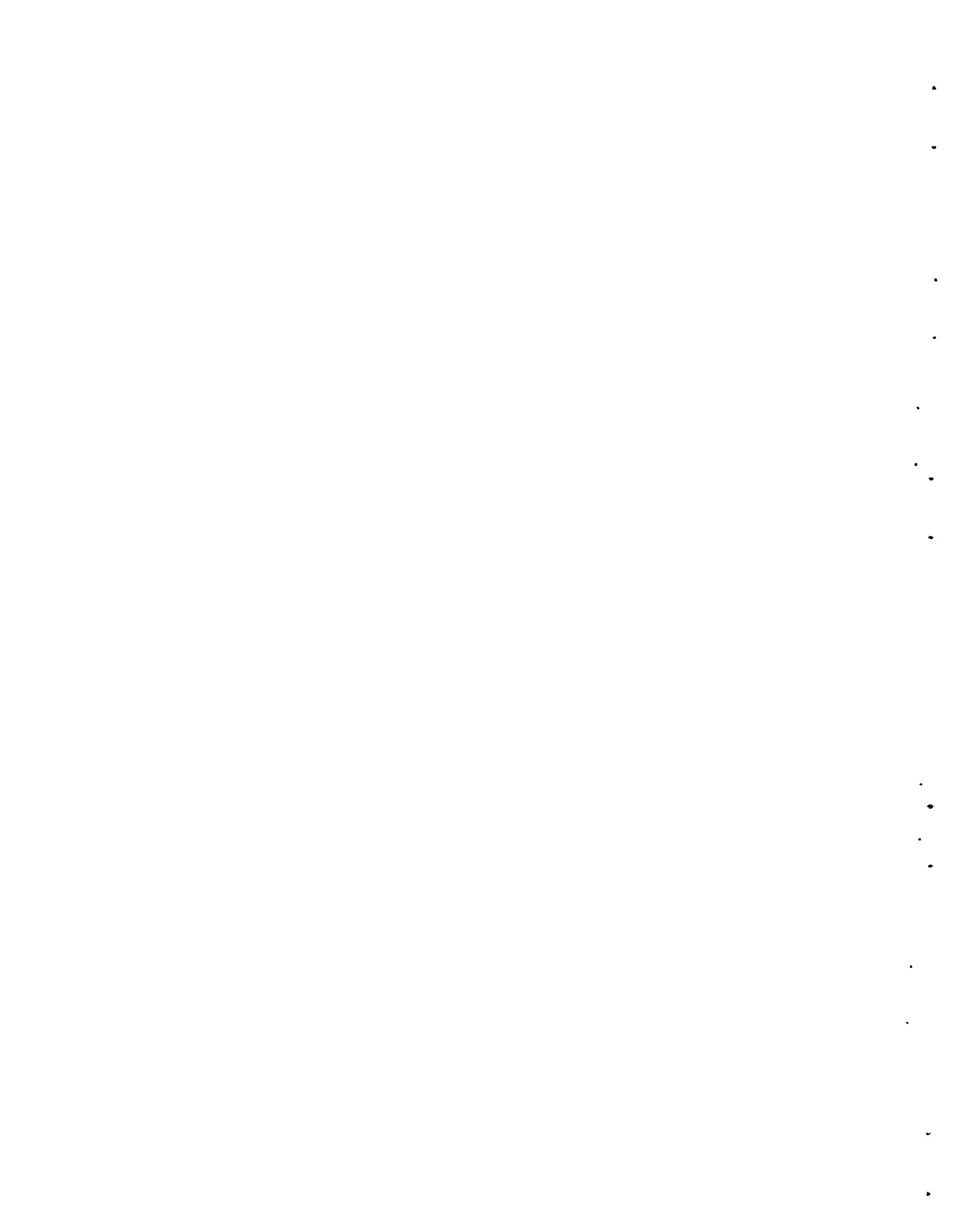
<u>Property</u>	<u>A</u>	<u>B</u>	<u>B**</u>
Sonic modulus	0.989	9.44	8.6
Tensile strength	0.987	7.98	8.2
Compressive strength	1.004	6.28	6.8

It is seen from the values of B that the sonic modulus decreases somewhat more rapidly with oxidation than does the ultimate tensile strength which, in turn, decreases more rapidly than the ultimate compressive strength. The values of A and B are probably least reliable in the case of the tensile strength because of greater scatter in the data. Both the sonic modulus and the compressive strength closely follow the above logarithmic equation.

To investigate further the actual depth of penetration of oxidant into the graphite during oxidation, a series of transverse samples was oxidized to about 15% weight loss at temperatures ranging from 600 to 850 °C. Successive shells were then machined from the cylindrical samples and the density of these shells determined from the weight removed and the changes in the sample dimensions. In this manner the radial variation in the apparent density was obtained. The density distributions indicate that at 600 °C oxidation is essentially homogeneous, an expected result. At 700 °C a slight gradient exists, but the oxidant probably penetrates to the center of the sample, at least through the system of macropores. At 750 °C the gradient is somewhat steeper but relatively deep penetration occurs, again probably only through the larger pores. At this temperature even after 15% oxidation, the utilization factor is only about 0.4, which indicates that the major portion of the micropore system is available to the oxidant. At the two highest oxidation temperatures employed, 800 °C and 850 °C, very steep density gradients occurred, and it appears that the oxidant was limited to about the outer 45% and 30% of the sample volumes

\*C. Rounthwaite, G.A. Lyons, and R.A. Snowdon, "Influence of Thermal Corrosion on the Strength, Permeability and Frictional Properties of Nuclear Graphite," London Carbon Conference, April 1965.

\*\*These values of Rounthwaite et al, are average values for both parallel and transverse samples. They have assumed in each case that A = 1.



respectively. Moreover, it is likely that only the macropores in these volumes were available to the oxidant, because the utilization factors after 15% oxidation are approximately 0.2 and 0.06 at 800 °C and 850 °C, respectively.

It is readily apparent that no attempt should be made to relate the magnitude of the utilization factor to penetration of the oxidant into the graphite samples. It has been previously shown that the loss in sonic modulus with extent of oxidation is independent of the rate of oxidation up to temperatures near 750 °C. The present density profile measurements explain this result. Oxidant penetration throughout the sample volume by means of the system of macropores is reasonably complete at temperatures near 750 °C, irrespective of the fact that less than half of the internal surface area is available for reaction.

#### Compatibility Studies of Sodium with Graphite

Seven irradiated CSF graphite samples were heated in contact with sodium for 100 hours at 537 °C (1000 °F). Four samples were irradiated at about 500 °C to exposures ranging from  $1.5 \times 10^{20}$  to  $2 \times 10^{21}$  nvt ( $E > 0.18$  MeV). Three samples were irradiated at 30 °C to exposures of  $1 \times 10^{19}$ ,  $6 \times 10^{19}$ , and  $1.2 \times 10^{20}$  nvt ( $E > 0.18$  MeV). The samples were sealed in stainless steel capsules after the capsules had been filled with sodium. The capsule welding and opening operations were performed in a helium-filled glove box. The interaction of graphite with sodium caused an expansion in the samples ranging from 0.7 to 1.0%. In NAA-SR-11309, 3.9% expansion was reported for type TSP graphite irradiated to  $1.1 \times 10^{21}$  nvt. The smaller expansion for the higher exposure CSF graphite may be due to the different type of graphite used in the present studies. Some preliminary work on unirradiated CSF graphite indicates that the expansion is nearly complete after three hours treatment with sodium at 400 °C.

#### IRRADIATION DAMAGE TO REACTOR METALS (A. L. Bement)

##### Alloy Selection

Assembly of the second liquid metal capsule is nearing completion. This capsule uses sodium as the environmental medium rather than NaK alloy to more closely approximate the operating condition of the sodium cooled fast breeder concept. Problems associated with sodium handling are being surmounted. The sodium will be maintained in the liquid state at all times during irradiation by means of a heater immersed in the metal at the capsule central axis. The irradiation assembly containing 32 AISI 316 stainless steel mechanical test specimens will be charged in ETR Cycle 83.

Final preparations are being made for insertion of a characterized, refractory metal, specimen and container assembly in the vertical section of the model gas loop. The assembly will be examined at the end of each five-day cycle for any physical or mechanical changes

•

•

•

•

•

•

•

•

•

•

•

•

•

•

caused by the loop environment. Thermocouples placed radially and axially will monitor the temperature flow characteristics of the assembly. Information gained from this experiment will aid in design of the in-core assembly for the ATR gas loop.

The AISI 316 stainless steel order from Allegheny Ludlum has been poured. The flat stock will be rolled at Pennsylvania sites. Two 12" x 12" ingots were shipped to Watervliet, New York, for processing to the specified round shapes.

#### In-Reactor Measurements of Mechanical Properties

The in-reactor creep test at 840 °C on annealed 304 stainless steel was not started due to heater failure. The capsule will be replaced so that the required test data can be obtained.

In-reactor and ex-reactor creep tests are continuing at 300 °C and 55,000 psi, and at 400 °C and 36,500 psi. The test at 350 °C and 45,000 psi was terminated after heater failure.

The minimum rate observed at 300 °C and 55,000 psi is  $6.5 \times 10^{-7}$ /hr. The specimen had been previously stressed at 36,500 psi and 45,000 psi. No minimum creep rate has yet been obtained for the 400 °C, 36,500 psi in-reactor creep test. Creep rates obtained for the 350 °C, 36,500 and 45,000 psi test prior to heater failure were  $3 \times 10^{-7}$ /hr and  $1.4 \times 10^{-6}$ /hr, respectively. The capsule will be recovered for future specimen examinations.

Construction of the high temperature capsule is continuing. Electrical installations for capsule checkout were started and will be completed this month.

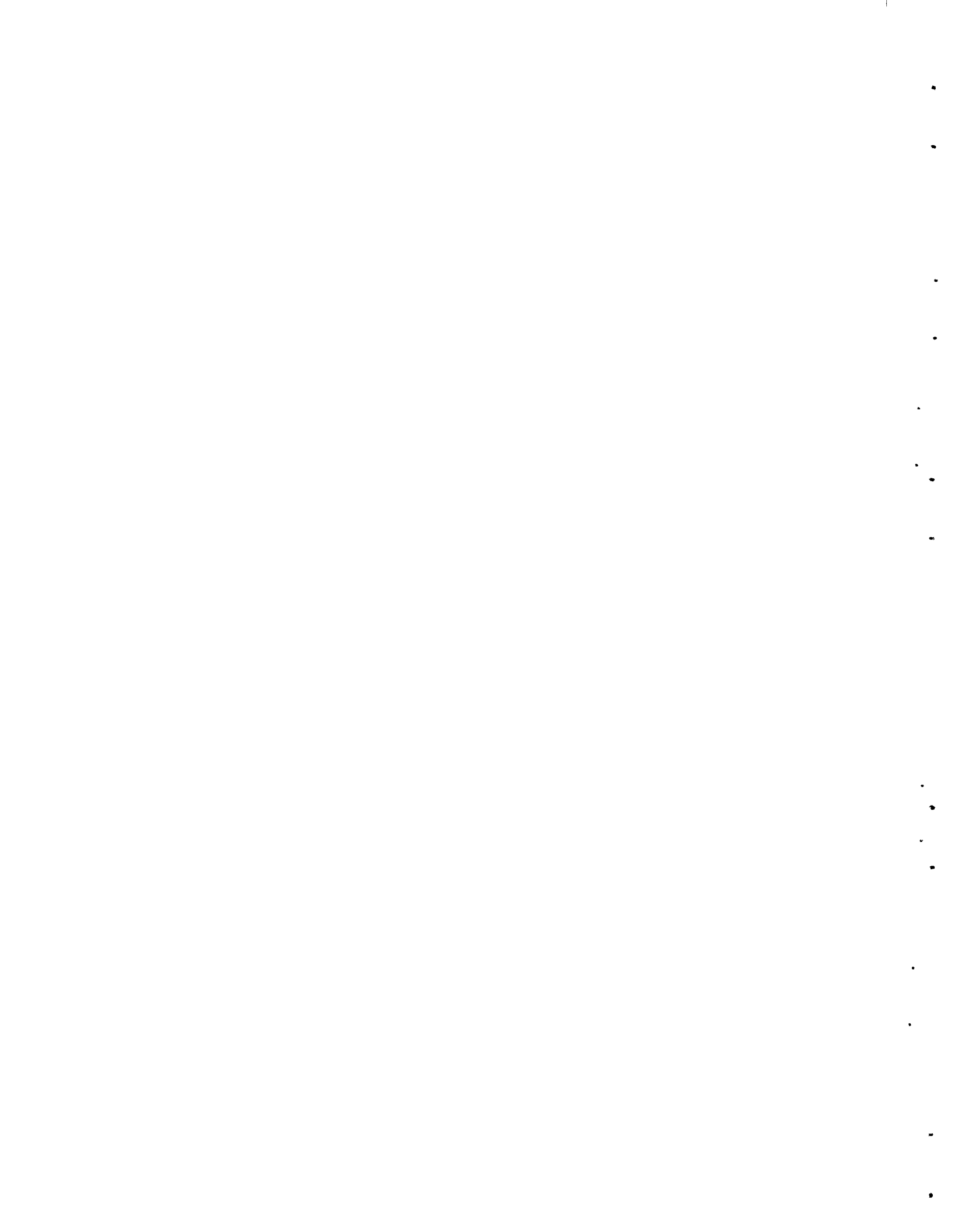
Appropriation requests and specifications were written for the purchase of additional control systems for installation in the reactor facilities.

#### Irradiation Effects in Structural Materials

##### Stainless Steels

The purpose of this phase of the program is to determine the combined effects of irradiation and environment on the mechanical properties of stainless steels. Radiation-induced property changes will be determined from irradiations and tests conducted at various temperatures on several alloys. Particular emphasis will be placed on determining the existence of metallurgical instabilities and the mechanisms by which they are enhanced in a nuclear environment.

Electron microscopy examinations have been employed to characterize the microstructure of AISI 304 and 348 stainless steels in both the annealed and highly cold worked condition prior to irradiation. Specimens from different heats have been examined. Samples from heats of AISI 316 and 321 stainless steel are also being studied. This thorough characterization is necessary for detecting subtle changes caused by neutron irradiation.





Electron micrographs were obtained from a bulk specimen of AISI 348 stainless steel which had been irradiated at 60 °C to an exposure of about  $1.0 \times 10^{20}$  nvt (>1 Mev). Carbide particles were observed primarily in the matrix of the material and did not appear to have increased in either size or number due to a sufficiently low irradiation and testing temperature. The particles were removed by an extraction process and identified as niobium carbides by means of x-ray diffraction. These particles were also examined on the electron microprobe. The particles were so small that their composition could not be determined.

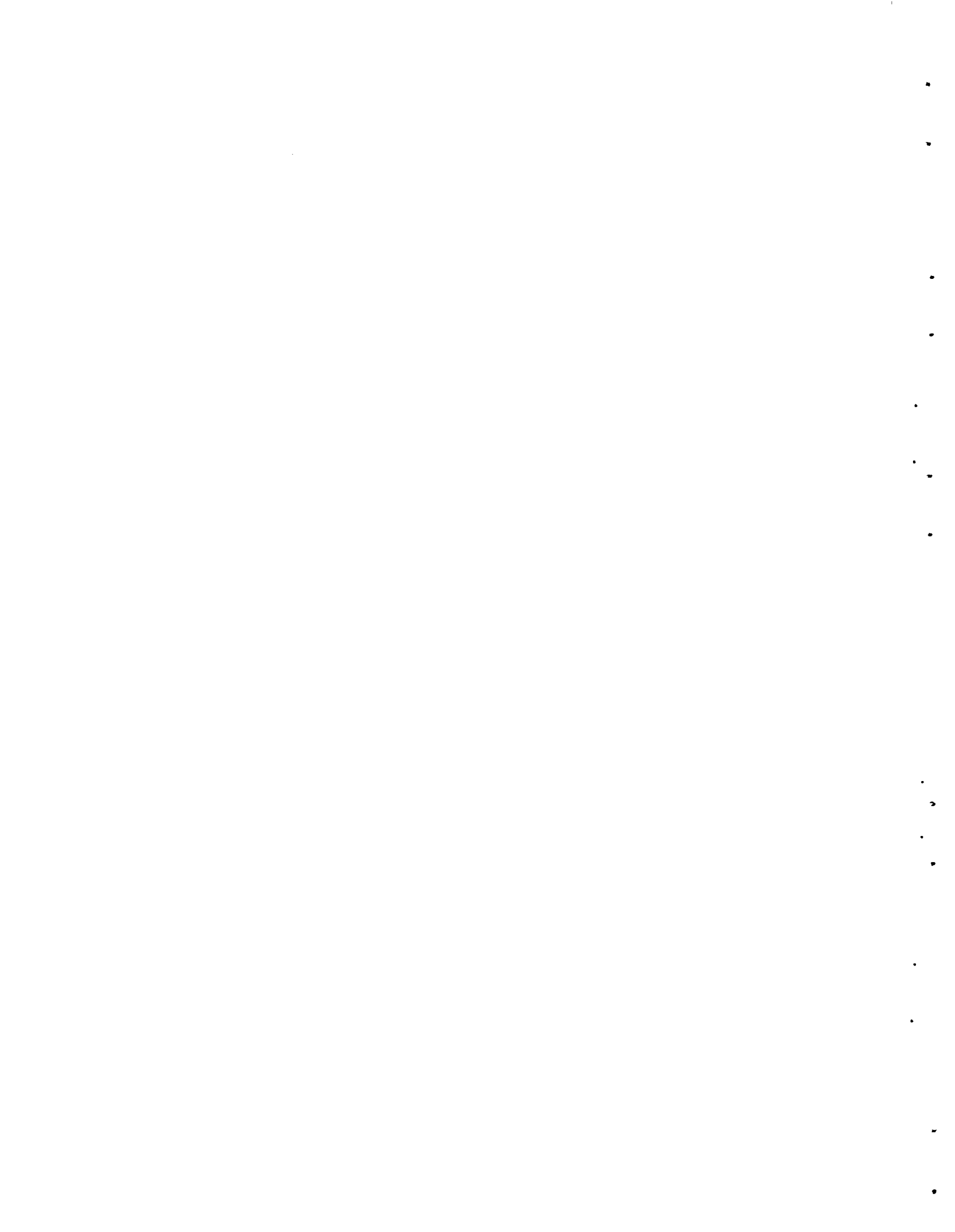
Irradiation at 60 °C resulted in the appearance of many very small clusters in the annealed AISI 348 stainless steel. These defect clusters can grow and annihilate one another depending upon various factors which are usually temperature dependent. A large portion of the mechanical property changes due to displacement-type damage is recoverable upon postirradiation annealing at temperatures between 400 to 600 °C. Therefore, thinned bulk specimens in the irradiated condition were annealed at 450 °C for one hour in vacuum and then examined in the electron microscope to determine what changes in microstructure occurred. Only a small portion of the defects were removed, and it appeared that only the smaller-sized defect clusters were affected. The larger clusters appear to be stable even at 450 °C for short times. Additional bulk specimens are currently being examined after annealing at temperatures to 600 °C. Specimens irradiated at temperatures to 750 °C have also been obtained and are currently awaiting examination. A shielded facility has been constructed and is currently being checked for use in preparing electron microscopy specimens from radioactive bulk specimens.

#### Nickel-Base Alloys

The purpose of this program is to determine the effects of modified microstructures on the irradiation stability of nickel-base alloys. Structural modifications are made by preirradiation thermal and/or mechanical treatments and are evaluated by tensile tests, stress-to-rupture tests and metallographic examinations.

A formal report entitled "Improved Postirradiation Stress-Rupture Properties of Hastelloy X-280," BNWL-231, by I. S. Levy, detailing the results of the stress-rupture tests recently completed, has been sent to Technical Publications for printing. A paper entitled "Post-irradiation Mechanical Property Improvements in Hastelloy X-280 and Inconel 600," BNWL-SA-724 A, by I. S. Levy, has been submitted to the American Nuclear Society for presentation at the Winter Meeting in Pittsburgh. A paper correlating unirradiated tensile properties with the microstructures of pretreated Hastelloy X-280, entitled "Electron Microscopy of Tensile Specimens of Thermomechanically Treated Hastelloy X-280," BNWL-SA-608, by I.S. Levy, B. Mastel, and J. L. Brimhall, has been submitted to Trans. AIME for publication.

Electron microscopy has continued on sections from the stressed areas of irradiated and unirradiated standard solution treated Hastelloy



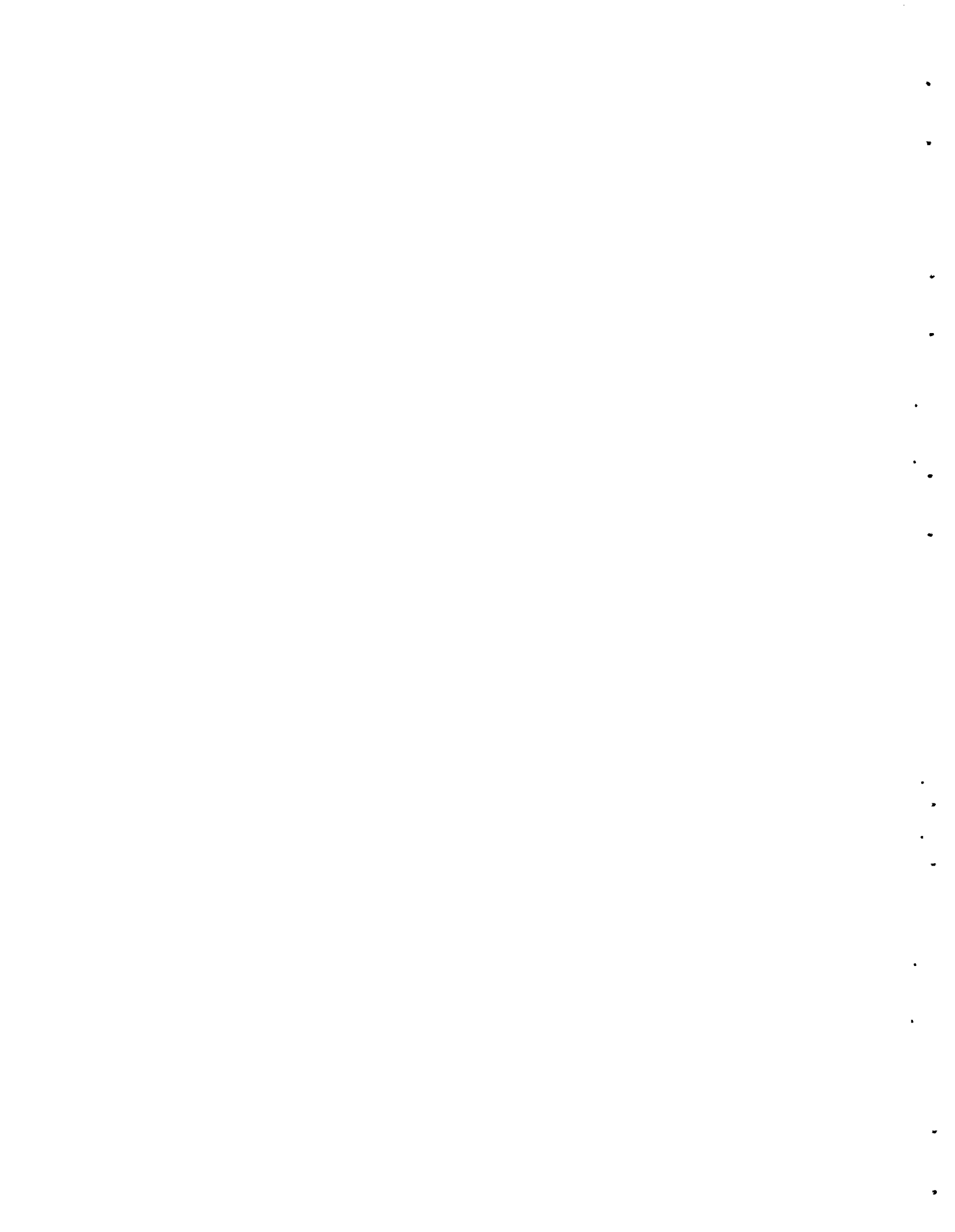
X-280 specimens that were tensile tested at 1350 °F (730 °C). Last month it was reported that transmission microscopy showed matrix precipitates in the unirradiated specimens, but none in the irradiated specimen. This month, replica microscopy, using similar 20-mil thick wafers from the same areas of the specimens and using the same electrolytic etch as was used for the transmission microscopy, showed that, in reality, the unirradiated specimens had two forms of matrix precipitate, one extremely small and one quite large. The replicas showed further that the effect of irradiation was to inhibit precipitation of the small precipitate, to increase the size of the large precipitate, and to produce this larger precipitate primarily around grain boundaries. This material had very low ductility after irradiation. This evidence reinforces the suggestion presented last month for the mechanism of irradiation embrittlement in this alloy. Defects, caused by irradiation at 540 °F (280 °C) in the standard solution treated material, increased diffusion to the grain boundary, under the influence of test soak and subsequent tensile strain at 1350 °F (730 °C), of those elements which would otherwise have precipitated in the matrix. It has been shown that ductility can be improved 100% by a preirradiation aging at 1500 °F (815 °C) for 24 hr. The irradiated specimen given this treatment showed gross matrix precipitate after tensile straining at 1350 °F (730 °C).

This suggests that clustered solute atoms, formed during the 1500 °F (815 °C) aging treatment, interact with the irradiation-induced defects at 540 °F (280 °C) to form complex aggregates. These aggregates promote precipitation in the matrix during subsequent high temperature testing, thereby restricting diffusion of the embrittling constituents to the grain boundary.

A similar mechanism can be used to explain the results of tensile tests and metallography on Inconel 600. Experimental treatments tested thus far show that improvements of up to 138% in total elongation with no reduction in yield strength were possible (compared to the standard treatment) for specimens irradiated at 540 °F (280 °C) to  $1 \times 10^{20}$  nvt (fast) and then tensile tested at 1350 °F (730 °C). Metallography (1000X) of the unstressed sections of unirradiated specimens subsequent to testing shows that the standard treatment had heavy, continuous grain boundaries and no matrix precipitate, while the specimen receiving the treatment that resulted in the best postirradiation ductility showed a noncontinuous grain boundary precipitate and a matrix precipitate.

Stress-rupture tests on unirradiated Hastelloy X-280 specimens, which are controls for those irradiated specimens already tested and reported on, have commenced this last month. These are being conducted in air at 1350 °F (730 °C) and at 18,000 psi, the 1000-hr rupture stress for standard treated unirradiated material.

Twenty-six tensile and 22 stress-rupture specimens of Hastelloy X-280, Inconel 600, and Inconel X-750, which were irradiated at 1300 °F (705 °C) to a goal exposure of  $1 \times 10^{20}$  nvt (fast), have been discharged. Tensile tests are scheduled to commence next month.



### Fracture Mechanics

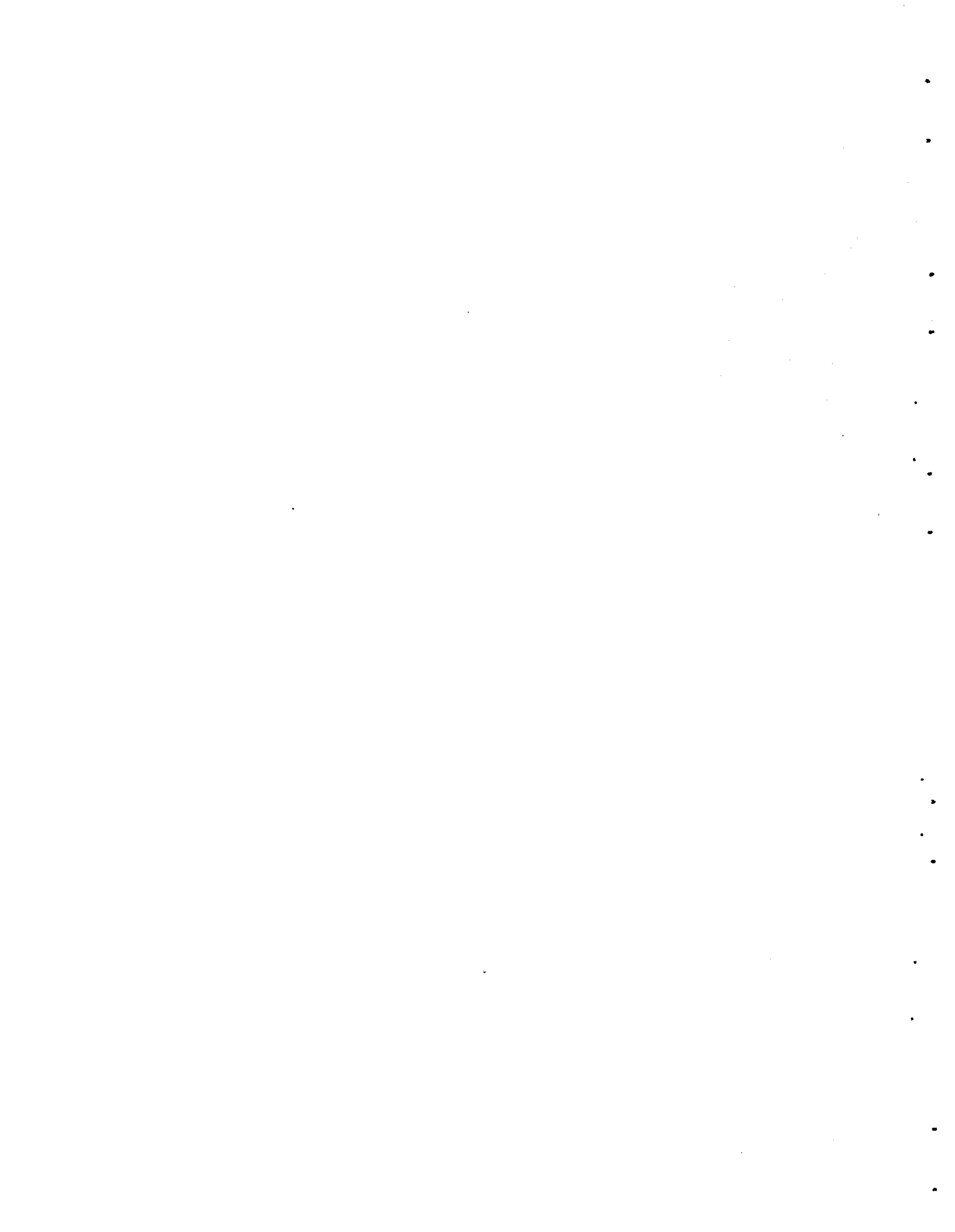
The fracture toughness of normalized A302-B exposed to one-half cycle in the G-7 loop of the ETR has been determined. The specimens were placed in the X-3, A-3 position and were estimated to have obtained an average exposure of  $5 \times 10^{18}$  neutrons/cm<sup>2</sup>. There was probably a substantial exposure gradient along the specimen, however, since the X-3 position extends out of the core of the reactor. It was found that 280 °C irradiation to  $5 \times 10^{18}$  neutrons/cm<sup>2</sup> does not affect the fracture toughness. The toughness ( $K_{Ic}$ ) observed for the irradiated material for cracking along the rolling direction was essentially the same as data obtained from unirradiated specimens.

There was a decrease in the stress intensity factor at arrest,  $K_{Ia}$ , indicating that irradiation increased the rate sensitivity of the material. In view of this increase of rate sensitivity, it is thought that PNL results correspond with notched Charpy impact data which indicate a transition temperature increase of 50 °F (10 °C) for a 550 °F (290 °C) irradiation to the same neutron exposure.

Another quadrant, which was exposed to approximately  $1 \times 10^{19}$  neutrons/cm<sup>2</sup>, has recently been discharged from the same position in the G-7 loop and will be tested when available. The results of these forthcoming tests will allow the determination of the exposure dependence of both  $K_{Ic}$  and  $K_{Ia}$ .

The decrease in fracture toughness of annealed Zircaloy-2 after an exposure of five cycles (2820 hr) in the ex-reactor hot water loop, which was described in the May report, has been found to be due to hydrogen pickup from the water. Results of a recent fusion analysis indicated that the hydrogen content of the specimens had increased from approximately 10 ppm residual hydrogen to 20 ppm. The hydrogen in solution at 280 °C in the ex-reactor loop specimens would appear as hydride platelets of ZrH<sub>2</sub> at room temperature and would cause a large reduction in the fracture toughness.

For the purpose of measuring the instantaneous position of a moving crack tip, a device has recently been developed by the Electronic Measurement Research Unit of Pacific Northwest Laboratory. Basically, the instrument is an eddy current device which employs a very high operating frequency (20 MHz) to provide the necessary band width. The probe is a flat coil mounted in plastic which in turn is tightly taped into position into the side groove of DCB specimens. The active length of the coil is 0.4 inch. As the crack tip moves past the coil, the impedance of the coil changes linearly with crack tip position. By recording coil impedance on an oscilloscope screen while the crack is moving in an unstable and rapid manner, it is possible to determine the instantaneous crack velocity. Because of the high operating frequency, the eddy current which is induced in the metal below the probe extends only a few thousandths of an inch into the metal. Thus, the crack velocity that is measured is that at the very surface of the metal. In operation, the effect of small changes in coil-to-metal spacing is compensated and the instrument is then



calibrated by measuring the probe impedance as a function of position with respect to a machine slot in a DCB specimen.

A typical oscilloscope record of a cracking event indicates mean crack velocities of about 110 feet/sec at room temperature for 7075-T6 aluminum, although instantaneous velocities as high as 750 ft/sec have occurred. One interesting feature of these results is the presence of the sharp spikes which have the appearance of a sudden and rapid increase in crack length followed by a rapid decrease or closing of the crack. These spikes have been found to occur in all the records which have so far been obtained. It is significant that the first spike usually occurs after an elapsed time of about 35  $\mu$  sec, which corresponds to the time of traverse of a longitudinal shock wave from the crack tip to the end of the specimen plus its return to the crack tip. As the stresses associated with a longitudinal wave generated by the sudden propagation of a crack are smaller behind the wave than in front of it, it will reach the free end of the specimen as a compression wave and be reflected as a tension wave. It seems a reasonable speculation that the return of this tension wave to the tip of the crack could cause a surge in the crack velocity, but it is yet difficult to justify the subsequent closing of the crack after passage of the tension wave.

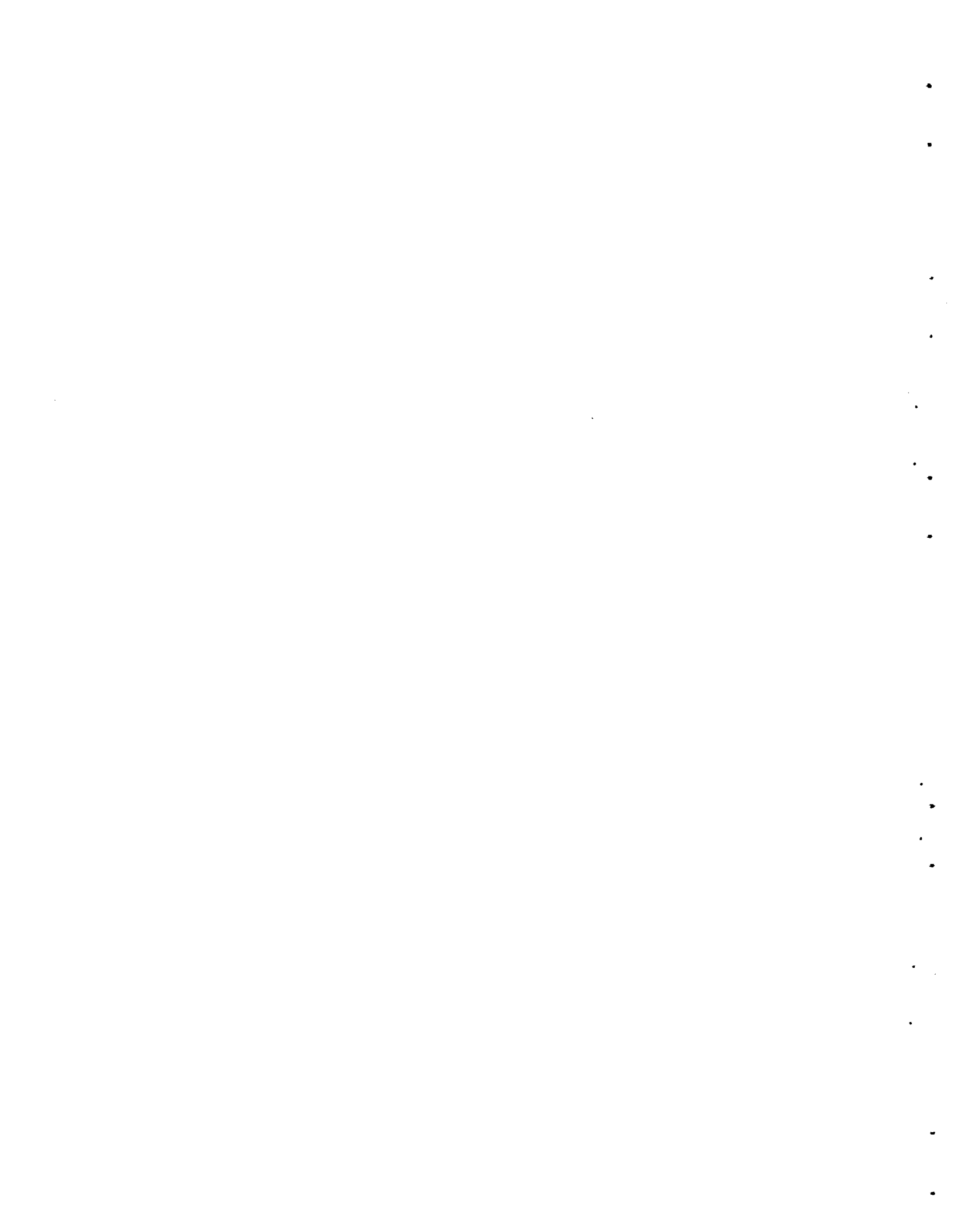
Although these results are very preliminary, the performance of the eddy current instrument has been encouraging. However, before attempting to determine the instantaneous energy absorption rate during a crack propagation event, a detailed analysis must be conducted to interpret the meaning of the crack length spikes discussed above.

### Advanced Metallurgy Studies

#### Fast Neutron Applications

An analysis has been made of the combined aspects of hydrogen and helium behavior in iron and nickel-base alloys. Two of the possible hydrogen-helium damage process interactions that have been identified in this analysis are of particular concern, should there be any tendency for neutronic hydrogen to segregate at, or otherwise interact with, grain boundary regions. Thus, it has been proposed that the continuous, nonequilibrium growth of intergranular helium bubbles under the influence of an applied stress is an essential step in the high temperature helium embrittlement process. The chemisorption of hydrogen on the internal surfaces defined by these bubbles can significantly reduce both the critical bubble size and the critical applied stress required to initiate this unstable bubble growth behavior. At lower temperatures, the growth of cracks formed by the coalescence of intergranular helium bubbles can be enhanced by the embrittling action of hydrogen, and appreciably so for martensitic and ferritic materials.

The general approach and specific experimental procedures required to investigate the intergranular behavior of hydrogen in fast reactor alloys have been developed, and preliminary studies will begin





as soon as the permeation apparatus becomes operational. The effect of grain boundary precipitates and related variations in intergranular composition on the apparent diffusivity of hydrogen will be evaluated using steady-state permeation methods, while dynamic permeation techniques will be used to detect possible temperature-dependent hydrogen-carbide interactions. Particular attention will be given to those austenitic materials whose intergranular regions can, for certain service conditions, become depleted in essential austenite-stabilizing elements and transform to the hydrogen-sensitive martensitic phase.

#### ATR GAS LOOP OPERATION AND MAINTENANCE (G. A. Last)

##### ATR Gas Loop Support

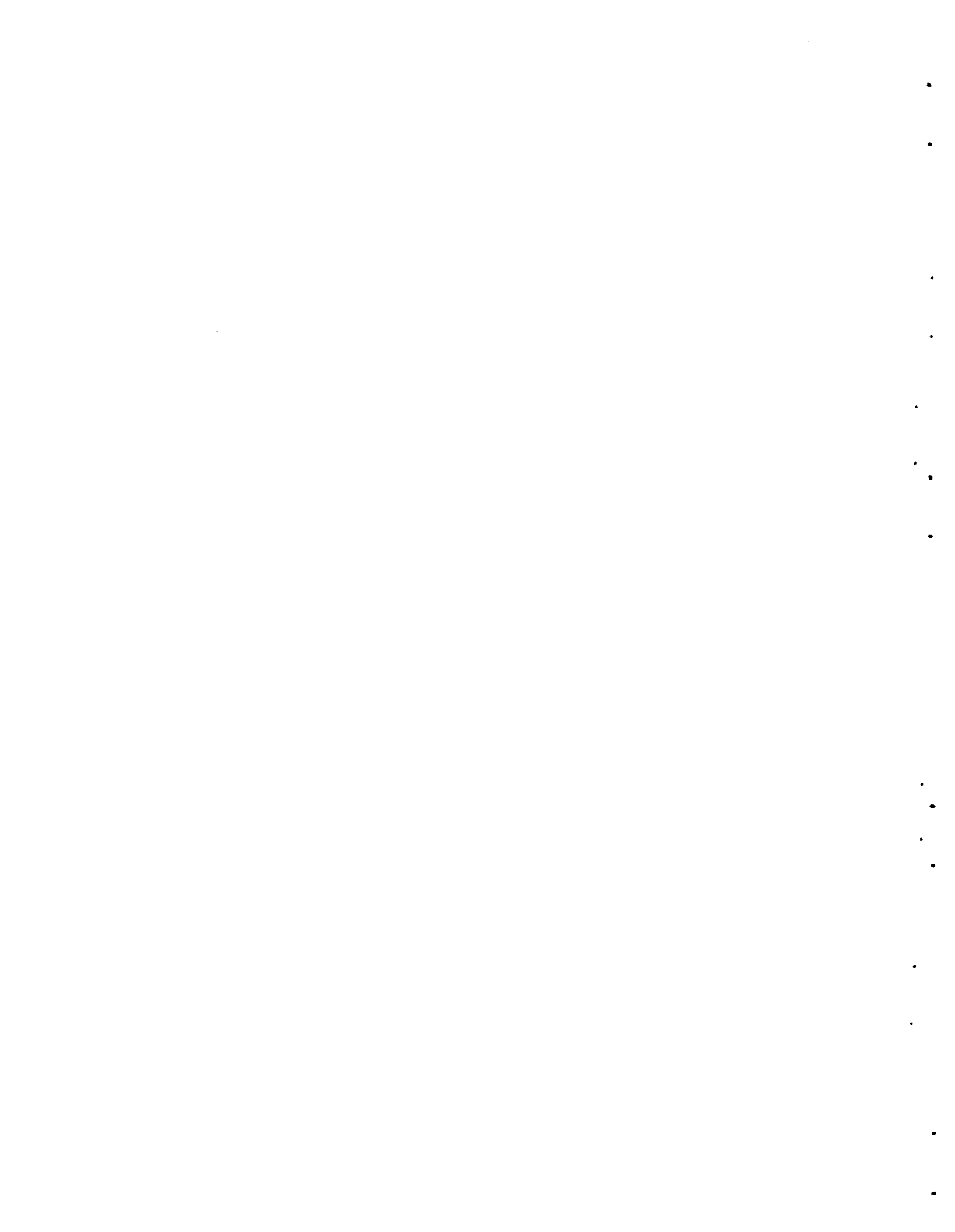
###### Model Gas Loop

The three-shift five-day per week operating schedule for the model gas loop has continued the past month. The extensive testing of the model heater is being done to determine whether or not the design parameters used on the ATR heater will meet the stringent ATR Gas Loop requirements. The testing program for the model heater includes:

1. Operation at various flows and temperatures to determine the heater's pressure drop and heat transfer characteristics. At several flow levels various power ratios between the nichrome and molybdenum heater sections will be run while maintaining a constant outlet temperature.
2. Step power settings to determine the short time transient characteristics of the heater.
3. Thermal cycling to insure the structural integrity during startup and shutdown.
4. Shutdown cycles which are equal to or surpass the most severe temperature shocks anticipated during ATR loop operation, such as reactor scram, loss of all power, etc.
5. Extensive operation at maximum temperature to insure long term reliability.

The model heater has been operated for a total of 683 hours with 21 thermal cycles between room temperature and various heater outlet temperatures. The heater has operated about 60% of the time at an outlet temperature of 2100 °F.

Minor changes were made to improve the loop operation. The dual gas cleanup system was installed and is operating very satisfactorily. With this system one bank can be in operation while the second is being regenerated. A regenerative heat exchanger installed in this system has reduced our liquid nitrogen use rate by 50%. The horizontal test



section was opened this month, and it was found that thermal expansion had caused deformation of the inner liner at a complex "T" joint. The inner liner was removed and replaced with a new section which allows greater expansion without deformation. A minor re-design was made to provide improved alignment of the liners for better gas passage and for easy insertion of test specimens. The flow instrumentation was recalibrated during the same outage.

A rapid temperature cool-down test was made from 2100 °F by turning off the heater power but leaving the compressor in operation. The cool-down rate for the first five minutes of this test was about 510 °F for the outlet gas; the second five minutes an additional 200°; the third five minutes 150°. At the end of one hour the outlet temperature was down to 675 °F.

A second type cool-down test was made by turning off the heater and the circulator. This would simulate a total power failure. The heater outlet gas decreased at the same rate as above, but the ceramic temperature cooled down at about one-half rate observed when just the heater was turned off. Several more of these tests are planned during this portion of the program.

#### ATR Gas Loop Heater

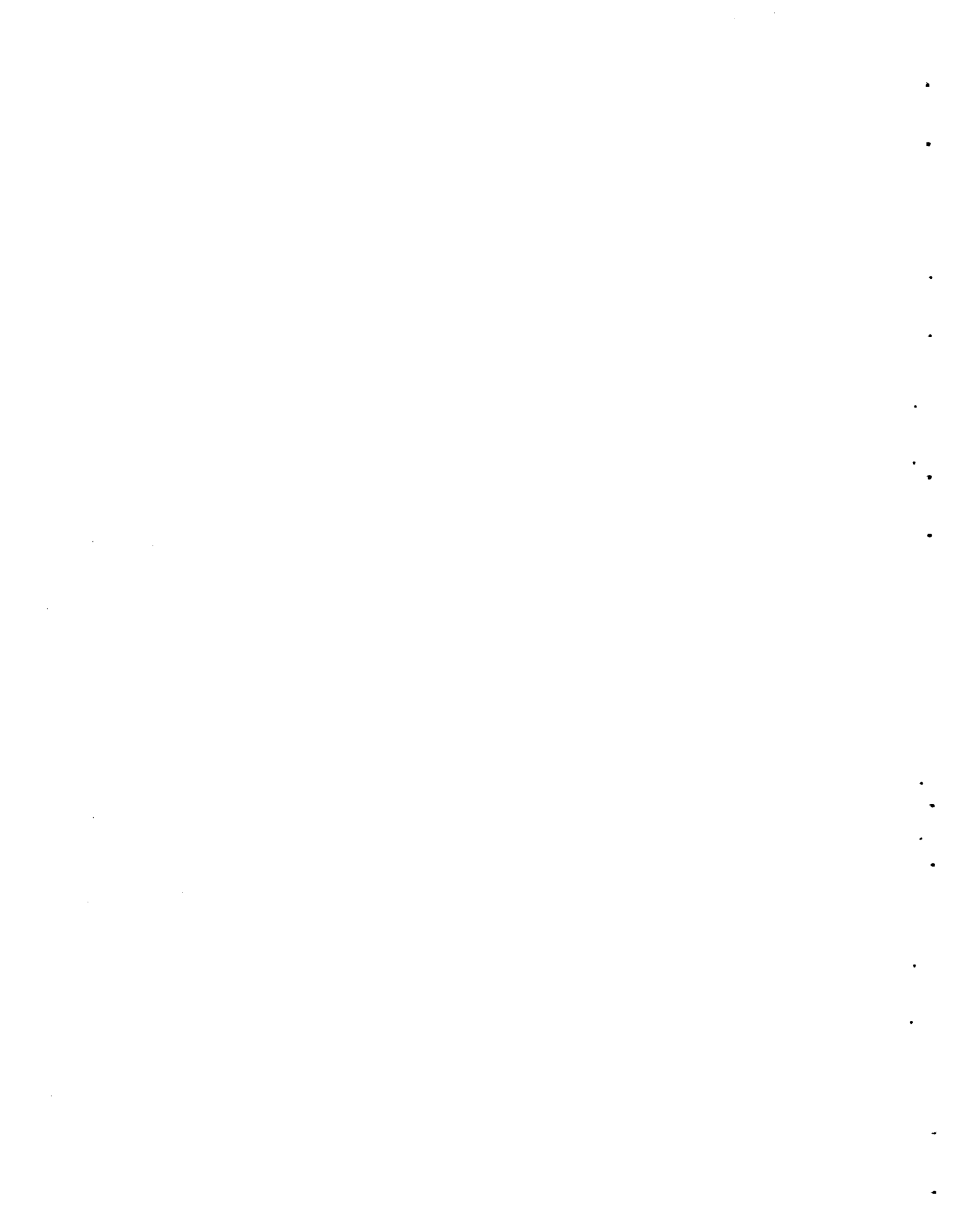
The ATR gas loop heater is being designed to heat helium flowing at a rate of 4140 lb/hr to a temperature of 2100 °F (1150 °C). The heating is accomplished in two stages with electric resistance heating elements. The gas first passes through an annular ring of nickel-chromium tubes, makes a 180° turn, and then passes through a center core of molybdenum tubes. Both tube banks are supported with aluminum oxide ceramic. The heater internals are insulated from the heater shell with metallic foil insulation.

The performance of the ATR gas loop is being simulated with an analog computer by an offsite group. Various constants, which are necessary for this analysis, have been calculated for the heater and transmitted to this group. Among these constants was the thermal response time of the thermocouple wells. A transient heat transfer program, Tiger V, was used to obtain the time constant. Results were obtained for both high and low gas flow rates.

#### Model Gas Loop Heater

##### Metallography of Molybdenum Heating Elements

Metallographic analysis of specimens from the extreme ends of the molybdenum heating elements has been initiated. In cutting samples from the elements, it was quite apparent that material from the outlet end of the heater is more brittle than material from the inlet end. In sectioning a standard element (extra material which was not part of the operational heater), the weld and weld-affected zones around the fin-connector joints exhibited brittle behavior with extensive cracking. Material away from the weld zones could be readily sheared without any visible evidence of cracking.



Samples from a separate lot of molybdenum sheet (thickness comparable to that of heat element material) have been tensile tested at room temperature and at approximately 2500 °F. The gripping employed for the sheet specimens performed satisfactorily at both temperatures. The tensile machine has been calibrated to obtain corrections for the force exerted by the vacuum chamber bellows on the load cell and for the spring constant of the bellows. The first effect can be readily subtracted out, while the second effect was too small to be measurable. Hence, the equipment is capable of giving good results, even at the small loads anticipated for these specimens at high temperatures.

#### Gas-Cooled Loop Vendor Data Review

ATR Gas Loop contract submittals through number 4219 have been reviewed and comments transmitted to Ebasco Services. Major equipment covered in this period includes purification system, handling cask, and transfer facility instruments. A major submittal on the main instrument panel is presently being processed. A review of Ebasco's markup of circulator control circuit data was made and comments submitted.

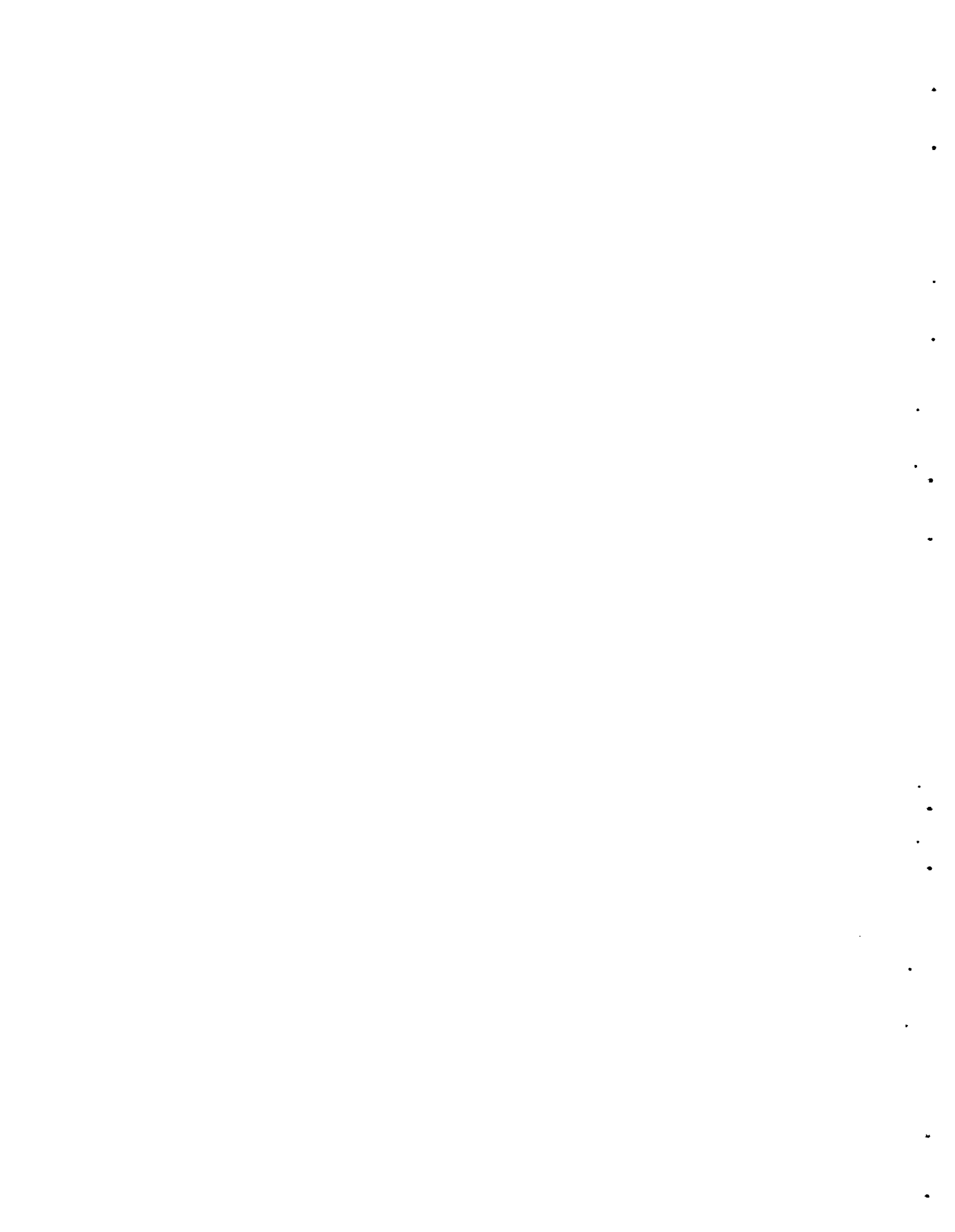
#### Meetings and Inspections

General Electric performed a demonstration of their bearing simulator operation on June 2, 1966. The simulator was operated up to 23,400 rpm and cycled through two dry starts and stops. Prior to the demonstration, more than 100 successful dry start/stops had been performed by General Electric.

#### Shielding Material Compatibility Studies

Iron balls of mixed sizes to give maximum packing density are proposed as the shielding material for the primary ATR gas loop filter. Alternate material choices are the oxides of lead (PbO), tungsten (WO<sub>3</sub>), or uranium (UO<sub>3</sub> or U<sub>3</sub>O<sub>8</sub>). The shielding material may see a temperature as high as 800 °C; however, insulation could decrease this temperature considerably. It is of interest to predict the behavior of the shielding material and associated structural materials at temperatures approaching 800 °C.

Representative samples of the iron balls were exposed to three conditions near 800 °C: high vacuum, flowing grade A helium and air at atmospheric pressure. Light sintering of the balls took place after a four-hour exposure to high vacuum at 780 °C. The ball compact was easily broken apart, and the balls showed no visual sign of deformation. After exposure to flowing helium at 800 °C for four hours (minimal oxidizing conditions), the balls showed a slight tarnish film and were not stuck together. In air at 800 °C and also exposed four hours, the balls were again in a sintered compact. Gross oxidation occurred and apparently aided in the sintering process. The kinetics of sintering would probably be increased by increasing the weight of the ball mass.



### Gas Chromatograph - Total Impurity Analyzer

The BNW gas chromatograph was developed further into an automatic model that performed high sensitivity gas analyses on the model gas loop. Impurity detection limits were consistently below 1 ppm, and the unit continued to operate reliably during the last nine months of the fiscal year with essentially no maintenance.

The novel features of the BNW instrument were built into an industrial process chromatograph by Greenbriar Instruments. The Greenbriar Chromatograph and a modified version for total impurity analysis were delivered to BNW in June for further testing on the model bop prior to installation on the ATR Gas Loop. Tests at the Greenbriar plant confirmed the sensitivity factors obtained at BNW. It now appears a commercial market is developing for the industrial chromatograph built by Greenbriar.

### METALLIC FUELS DEVELOPMENT (J. E. Minor)

#### Irradiation of Thorium-Uranium Fuel Elements

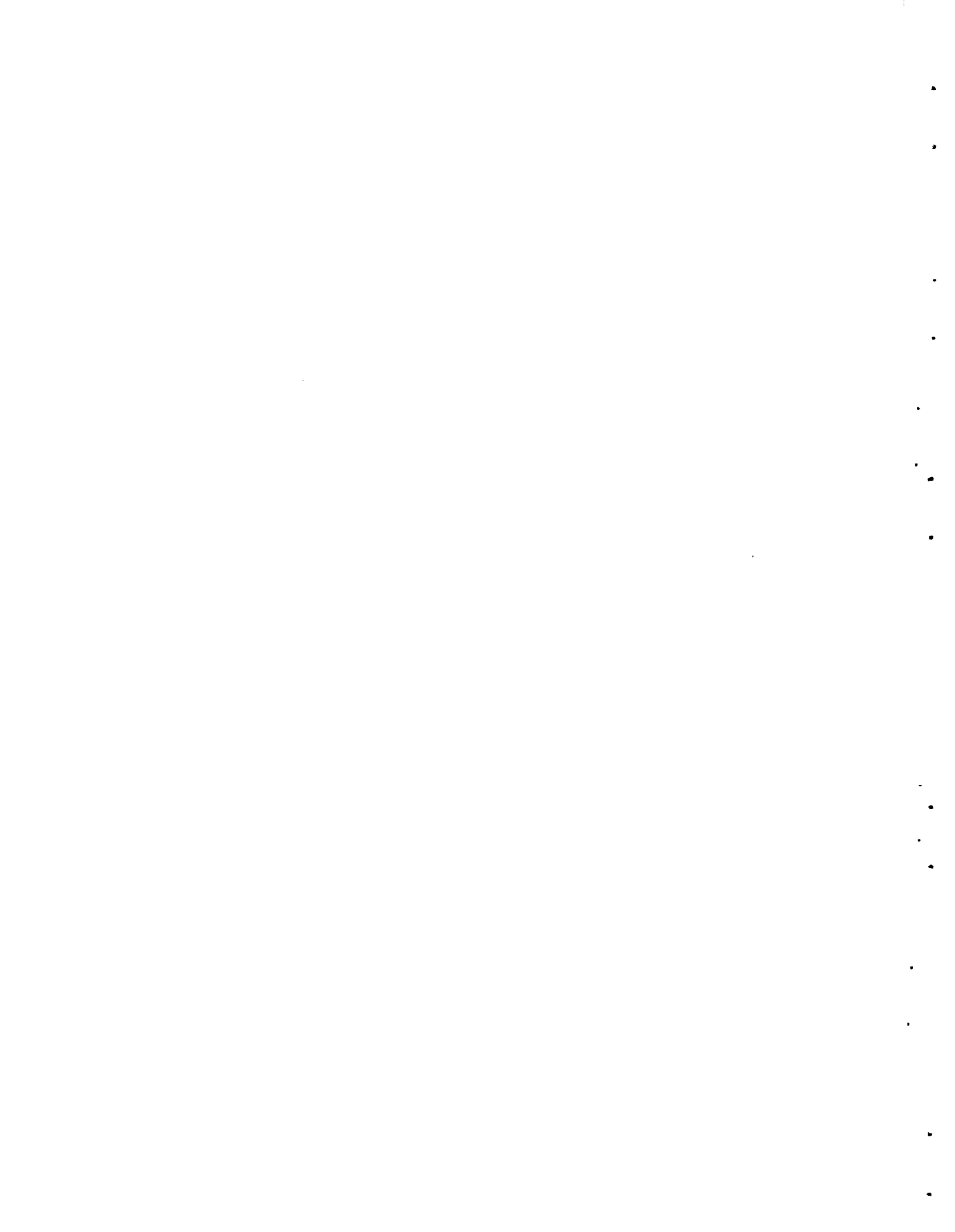
Three tubular Zircaloy-2 clad thorium 2.5 wt% uranium, 1.0 wt% zirconium fuel elements are being irradiated this cycle in the ETR P-7 loop. The highest exposure fuel element is currently operating at a maximum core temperature of 465 °C and at the end of the current cycle will have accumulated approximately 14,500 MWd/ton. The element showed a fuel volume increase of 2.3% at the end of the last cycle. This volume increase is slightly greater than that required to accommodate the solid fission product atoms.

One element, diverted from the irradiation testing, was returned to the Pacific Northwest Laboratory and was defect tested in a high temperature, high pressure, water loop (IRP Facility of Corrosion and Coolant Chemistry). Examination of this element after removal from the IRP loop is continuing in Radiometallurgy.

#### High Exposure Uranium Irradiation Test

Results from the irradiation of uranium metallic fuel to date have demonstrated that swelling of the uranium places restrictive limits on the temperature and burnup that can be achieved in a reactor fuel element. Irradiation studies have shown that uranium swelling can be reduced significantly by appropriate alloying of the uranium and by external restraint. It has also been observed that under irradiation uranium takes on plastic characteristics such that it flows under small applied loads.

A fuel element irradiation test is being designed which capitalizes on these known characteristics. The test fuel specimens will be designed to operate successfully at high temperatures to burnup greater than 10,000 MWd/ton. The fuel rods will be clad with various thicknesses of Zr-2 ranging from 0.025" to 0.050". A void of 10% or





more of the fuel volume will be provided in the center of the uranium core. The combined effect of the uranium plasticity and the restraint from the cladding will cause the uranium swelling to be accommodated by the central hole. Two uranium compositions will be used in the test--U + 350 ppm Fe + 800 ppm Al and U + 150 ppm Fe + 100 ppm Si. Primary extrusion of the alloy billets has been completed. The extrusion conditions are:

	<u>Alloy</u>	<u>Die</u>	<u>Preheat</u>	<u>Extrusion Reduction</u>
#1	350 Fe-800 Al	2.210	3 hr, 620°C	3.4:1
#2	150 Fe-100 Si	2.250	4-1/2 hr, 620°C	3.3:1

Coextrusion components were designed and fabricated and assembly of the coextrusion billets has been completed. Irradiation is planned to begin in the ETR-M3 water loop by August 15, 1966, and an exposure of 10000 MWd/ton is expected by August 15, 1967, on the higher power generating specimen.

#### Chemonuclear Fuel Development

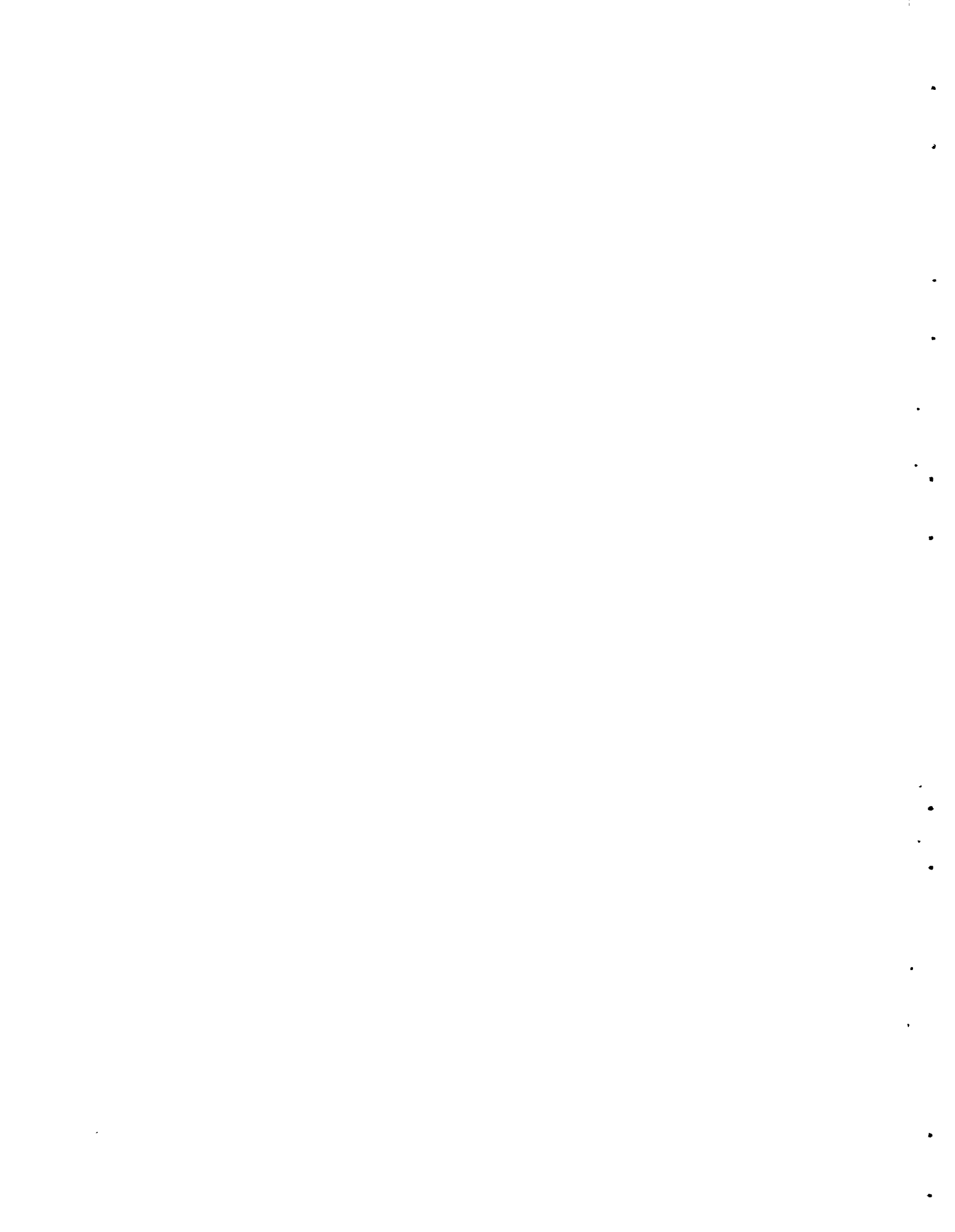
Vacuum evaporations of platinum, palladium, and uranium have been proceeding to evaluate the effects of temperatures, power levels, bakeout cycles, substrate speeds, and deposition rates on the coatings of sample rods. Nearly all parameters for optimum plating cycles have been determined. The length of the bakeout cycle required has restricted the plating cycles to one cycle in an eight-hour day and two cycles in approximately 11 hours. Original plans called for the plating of a batch of rods with all coatings in a single plating cycle. Due to variations in deposition rates over long cycles and the critical coating thicknesses required, a more tedious method involving a minimum of four plating cycles per batch of rods will be necessary to ensure proper coatings and uniformity.

### ENGINEERING DEVELOPMENT

#### NEUTRON FLUX MONITORS (G. C. Fullmer)

##### Regenerating Detectors

Satisfactory experimental data are being obtained with the two developmental (U<sup>234</sup>-U<sup>235</sup>) regenerating in-core neutron flux detectors installed in a test facility of the KW-Reactor. For these detectors, the contained U<sup>234</sup>, originally equal to 90% of the total coating employed, transmutes, by thermal neutron capture, to fissile U<sup>235</sup>; this process serves to retain relatively constant detector sensitivity for very long exposures. Review of the data obtained to date indicated that a second series of tests, using new chambers, would be required to better define the operational characteristics and to insure that the established concepts could be exploited on a commercial basis.



In view of this planned further testing effort, specifications were prepared and sent to representative manufacturers for rapid procurement of matched sets of detector chambers with integral cable assemblies. All chambers will be physically identical except for the coatings employed. Standard manufacturing techniques will be used in all cases to assure the eventual adaptation of the regenerating concept for commercial use. Each chamber will be of 0.25-inch diameter with a triaxial cable attached. Two chambers will not employ fissile material coating on the electrodes, two will be standard-form enriched  $U^{235}$  coated units, and three will utilize the established regenerating coating mixture of approximately 90%  $U^{234}$  and 10%  $U^{235}$ . These detectors will be tested in the laboratory and then inserted, as a compact assembly to assure similar exposure, into a suitable test facility.

Theoretical considerations were continued regarding extension of the regenerating concepts to the measurement of fast neutron flux.

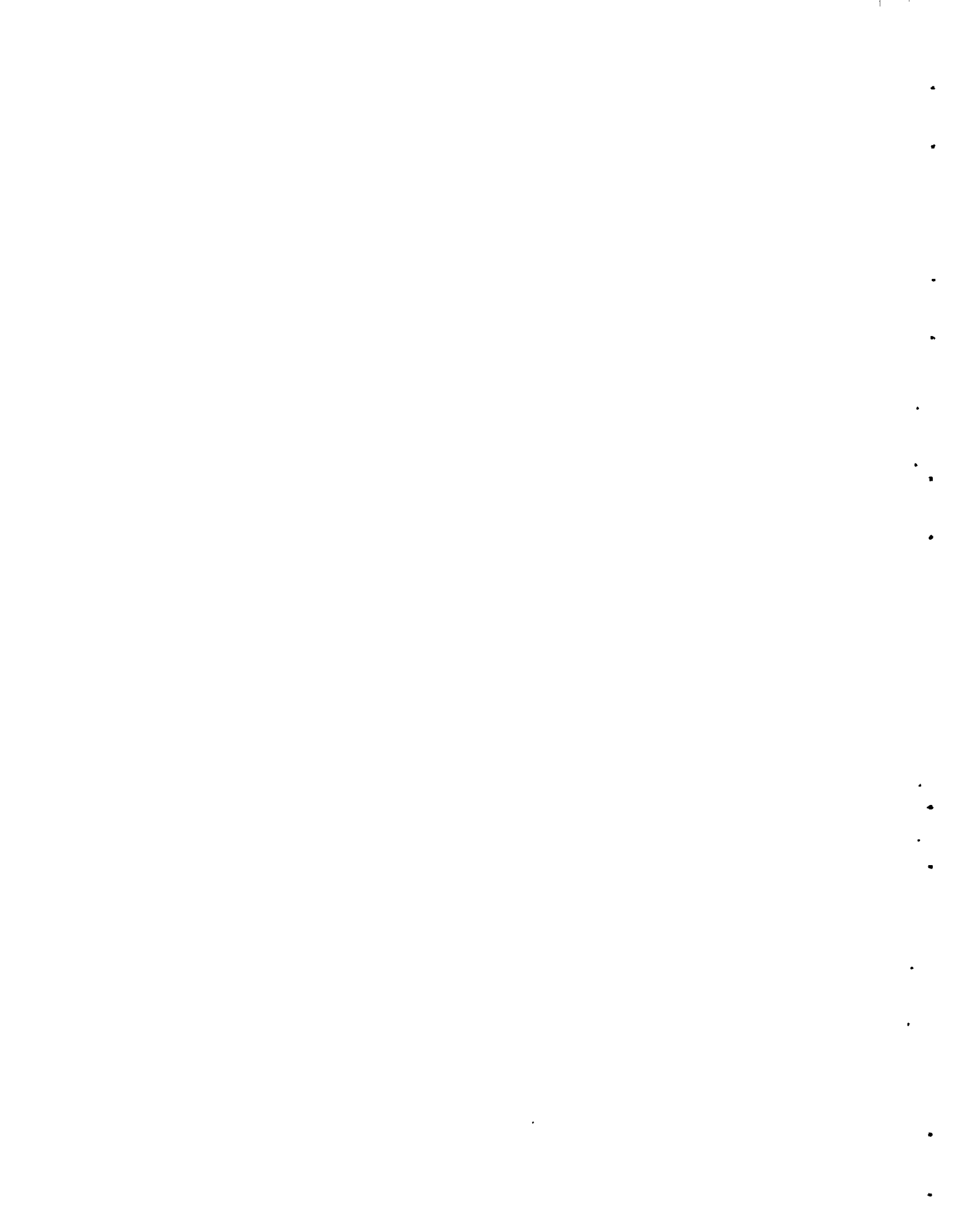
#### Beta Current Generator Detectors

A second experimental dual-chamber, twin-lead beta current generator detector assembly was fabricated, where one chamber uses boron-11 and the other contains carbon, on an electron-balanced basis. This twin method, which demonstrated promise for the first experimental assembly, is an improved approach which should provide nearly equal gamma response with each chamber. Thus, subtraction of the generated electrical currents is expected to yield a net current that is directly related to the in-core neutron flux, where the neutron flux-caused current is generated during decay of  $B^{12}$  (created by thermal neutron capture in the  $B^{11}$ ) to  $C^{12}$  with emission of 13.4 MeV betas with a half-life of about 20 milliseconds.

After laboratory tests and high level  $Co^{60}$  gamma tests, to about  $5 \times 10^6$  R/hr, are completed, the assembly will be inserted into a reactor test facility for in-core experimentation. Although the low thermal neutron cross section of boron-11 (about 5 millibarns) provides the generation of electrical current in the range of only about one nanoampere per  $10^{13}n \text{ cm}^{-2} \text{ sec}^{-1}$ , this cross section insures an extremely constant sensitivity during in-core exposure. This constant sensitivity, coupled with the fast response time inherent in the 20 millisecond half-life of  $B^{12}$ , can conceivably provide a useful in-core neutron flux detector, worthy of commercial exploitation, without the need for computer response-adjustment programs. In addition to the described thermal flux studies, theoretical considerations were pursued regarding the extension of the beta current generator concepts to fast flux measurements; candidate isotopes are being explored.

#### Microwave Detectors

Difficulties are still being encountered in the development of a satisfactory sealing technique for use with the in-core microwave resonant cavities. An appropriate seal will permit elimination of



the internal quartz capsule, now used to contain the gas samples. Considerable improvement of system sensitivity for in-core neutron flux measurement, where microwave phase shift techniques are utilized, would then be expected on the basis of tests to date. Alumina sealed waveguides are being procured, and soldered glass seals are being investigated, to aid in achieving the desired physical assembly.

MICROWAVE AND INFRARED DETECTION OF COOLANT IMPURITIES AND MEASUREMENT OF IN-REACTOR TEMPERATURES (G. C. Fullmer)

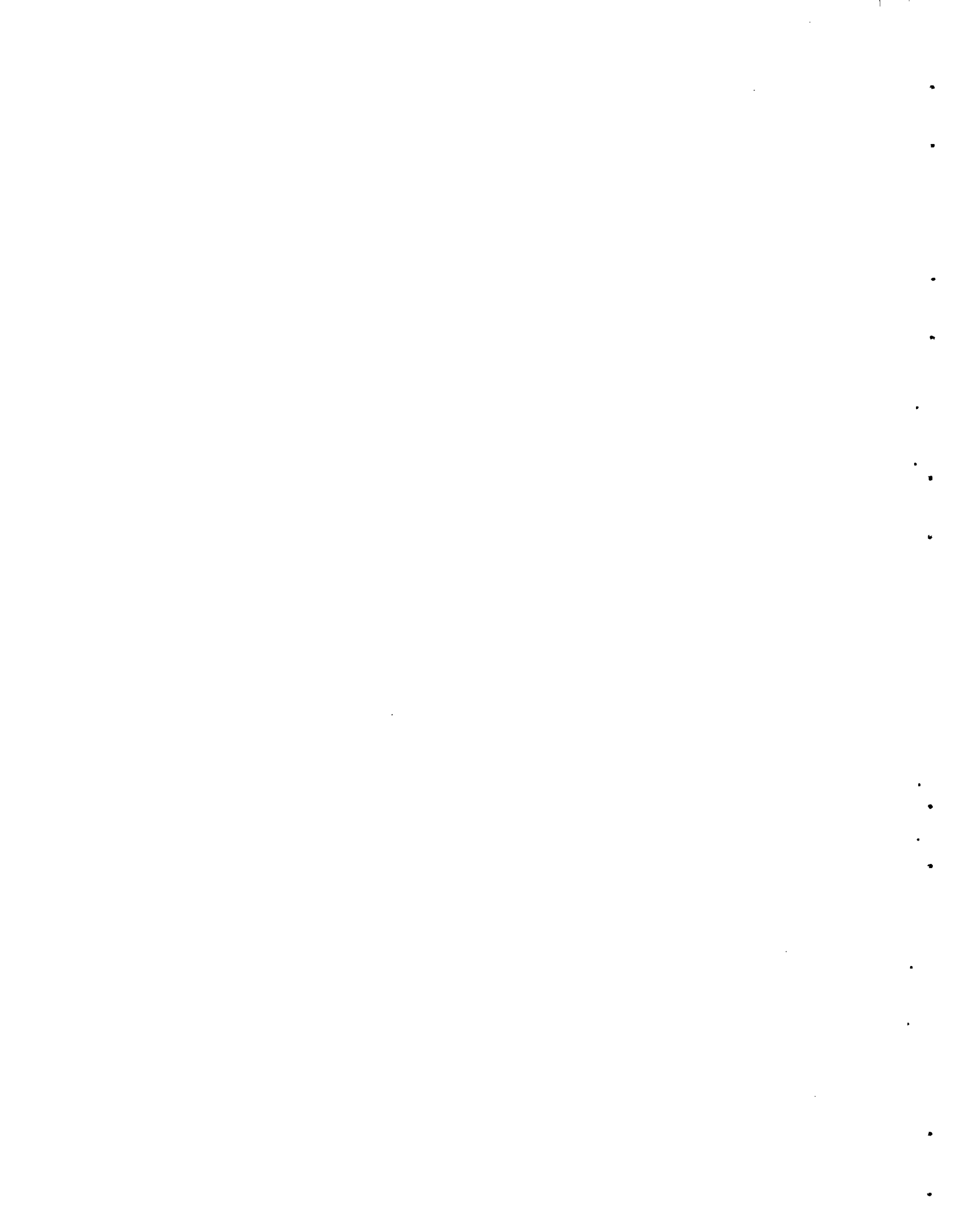
Microwave Techniques

Further tests utilizing microwave frequency shift methods demonstrated modest further stability improvement for moisture-in-gas detection levels in the range of 700 ppm. Consideration of the problems involved indicates that further electronic circuitry stability improvements will be required before the anticipated sensitivity of about 70 ppm can be achieved. Theoretical considerations of the dielectric properties of water and water vapor were continued in an effort to achieve a better understanding of the usefulness of microwave techniques for measurement of moisture in reactor coolant gases, especially at the elevated temperatures expected in the planned applications.

Infrared Techniques

Satisfactory operation is being achieved with the rotating filter wheel mechanism, developed for use in the absorption hygrometer. Previously, attempts had been made to employ single layer germanium filter films with optical thicknesses equal to 1.5 times the central wavelengths of the particular infrared passbands of interest. Although some water vapor sensitivity was noted, the passbands proved to be excessively broad. The new rotating filters were made by depositing a multilayer dielectric coating of the form HLHHLH on a glass substrate, where H represents a quarter-wave optical thickness germanium and L represents the same optical thickness of silicon dioxide. Two opposite quadrants on the filter wheel have a passband peaking at 2.65 microns with a width at half-maximum transmission of 0.05 micron. The peak transmission is 85% and coincides with a specific water absorption band. The other two opposing quadrants of the assembly peak at 2.42 microns, with other characteristics very similar to those of the 2.65-micron quadrants. Since no water vapor absorption occurs at the 2.42-micron wavelength, this passband is used to generate a reference signal against which the signal at 2.65 microns may be compared.

In further development on the filter assembly, a compensating wedge filter, which is driven by a servo motor and discriminates against one of the two (2.42- or 2.65-micron) passbands, was also fabricated. This filter is made in the form HLHLH with optical thickness varying across the unit. Filters with desirable features have been produced; however, further improvements in sensitivity can be anticipated with revision of the filter design or change in type of detector.



PLUTONIUM RECYCLE PROGRAM (F. G. Dawson)FUELS DEVELOPMENTPRTR Fuel Element Performance

Beta-gamma and alpha-autoradiographs of a longitudinal section of the bottom end region of rod FB-06 from FE-6504 indicated higher activities in the once-molten fuel region of the UO<sub>2</sub> - 1 wt% PuO<sub>2</sub> graded enrichment zone than in the surrounding nonmolten fuel.

Examination of the beta-gamma autoradiograph revealed that the centrally located dark region on the autoradiograph coincides with the well defined cellular or as-cast-appearing structure outlining the once-molten fuel region on the photomosaic.

The boundary of the centrally located dark region on the alpha-autoradiograph, which chemical analysis showed to contain 4 wt% PuO<sub>2</sub>, is more diffuse and lies beyond the well defined cellular region on the photomosaic. These comparisons indicate that plutonium diffused into the UO<sub>2</sub> - 1 wt% PuO<sub>2</sub> fuel region beyond the liquid-solid interface and that the centrally located dark region on beta-gamma autoradiographs probably defines the extent of the molten fuel region at the time of shutdown.

Plutonium Characterization Studies

Gamma energy spectra above 50 KeV have been obtained from the three Shippingport fuel elements utilizing a lithium-drifted germanium detector system. Determination of the spectra below 50 KeV will be made upon receipt of a silicon-drifted germanium detector. No significant quantities of photo peaks have appeared above 400 KeV with the exception of Cs<sup>137</sup> at 662 KeV, indicating that fission product carry-over will not cause excessive interference.

Tentative identification of the isotopes present has been made utilizing the existing spectrograms. Those isotopes present are U<sup>237</sup>, Am<sup>241</sup>, and Pu<sup>238</sup> thru <sup>242</sup>. Gamma spectroscopy is not a positive identification, and the final assay will be determined by the Analytical Chemistry Laboratories of the Chemistry Department.

The three plutonium samples are in the form of plutonium nitrate solutions which have concentrations varying from 10 to 12 grams of plutonium per liter. Small samples were withdrawn from each of the solutions, diluted and this dilution used to make sources of approximately  $5 \times 10^4$  dpm of plutonium activity. Spectrograms of these sources will be obtained and, utilizing the final assay data, relative yields of the individual photo peaks will be determined. This technique should eliminate any self-absorption within the source.

The surface and nonsurface dose rates of the 10 to 12 grams of Pu/l solutions will be measured. It will not be possible to extrapolate the results to higher concentrations because of the self-absorption that takes place within these relatively dilute solutions. Ordinarily, concentrations are in the range of 100 to 400 grams of Pu/l of solution.





RESOLVED\* PHOTO PEAKS OF PLUTONIUM  
SEPARATED FROM SHIPPINGPORT REACTOR FUELS

<u>Energy, KeV</u>	<u>Isotope</u>
43.8	Pu-238, Pu-242
52	Pu-239
60	Am-241
95	Ce-144
98	Pu-238, Am-241
100	Pu-238, Am-241 and possibly Cm-242 & 244
112	U-237, Am-241
114	U-237, Am-241
117	Unknown
129	Am-241
148	Pu-241
164	U-237
206	Pu-239, U-237
265	U-237
329	U-237, Am-241

\*Resolution at 60 KeV is 2.8 KeV FWHM.



### FERTF Test Element Design

A special FERTF test element is being designed for irradiation experiments at rod power generations as great as 30 kw/ft during the High Power Density Program. The basic design consists of a basket assembly containing a six-rod-ring of Mark I-R  $UO_2 - PuO_2$  fuel rods. A prototype stainless steel basket tube with six full length spacing ribs was completed. Charge-discharge tests in the EDEL-1 test loop are scheduled for July. The use of boron stainless steel for the basket tube, to allow higher plutonium enrichment in the fuel, is being studied.

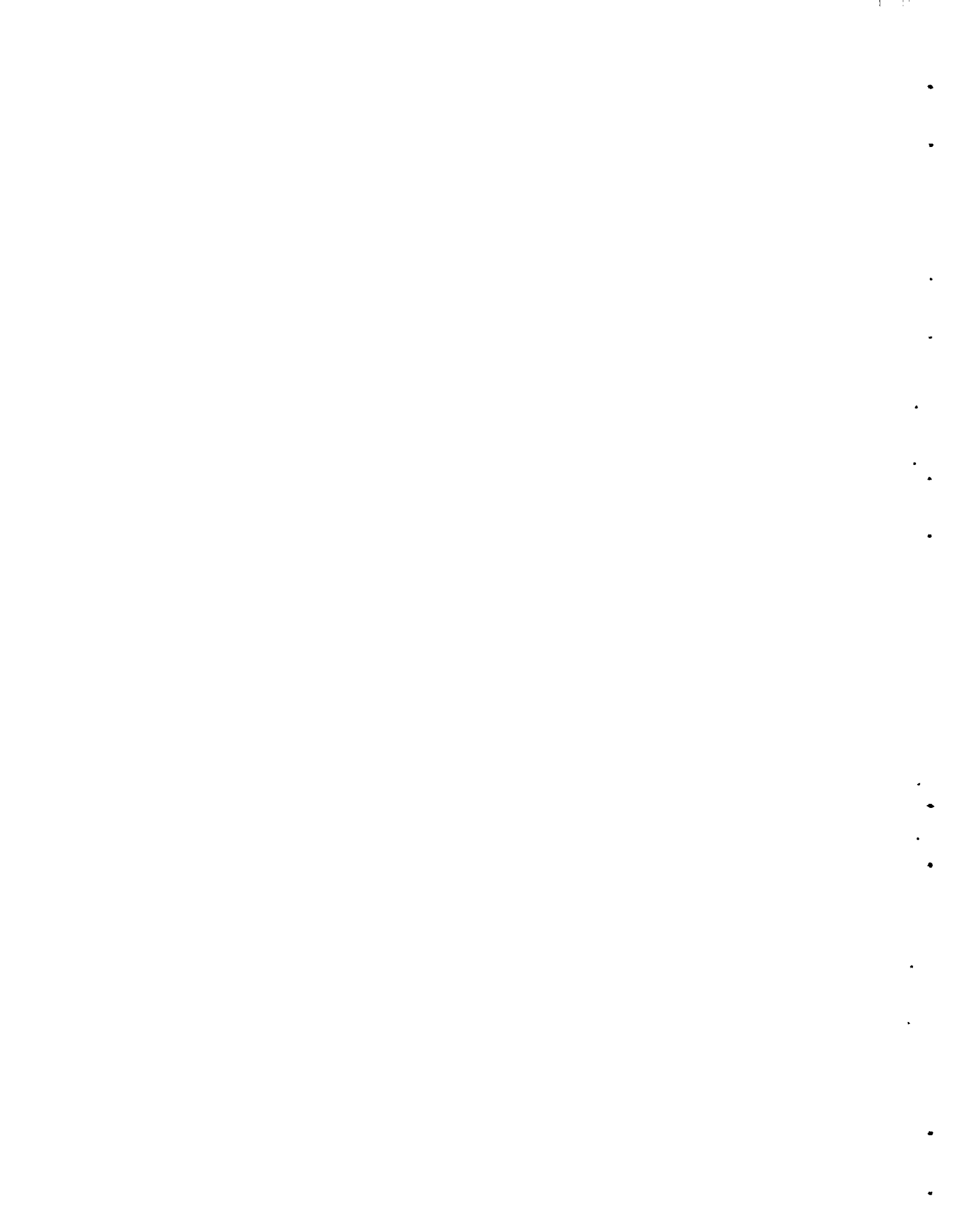
### Heat Transfer Calculations Concerning Fuel Element Basket for FERTF

Calculations were continued to determine temperatures in the FERTF (Fuel Element Rupture Test Facility) pressure tube if it is assumed that fuel is released from a fuel rod and that the hot fuel deforms the protective basket until it contacts the pressure tube. Calculations were made for one new case, with the fuel enclosed in a grooved basket. More detailed evaluations of three previously studied cases for ribbed baskets were made to obtain specific numerical data.

The calculations assume that a strip of fuel approximately 0.5 inch thick, 0.5 inch wide, and indefinitely long is in perfect thermal contact with the basket. The four cases which have been studied are:

1. Fuel contacting the 1/8 inch thick basket at a location where it has no supports between it and the pressure tube.
2. Fuel contacting the 1/8 inch thick basket at a location opposite a 1/8 inch thick rib between the basket and the pressure tube.
3. Fuel contacting the 1/8 inch thick basket at a location opposite a 1/16 inch thick rib between it and the pressure tube.
4. Fuel contacting a basket which is 1/4 inch thick with 1/8 inch deep axial grooves 1/8 inch apart around the circumference of the basket.

The calculations for the first case show that if perfect thermal contact between the basket and pressure tube is assumed, the maximum average temperature across the tube would be about 2100 °F (1150 °C). However, more realistic values of the thermal contact give temperatures of 1200 to 1500 °F (650 to 815 °C). At these temperatures, a Zircaloy pressure tube would be expected to fail; a Hastelloy pressure tube would be expected to have a time-to-failure of several to an indefinite number of hours.



The second case gives maximum basket temperatures of 735 °F (380 °C). At this temperature, either a Zircaloy or Hastelloy pressure tube would be expected to have an indefinite life.

The third case gives maximum basket temperatures of 890 °F (480 °C). At this temperature, a Zircaloy pressure tube would have a time-to-failure on the order of 10,000 hours and a Hastelloy pressure tube would have an indefinite life.

The fourth case gives maximum temperatures of 738 °F (380 °C) if coolant is maintained in the grooves. Either a Hastelloy or Zircaloy pressure tube would be expected to have an indefinite life at this temperature. However, if one of the grooves should become blocked so that the coolant flow were stopped, the pressure tube maximum temperature would be expected to increase to 1370 °F (740 °C). At this temperature, a Zircaloy pressure tube would be expected to promptly fail and a Hastelloy pressure tube would have a time-to-failure on the order of 1000 hours.

#### PRTR Fuel Rod Pressure Test

Fabrication, assembly, and nondestructive testing of the components for the fuel rod internal gas pressure sensing test in PRTR are proceeding on schedule. The test is designed to measure the operating gas pressure and temperature in the plenum regions of six fuel rods. Three 19-rod clusters each containing two rods with pressure sensing attachments will be assembled this month. Two of the elements contain UO<sub>2</sub> - 2 wt% PuO<sub>2</sub> fuel and one contains ThO<sub>2</sub> - 5 wt% PuO<sub>2</sub>.

#### Mark I-R Flux Wire Element Test

A Mark I-R high power density fuel element with an attached flux wire successfully completed flow testing in the EDEL-1 test loop. This special design, scheduled to be used in the Batch Core Experiment in the PRTR, includes a stainless steel clad aluminum-cobalt alloy flux wire extending the full length of the element. Thirteen circumferential bands hold and position the wire along the outside of the fuel element. After completing four weeks of operation in the EDEL-1 test loop under PRTR conditions (140 gpm coolant flow, 1050 psi pressure, and 510 °F coolant temperature), the element was found in perfect condition. The design is now considered acceptable for the PRTR.

#### FUELS REPROCESSING DEVELOPMENT

##### Optimum Reprocessing Plant Study

Work on the study to define economically optimum reprocessing plant size was continued. Three different demand projections have been defined representing situations where a reprocessor would capture a small, moderate, or major portion of the total market based on current nuclear power growth projections. It is necessary to express these



demand projections mathematically, and several different equation forms have been tested to find one that fits the situation. An expression of the form  $D = k a^{bx}$  was found to provide reasonably good curve fitting and will be used.

The method being used to define optimum plant size involves a minimum cost calculation for a specific series of capacity additions over a specified period of time and then selecting the number of capacity additions that result in the lowest "present value total cost." In the course of the calculation the size of each increment of capacity is calculated with the first increment being the one of the most interest. The calculations require finding solutions to a series of nonlinear simultaneous equations with a trial and error procedure. Assistance of the Mathematical Analysis Section of the Mathematics Department has been obtained to develop a computer program to solve this problem. The basic program has been prepared using equations based on a simplified expression of the growth rate of nuclear power and is being debugged. After debugging, the more complex expression for the growth rate will be substituted. The program should be ready for use early next month.

## REACTOR PHYSICS

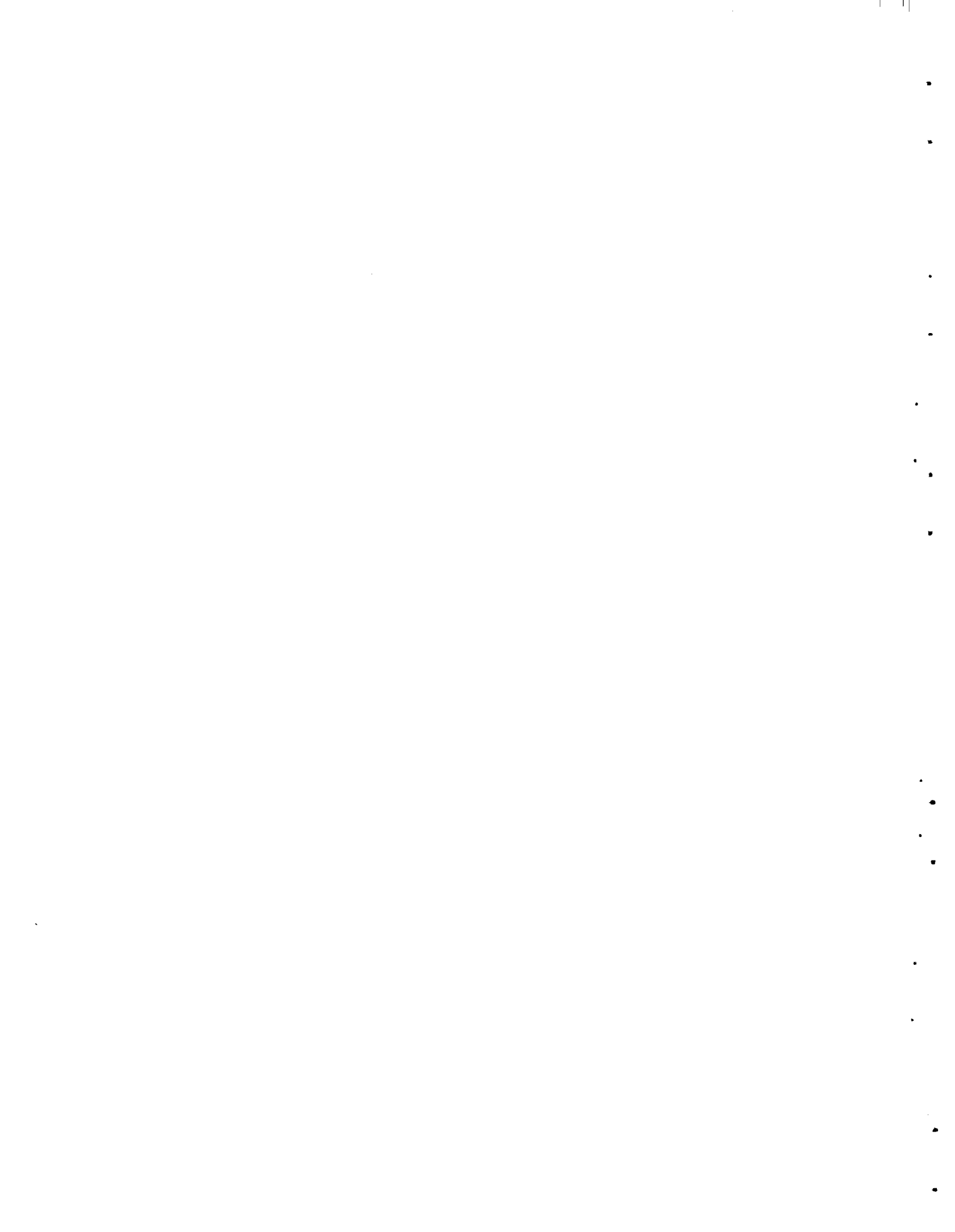
### D<sub>2</sub>O Moderated Systems

#### Photoneutron Effects on the Delayed Neutron Fraction

A problem in the calculation of delayed neutron fractions for systems cooled or moderated by deuterium is the determination of the effect of the neutrons produced by the  $\gamma$ -n reaction in deuterium. Gamma rays are emitted in the decay of fission products and these in turn, through the  $\gamma$ -n reaction, produce delayed neutrons which are added to those produced during the fission product decay.

Experimental measurements of the delayed neutron fractions and inverse lifetimes exist for a point source of fuel in an infinite media of deuterium. To apply this data to a realistic system, one must estimate the efficiency of the system in producing in the deuterium gamma rays with an energy above the threshold for the ( $\gamma$ -n) reaction relative to a point source in an infinite media of deuterium.

The first known attempt to compute this effectiveness in a rigorous manner with modern computers and transport theory methods is now in progress. The calculation has been completed for a 2 wt% PuO<sub>2</sub> 19-rod cluster in the PRTR. Results show that a deuterium cooled and moderated cluster is 28.06% as effective in producing gamma rays in deuterium as is a point source. If the cluster is cooled with light water and moderated with deuterium, the cluster is only 17.58% effective in producing gamma rays with an energy large enough for the ( $\gamma$ -n) reaction. For the deuterium moderated and cooled system this gives rise to about a 5% increase in the effective delayed fraction for the PRTR. Various other fuel assemblies including a Pu-Al 19-rod cluster will also be evaluated.





### Kinetics Studies\*

Reactor oscillation and noise experiments have been conducted in the Plutonium Recycle Critical Facility to obtain transfer function information under simulated PRTR operating conditions. A rotating neutron poison was the primary driving function while the moderator level was caused to fluctuate at a constant frequency. Analysis of the data is complete. The ratio  $\beta/\lambda$  of the delayed neutron fraction for both the oscillator data and noise data was obtained by fitting the analytic transfer function to the data by the method of least squares. The results are:

<u>Experimental Conditions</u>	<u><math>\beta/\lambda</math></u>
Rotating oscillator without moderator level fluctuations	10.7 $\pm$ 0.4
Rotating oscillator with moderator level fluctuations (simulated PRTR)	10.9 $\pm$ 0.3
*Noise analysis without moderator level fluctuations	12 $\pm$ 1
Noise analysis with moderator level fluctuations	Undeterminable

\*28 HPD elements instead of 27 HPD plus 11 Pu-Al elements as for the other determinations.

The results of the oscillator measurements were independent of whether the moderator fluctuations were present or not and were more accurate than the noise results. Also, the results from both the phase and amplitude data of the oscillation experiment were in agreement. Thus, it is concluded that the oscillator method should be well suited for transfer function measurements in the PRTR in the presence of extraneous noise signals.

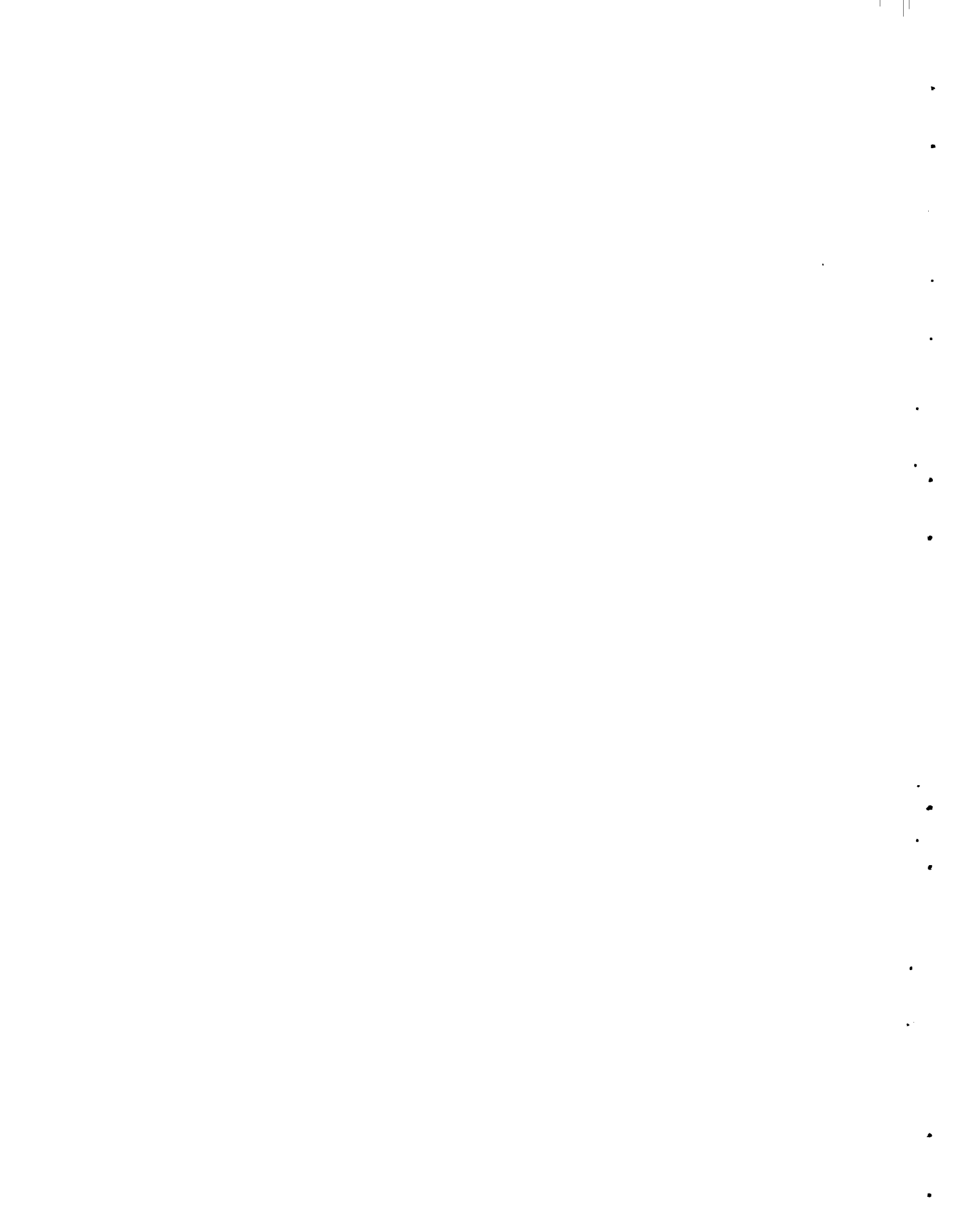
### HPD Core Experiment in the PRTR

Analysis of experiments performed in the Plutonium Recycle Critical Facility (PRCF) has continued. A series of calculations using computer code SWAP has been made to determine fuel element worths and kinetics parameters. Evaluation of these calculations is not yet complete.

Reactor noise data have been obtained from three magnetic tape recordings using the 10 channel noise analyzer. One of these recordings was made with the moderator level oscillating. The other two were made with 4.8 and 11.0 ppm B<sup>10</sup> in the moderator. Analysis of the data from the two experiments with various amounts of boron is about 50% completed.

---

\*This work is in partial fulfillment of the requirements for a M.S. Degree from the University of Washington.



A paper summarizing the analytical and experimental results of the HPDC experiment in the PRCF has been prepared and submitted for presentation at the 1966 Winter Meeting of the American Nuclear Society.

New calculations on the Fuel Element Rupture Test Facility (FERTF) have been made at the request of the Fuels Development Section of the Materials Department. These calculations determined the power generation rate in the FERTF with a Zircaloy process tube and a borated stainless steel basket. The problem of boron burnup was also investigated.

A reactor physics section for the FERTF Safeguards Analysis has been written and submitted to the Nuclear Safeguards and Engineering Section of the Environmental Health and Engineering Department. This section was based on analytical results, in conjunction with PRCF experiments.

Work has continued in the planning of tests in the PRTR. Details of lutetium and gold foil irradiations have been planned. The scope of the approach to power experiments has also been established.

Calculations have been begun to derive reactivity vs period curves for the High Power Density Core (HPDC) in the PRTR. These curves are being calculated as a function of boron concentration in the moderator.

#### Boron Concentration Measurements

Determination of  $B^{10}$  content of solutions of boric acid in  $D_2O$  has begun in the Thermal Test Reactor. The reactivity of standard solutions of known concentration has been measured to obtain a graph of reactivity worth versus boron concentration. These standard samples varied from 1 ppm to 25 ppm  $B^{10}$ . The data will be used to determine the boron concentration of the samples that were taken during the HPDC experiments in the PRCF and the samples to be taken during the PRTR operation with the HPD core.

#### PRCF Operation

A description of the experimental program planned for PRCF with a light water moderated, 2%  $PuO_2 - UO_2$  core was prepared and forwarded to the Commission. Safeguards review of the experiments showed no need for a supplement to the Safeguards Analysis Report nor for revisions to the operating specifications.

The  $D_2O$  to  $H_2O$  conversion was successfully completed in 17 operating days. The present core arrangement is for 1/2" x 36" long fuel in a 0.85" pitch. Two series of experiments using 2 wt% Pu mixed oxide fuel were performed: (1) uniform 8%  $Pu^{240}$ , and (2) 8%  $Pu^{240}$  in the inner zone and 24%  $Pu^{240}$  on the outside. Load to critical, rod worths, moderator level worths, and flux traverses were conducted for each loading. A uniform 24%  $Pu^{240}$  load to critical is presently under way.



The gamma scanner has been installed in the PRCF shop area. Scanning of a typical PRCF irradiated fuel element revealed insufficient counting rates and an inadequacy in the crystal shielding. The slit size and collimator length are being investigated to obtain optimum counting statistics during traverses.

### CAF Operation

Several series of approach to critical measurements were completed for the Phoenix fuel experiment. The assemblies consisted of 19 fuel elements containing 108 grams, 124 grams, and 151 grams of Pu per element. The elements are being loaded to 175 grams of Pu. The elements consist of repeating cells with each cell containing 2-1/96" diameter x 0.020" Pu-Al disks, 2 Al disks and 0.120" of polyethylene.

### Code Development\*

#### Computer Program RETREV

The computer program RETREV is used to retrieve neutron cross sections and associated data from Brookhaven's SCISRS library tape. SCISRS is described in BNL-883, and the library tape that is available on-site contains approximately 300,000 data points. The data are stored on tape in such a fashion that a user has available information concerning the accuracy of each data point and enough information to be able to duplicate the form of the input data, i.e., 14.00+0 implies one more significant figure than 14.0+0. RETREV was written in Fortran IV (70%) and Sleuth II (30%) for the Univac 1107 computer.

The request options available locally are the following: atomic number, mass, cross section type, energy in MeV, institution, year, and suppression of the printout of the comment section. Input is by NAMELIST and, unlike BNL's RETREV, only integers or floating point numbers are used. The 1107 version requires as input the desired Z(s), A(s), and appropriate request numbers (which can be found in BNL-883).

Eventually RETREV will be programmed to punch and plot the cross section data contained on the library tape; however, these options probably will not be added until all of the various types of cross sections can be retrieved. The unpacking routines for recreating the differential cross sections and the secondary energies have not been written.

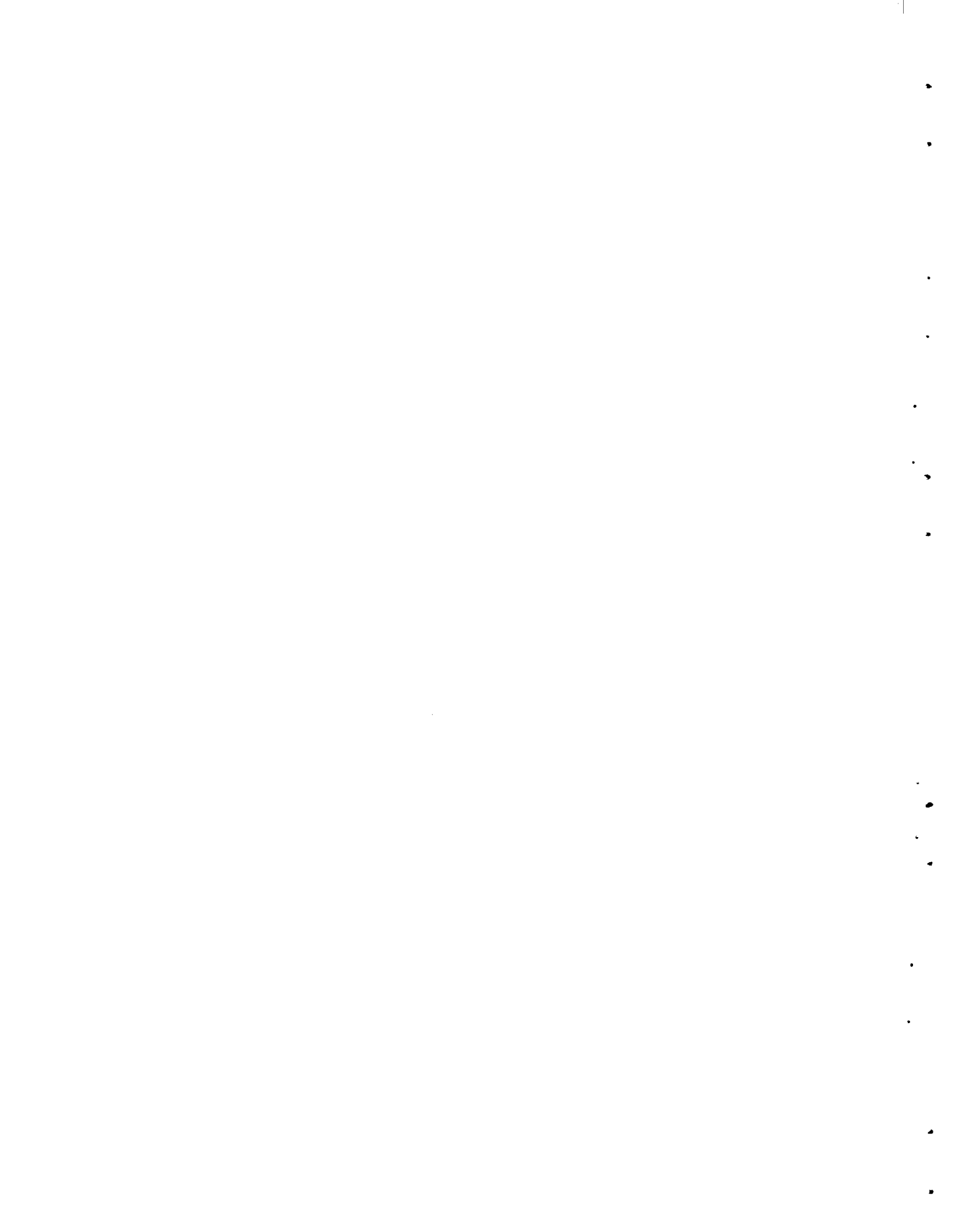
A relocatable deck is available for general on-site use.

#### BNW Master Library

Carbon 12 was modified to include the fast absorption cross section from KFK-120. Carbon will be reupdated later using KFK-120 data at a much finer energy mesh than the one currently in the library record.

---

\*Partially funded by O2.



The aluminum 27 record was modified to include the peak of the 5.9 KeV resonance. The record as obtained from the ENDF/A library did not have a peak cross section and resulted in low, average cross sections between 4.0 and 10.0 KeV. Chromium and nickel were also updated using the KFK-120 data. Updating the isotopes of iron by Theoretical Physics personnel is continuing and any changes are immediately added to the appropriate records on the master library tape.

A keypunch error in the Pu-239L record was corrected. The error had apparently been in the library for some time. The fission cross section at 145 eV was 91 barns and should have been only 9.1 barns. The average fission cross section between 100 and 215 eV dropped approximately 4 barns.

A new version of U<sup>236</sup> is about ready to place on tape.

#### HAMMER

The BNL-SRL lattice analysis code HAMMER has been successfully converted for use at this installation. It is available for either the IBM 7090 or the Univac 1107.

#### EXTERMINATOR

The Univac 1107 version of the 2-dimensional diffusion theory code EXTERMINATOR runs approximately 2 - 2-1/2 times as long as the version for the IBM 7090. Work was begun this month to determine the cause and, if possible, to reduce the running time. It has been determined that the code is I/O bound. The program is being revised to add the necessary parallel logic for reducing the I/O waiting time.

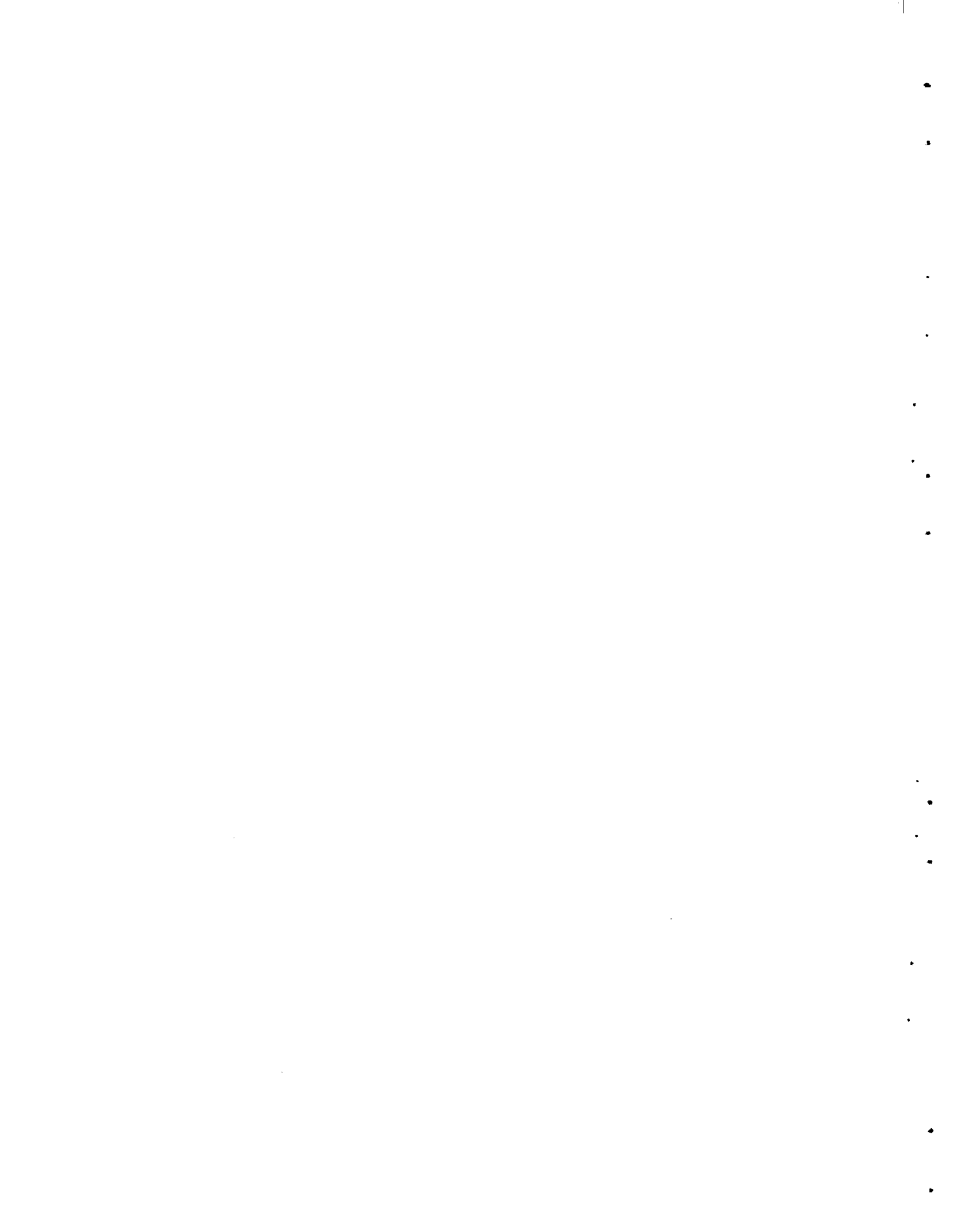
### Neutron Physics

#### Slow-Neutron Scattering

The Rotating-Crystal-Spectrometer (RXS) was used for a single measurement of the double-differential scattering cross section of 0.1 eV energy neutrons from a thin sample of room temperature D<sub>2</sub>O. Assuming that the reduced data will show no experimental discrepancies, this completes the planned scattering measurements on D<sub>2</sub>O.

The RXS was used for a measurement of the double-differential scattering cross section of 0.608 eV energy neutrons from room temperature H<sub>2</sub>O. A single measurement for an incident neutron energy of 0.4 eV remains to be done to complete the planned RXS measurements for room temperature H<sub>2</sub>O. Preliminary calculations were made to attempt to fit the H<sub>2</sub>O scattering law results obtained on the RXS with trial phonon frequency distributions using the LEAP program.

The RXS was used to measure the double-differential scattering cross sections of 0.304- and 0.152-eV energy neutrons from a 0.015 inch thick sample of solid H<sub>2</sub>O at a temperature of -6 °C.





The triple-axis spectrometer was used to measure the double-differential scattering cross sections of neutrons from H<sub>2</sub>O at 95 °C. Measurements were made at several different energies to allow re-normalization of previously obtained data which contained systematic errors.

Investigation continued on a method of high resolution monochromatization using multiple-Bragg diffraction. Part of the previous analysis was found to be in error, and the calculational program was corrected.

#### Fast Neutron Cross Sections

A paper on the "Existence of the 2.86 MeV Level in B<sup>10</sup>" was completed and submitted for publication.

Work continued on a paper which presents evidence for the non-existence of a bound state of the di-neutron from n-d total cross section measurements.

An effort was made to reprocess all of the previously obtained fast neutron total cross section data. This reprocessing which was essentially completed was necessary to perform the covariant error analysis. The final processing by the program LILNED which combines the results of two or more separate measurements was about 25% completed.

#### Cross Section Evaluation

At a meeting of the Cross Section Evaluation Working Group, BNW was assigned the responsibility of providing complete sets of evaluated data for several isotopes for the Evaluated Nuclear Data File/B. The isotopes assigned were H<sup>1</sup>, H<sup>2</sup>, Xe<sup>135</sup>, Sm<sup>149</sup>, Eu<sup>151,153</sup>, Dy<sup>164</sup>, Lu<sup>175,176</sup>, and Au<sup>197</sup>. In addition, we plan to provide data for Cu<sup>63</sup> and Cu<sup>65</sup>. Work has begun on obtaining the results of previous evaluations and new data.

#### REACTOR ENGINEERING DEVELOPMENT

##### BWR and PWR Core Design Studies

A computer code sizing water-cooled reactor cores within heat transfer limitations has been written. The code subroutines analyze three core geometries and facilitate two-phase flow pressure drop calculations. Sufficient data can be obtained to supply input to reactor nuclear analysis codes for fuel cycle considerations.

##### Chemical Shim

The boric acid test of the PRTR dump valve was completed. The valve has been disassembled and the springs removed for examination.

The chemical shim test in the Environmental Test Facility has been completed. Total operating time for this last test run was 108 days. Nominal boron concentration was 50 ppm. During the test, coupons were removed monthly from the storage tank for examination and evaluation.

•

•

•

•

•

•

•

•

•

•

•

•

•

•

•

### Shroud Tube Removal Machine

Fabrication of the remaining parts of the Shroud Tube Cutter is in progress. It is doubtful that all parts will be completed by July 1, as scheduled. Some small parts ordered offsite have not been received and may cause some additional delay.

The six-inch weld cutter was installed on the machine and a top weld cut made on the six-inch mockup shroud tube; no difficulties were encountered. The cut was clean with very little burr. Some modifications are being made on the six-inch weld cutter to facilitate its passage through the tube to make the bottom weld cut.

Preparation of the first draft of an operating and maintenance manual for the machine is estimated 80% complete.

### Rupture Loop Particle Removal Study

Detailed design was completed, material is presently being ordered, and purchase requisitions for auxiliary equipment have been prepared. Fabrication should start in early July, 1966.

### PRTR Moderator-Reflector System

Revisions to the reflector-moderator systems permitting use of light water as a reflector are 80% complete.

The reflector helium sweep blower by-pass regulating valve has been received. This item completes receipt of all engineering procured material.

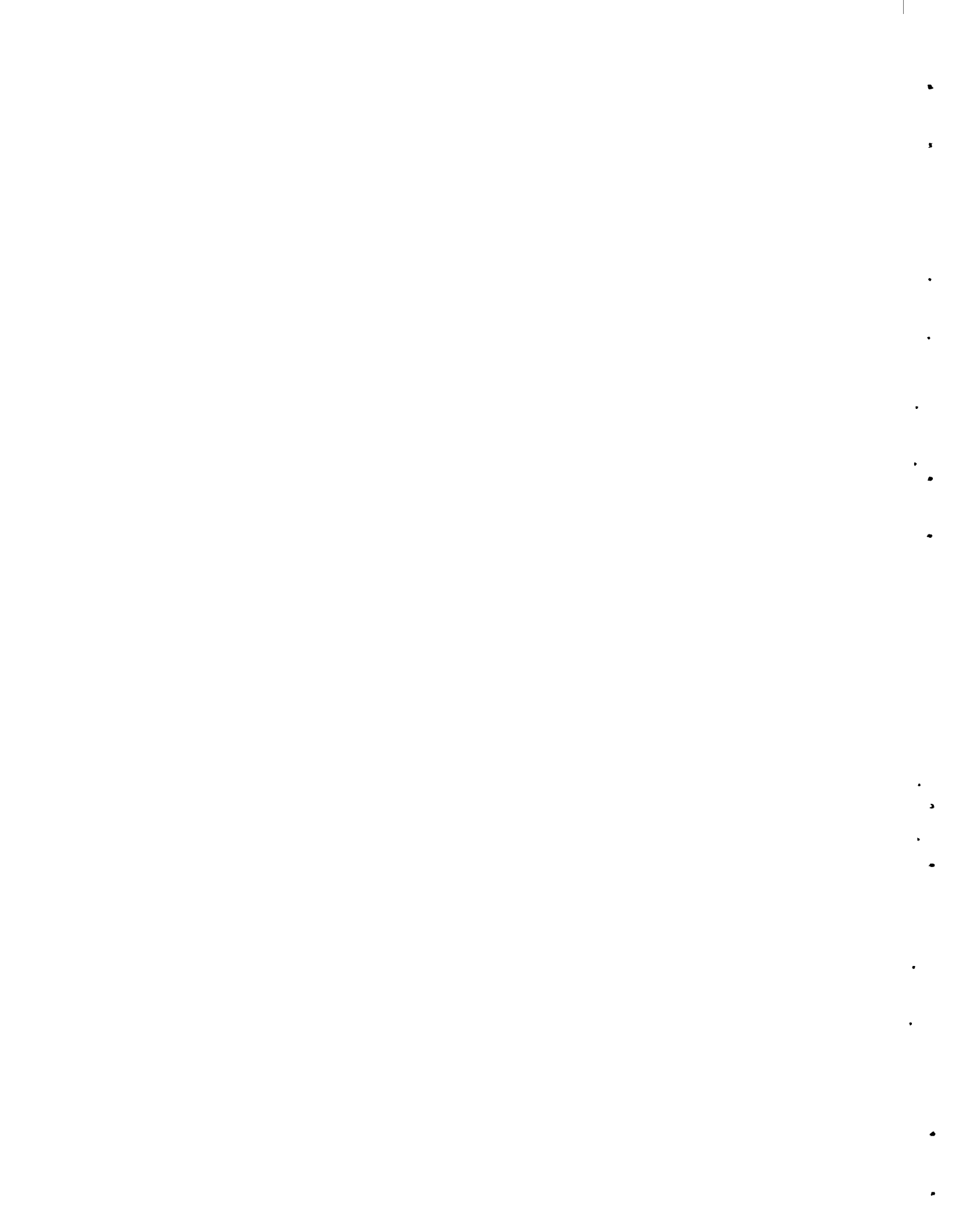
## MATERIALS DEVELOPMENT

### PRTR Corrosion Monitoring

Material corrosion in the PRTR moderator, reflector and primary shield is monitored by continuous corrosion probes. Probes of 6061 aluminum alloy in the moderator and reflector system and a probe of 1010 carbon steel in the primary shield system all showed rates of less than 0.01 mil/month during the past month.

### PRTR Primary Shield Leak Corrosion Tests

Laboratory corrosion testing to examine potential corrosion problems resulting from the leak in the bottom PRTR primary shield has continued. The latest test to evaluate aluminum corrosion resulting from the shield coolant contacting the moderator system aluminum shim wells and piping was completed. The test was conducted in a small laboratory loop simulating the shield system containing coolant at 60 °C, PH-10, 15-60  $\mu\text{mho/cm}$  conductivity and 0.08 - 2.4 ppm  $\text{O}_2$ . A continuous aluminum corrosion probe located in the loop corroded at a rate of 1.8 mils/month during the first week as reported earlier. At the end of this period, the corrosion probe underwent a rapid reduction



in aluminum corrosion rate to less than 0.01 mils/month, where it remained for the next three weeks of the test. Thus, once the protective aluminum oxide layer was formed, the uniform equilibrium corrosion rates in degraded ammoniated coolant are planned. Carbon steel corrosion rates determined by a corrosion probe were negligible during the entire testing period.

#### Chemical Shim Corrosion Studies

Pilot plant testing of a PRTR dump valve, shroud tube bellows assembly and shim rod assembly with borated water has been conducted. These tests were examining the effects of using  $H_3BO_3$  in the moderator system. Examination of the components will be conducted during the next reporting period.

#### Ceramic Fuel Dissolution Studies

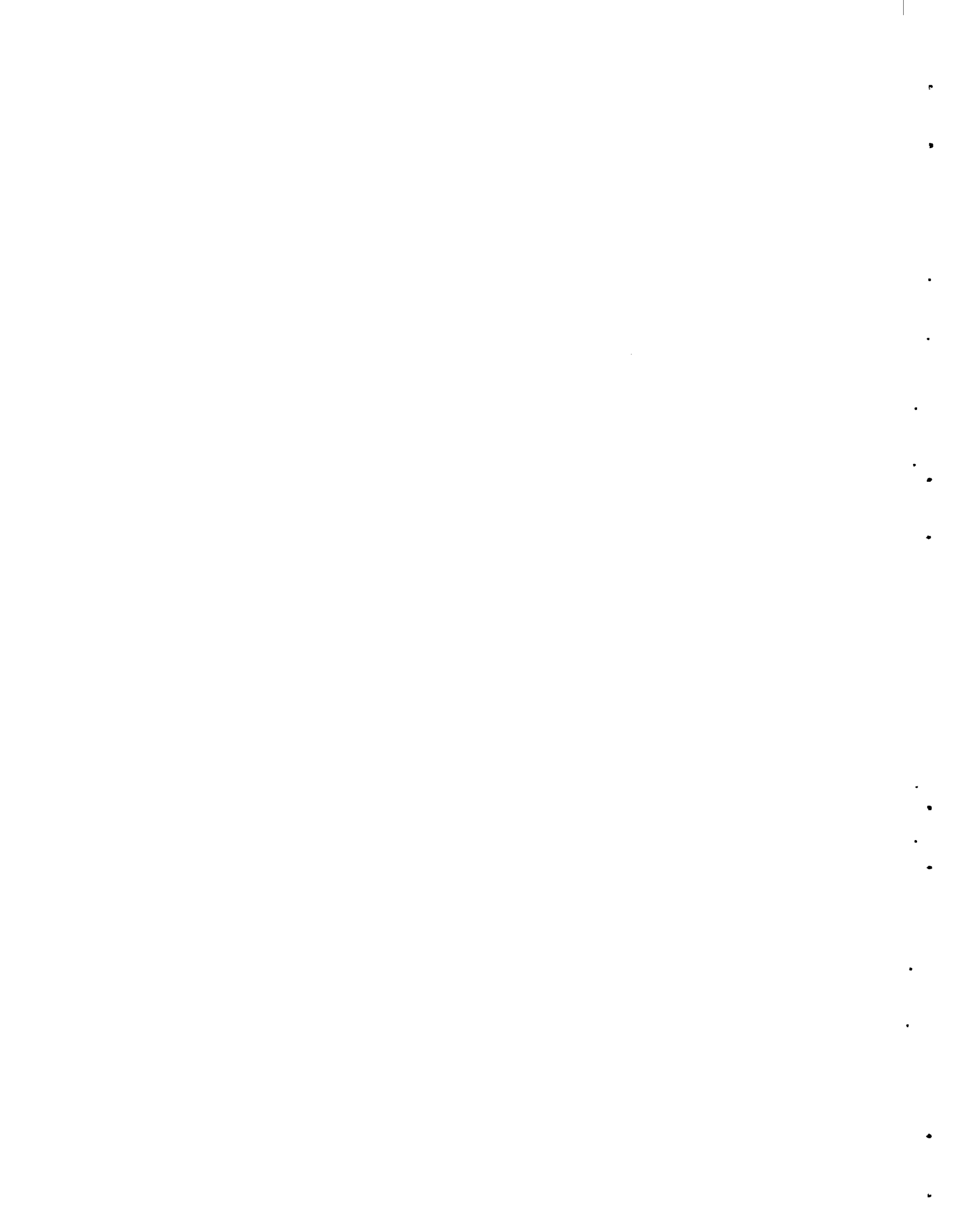
Ceramic fuel dissolution work during the past month has been directed toward determining the dissolution rates of sintered  $PuO_2$  in concentrated  $H_3PO_4$ . Preliminary data show that the rates were much lower than those found for the high fired  $PuO_2$  at comparable temperatures. The sintered material was treated at 1650 °C and the high fired  $PuO_2$  was fired at 900 °C. The higher treatment temperatures evidently altered the oxide structure, making it more difficult to dissolve.

#### PRTR Pressure Evaluation

The PRTR reactor safeguards program includes study by destructive examination of the effect of reactor environment upon the Zircaloy-2 pressure tubes. Work in progress is composed of measurement of elastic strain on unirradiated tube specimens while under different loading conditions, and crack propagation tests at various temperatures. The respective objectives are to describe elastic behavior of an anisotropic tube and to provide crack propagation data. This work is continuously improving the basis for judgment of irradiated specimens.

The third test of three required for determination of elastic constants necessary for describing stress, strain, and radial displacement of a pressurized orthotropic cylindrical tube is operational. A satisfactory pressure seal around the strain gage lead wires has been attained without a reduction of wire-to-wire resistance below about 10,000 meg ohms. The specimens were pressurized to 4500 psig with helium. At each 500 psig increment, the indicated strain from the inside and outside strain gage circuits was recorded. When plotted, these strain data were found to be linearly dependent upon pressure.

The effect of temperature upon propagation of a two-inch long simulated crack is being determined. Tests at 20, 80, and 107 °C have been performed. The calculated Lamé stress at propagation was 34,650, 31,750 and 31,850 psi, respectively. Assuming that the latter value is slightly high, the slopes of the line described by these points is minus 48.3 psi (stress)/C. Tests at higher temperatures will be performed.



PRTR pressure tube 5696, which had been discharged from channel 1948, was cut into test specimens at the PRTR basin, and its taper section was transferred to Radiometallurgy. A replica of a mark and its adjacent area on the inside surface of the taper was made to facilitate study of the mark. The shape and location of the mark support the idea that the mark is the result of contact by a tube alignment mandrel.

### CYCLE ANALYSIS

#### Economically Optimum Plutonium Lattices for Water Reactors

Reoptimizing uranium water reactor lattices for plutonium to minimize fuel cycle costs will usually soften the neutron spectrum and improve the value of plutonium.

The following three methods of optimizing the neutron spectrum without modifying the core or the vessel of a pressurized water reactor have been considered: (1) reducing the fuel density, (2) reducing the fuel rod diameter, and (3) increasing the lattice pitch. Table I lists the pro's and con's of these three optimizing methods.

Also, three interesting plutonium compositions representing the recycle and nonrecycle plutonium fuels that thermal reactor operators may encounter have been considered: (1) the plutonium composition from fast breeder blankets (94% Pu<sup>239</sup>, 5% Pu<sup>240</sup>, 1% Pu<sup>241</sup>, 0% Pu<sup>242</sup>, or as abbreviated: 94-5-1-0); (2) the plutonium composition from a first cycle water reactor discharge (62-17-16-5); and (3) the plutonium composition from a fourth cycle water reactor discharge (50-16-19-15).

The results are compared in two ways. The first type of comparison is shown in Table II, wherein each lattice modification is analyzed by holding the other two constant. The table shows that, except for nonrecycle plutonium (94-5-1-0), increasing the lattice pitch yields the lowest fuel cycle cost.

A second way of comparing the results shows that a combination of increased lattice pitch and reduced rod size yields additional savings of up to 0.24 mill/kWh<sub>e</sub> for the highly burned plutonium (50-16-19-15).

Furthermore, our calculations show that the value of first cycle plutonium is up to 28% more in an optimized lattice than in a uranium lattice.

#### Some Nuclear Characteristics of PWR's Recycling Plutonium

This study shows that the disadvantage in the power distribution with plutonium recycle, compared to that of U<sup>235</sup>-enriched refueling, vanishes after a PWR core has been successively refueled with recycled plutonium. This condition is called plutonium steady state recycle. Thus, the power distribution is distinctly different for plutonium first recycle and plutonium steady state recycle.

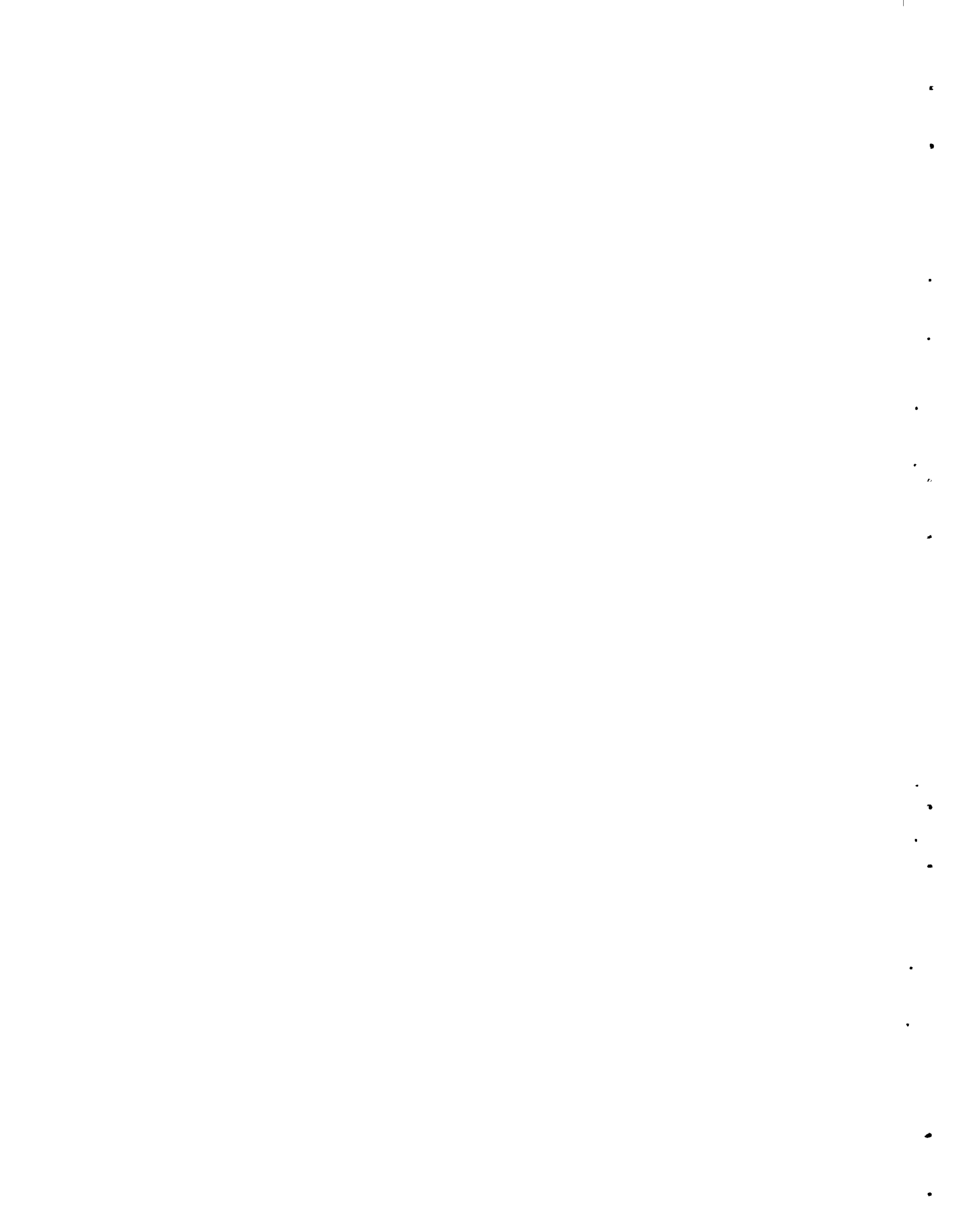




TABLE I

ADVANTAGE AND DISADVANTAGES OF  
SEVERAL METHODS OF LATTICE OPTIMIZATION

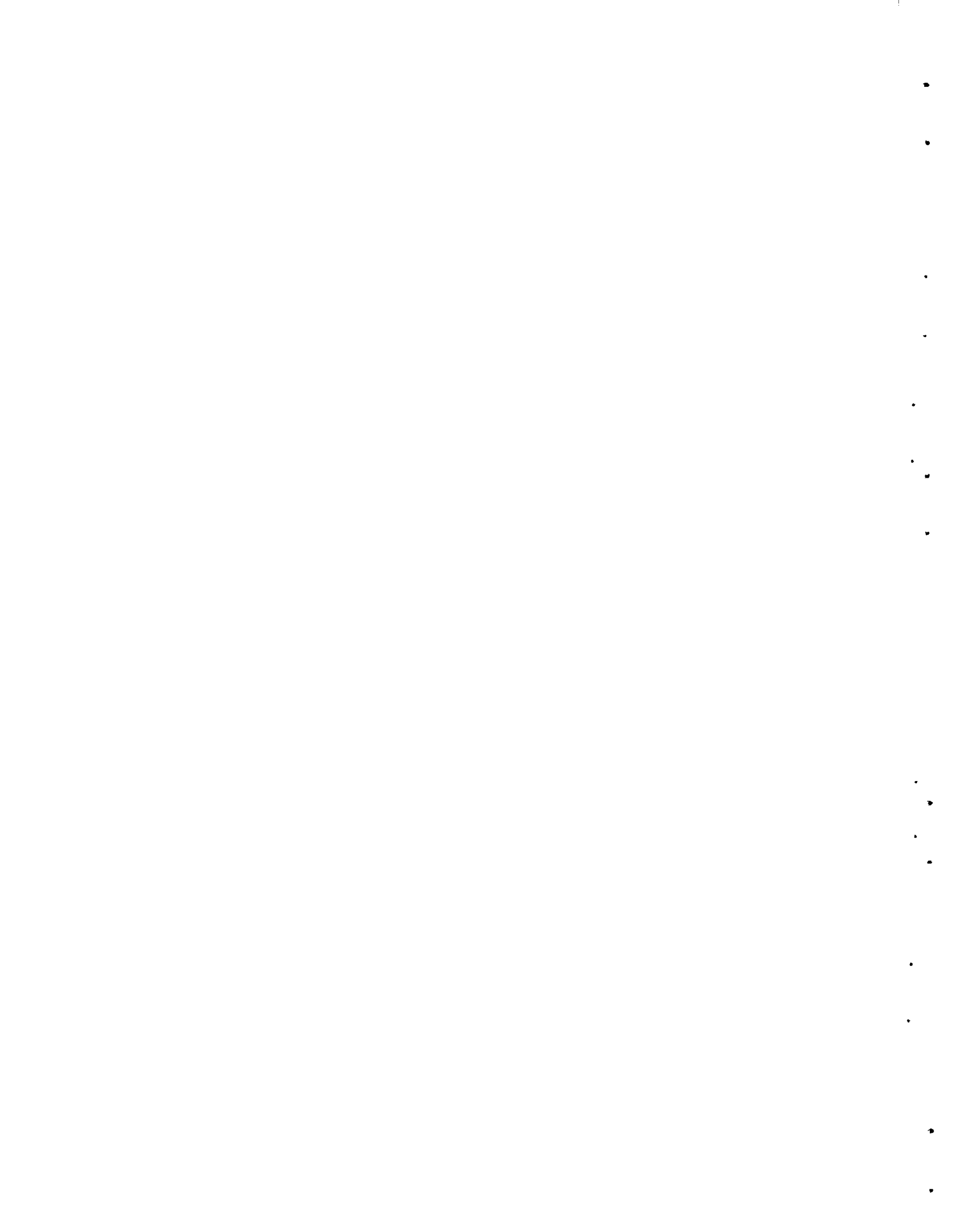
<u>Basic Variation</u>	<u>Advantages</u>	<u>Disadvantages</u>
Reducing Fuel Density	<ol style="list-style-type: none"> <li>1. Maintains heat transfer area.</li> <li>2. No modification of pitch or assembly.</li> <li>3. Higher specific power (high thermal conductivity of matrix materials).</li> <li>4. Lower inventory.</li> </ol>	<ol style="list-style-type: none"> <li>1. Fabrication cost increases.</li> <li>2. Limited economic range of changes in spectrum.</li> </ol>
Reducing Rod Size	<ol style="list-style-type: none"> <li>1. High specific power. (Avoiding melting by using thinner rods.)</li> <li>2. No modification of pitch or assembly.</li> <li>3. Large range of change in spectrum.</li> </ol>	<ol style="list-style-type: none"> <li>1. Reduced heat transfer area.</li> <li>2. Fabrication cost increases.</li> </ol>
Increasing Pitch	<ol style="list-style-type: none"> <li>1. No change in fabrication cost.</li> <li>2. Large range of spectrum change (but at discrete M/F values).</li> </ol>	<ol style="list-style-type: none"> <li>1. Assembly requires modification.</li> <li>2. Reduced heat transfer area in a fixed vessel size.</li> </ol>



TABLE II  
OPTIMUM LATTICE PARAMETERS FOR THREE FUEL COMPOSITIONS

Pu Comp., Pu <sup>240</sup> -Pu <sup>241</sup> -Pu <sup>242</sup>	Fuel Cycle Costs in a Reference Water Reactor Lattice	Reducing Fuel Density		Reducing Rod Radius		Increasing Lattice Pitch	
		Optimized Cost, (1) Mills/kWh	Density % Theor.	Optimized Cost, (1) Mills/kWh	Clad Rod Radius, cm	Optimized Cost (1) Mills/kWh	Lattice Pitch, cm
94-5-1-0	1.83	1.72	74	1.82	0.53	1.83	1.27
62-17-16-5	2.06	1.96	71	2.02	0.47	1.96	1.40
50-16-19-15	2.38	2.19	49	2.19	0.45	2.17	1.46
Slightly Enriched Uranium	1.84						

(1) These costs are based on: \$100/kg Fabrication  
 \$ 32/kg Reprocessing  
 10% Interest on both the Fuel Inventory and  
 the Fuel Cycle  
 \$10/g fissile Plutonium Credit (Note: the value  
 has not been decreased with the increasing  
 Pu<sup>242</sup> content).



Because of the incremental fabrication cost of plutonium enriched rods over  $U^{235}$ -enriched rods, it is desirable to minimize the number of plutonium-bearing rods required by plutonium recycle. As Table III shows, reducing the percentage of plutonium-bearing rods actually improves the power ratio between a plutonium recycle assembly and a slightly enriched uranium assembly, even though the individual plutonium-bearing rods within the assembly will be operating at a higher power than that of adjacent  $U^{235}$ -enriched rods. This improvement in the assembly power ratio is due to the self-shielding of the plutonium cross sections in the higher plutonium-enriched rods within the assembly. This self-shielding could be increased by using larger plutonium fuel particles, which have self-shielding characteristics similar to those of pencil plutonium configurations.

It was found that adjusting the lattice parameters to minimize the fuel cycle costs of plutonium recycle usually softens the neutron spectrum; but this, as Table IV indicates, will not drastically affect the power ratio during the plutonium first recycle. And during the plutonium steady state recycle the power distribution of a plutonium recycle assembly is no worse than that of slightly enriched uranium assembly.

Table IV also shows that as the burnup proceeds during the first plutonium recycle, the power ratio rapidly improves. This rapid improvement is due to the burnout of the large cross section plutonium isotopes.

The reactivity coefficients and a reactivity comparison between plutonium recycle and slightly enriched uranium refueling for first recycle and steady state recycle, are now being studied.

## TEST REACTOR OPERATION

### Operating Experience

Preparations for starting the batch core critical tests were completed in June. The non-nuclear critical tests which include determining moderator drop rates following a reactor scram were in progress at month end. Work accomplished during June included the following:

1. The primary system flush with degraded heavy water was completed. The primary system was then refilled with primary grade  $D_2O$ . The current primary system isotopic purity is 96.4%  $D_2O$ .
2. The core blanket system was returned to helium service with flow established through the moisture detection system sample lines.
3. The strainer downstream of the moderator pumps was removed and cleaned following a drop in moderator loop flow. The strainer basket was plugged with a fine black

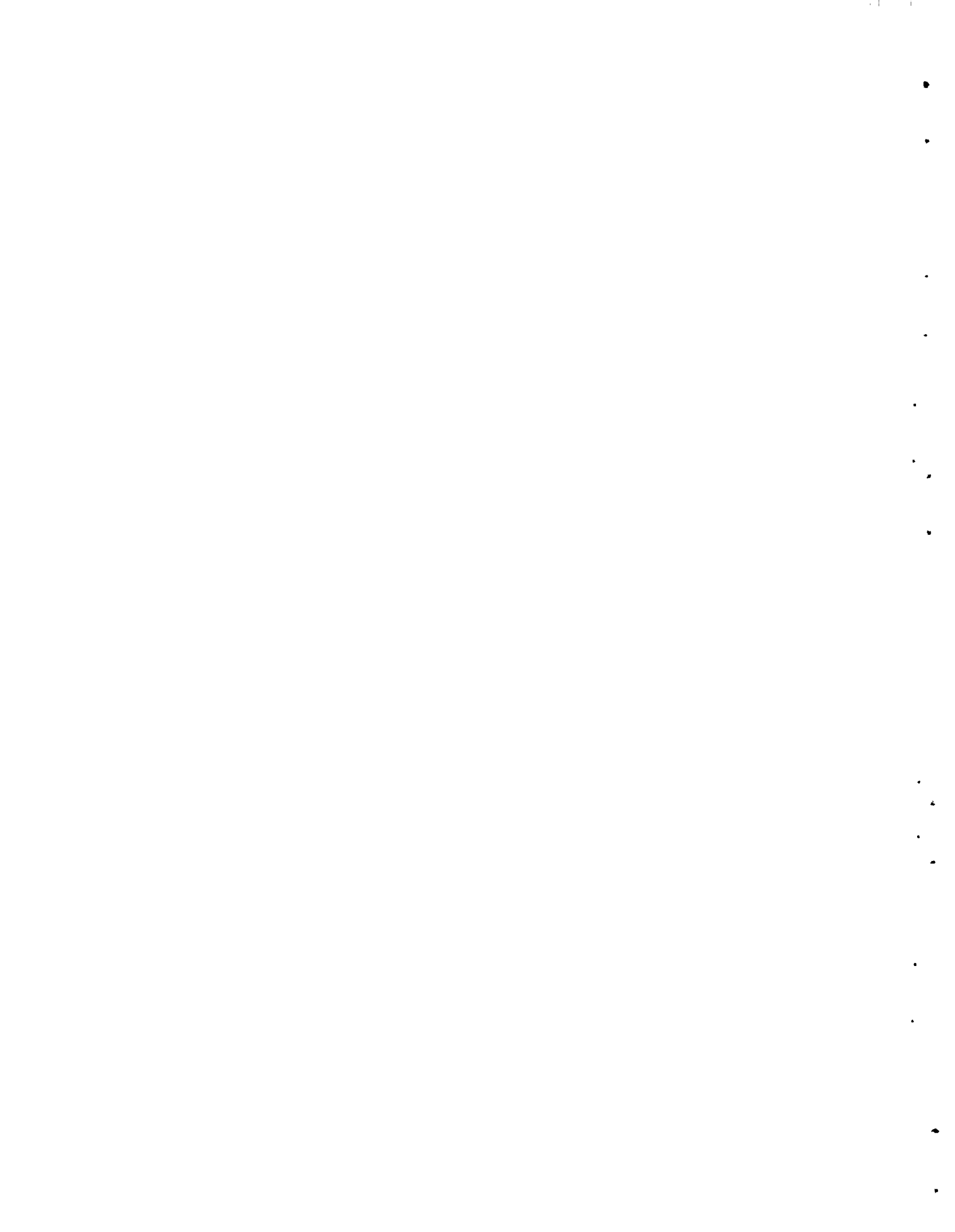


TABLE III

PLUTONIUM PLACEMENT AND ITS EFFECT ON THE POWER RATIO  
 BETWEEN A PLUTONIUM RECYCLE FUEL ASSEMBLY  
 AND A U<sup>235</sup>-ENRICHED FUEL ASSEMBLY

Percent of Pu- Bearing Rods in Recycle Fuel Assembly*	Power Ratio		Effective Pu <sup>239</sup> Fission Cross Section, barns	Enrichment of Pu-Bearing Rods in Recycle Assembly*		
	Power from Pu Recycle Assem.	Power from U <sup>235</sup> -Enriched Assem		U <sup>235</sup> Wt %	Fissile Pu, ** Wt %	Enrich., Wt %
0	1.00		--	2.80	0	2.8
100	1.34		1274	2.20	0.60	2.8
50	1.29		1156	1.60	1.20	2.8
33	1.27		1078	1.00	1.80	2.8
25	1.24		1036	0.60	2.20	2.8
27***	1.00		630	0.70	2.10	2.8

\*The remaining percent of rods in the recycle assembly are enriched only with 2.8% U<sup>235</sup>.

\*\*Recycle plutonium composition is 62% Pu<sup>239</sup>, 17% Pu<sup>240</sup>, 16% Pu<sup>241</sup>, 5% Pu<sup>242</sup>.

\*\*\*Pencil Pu in natural uranium.

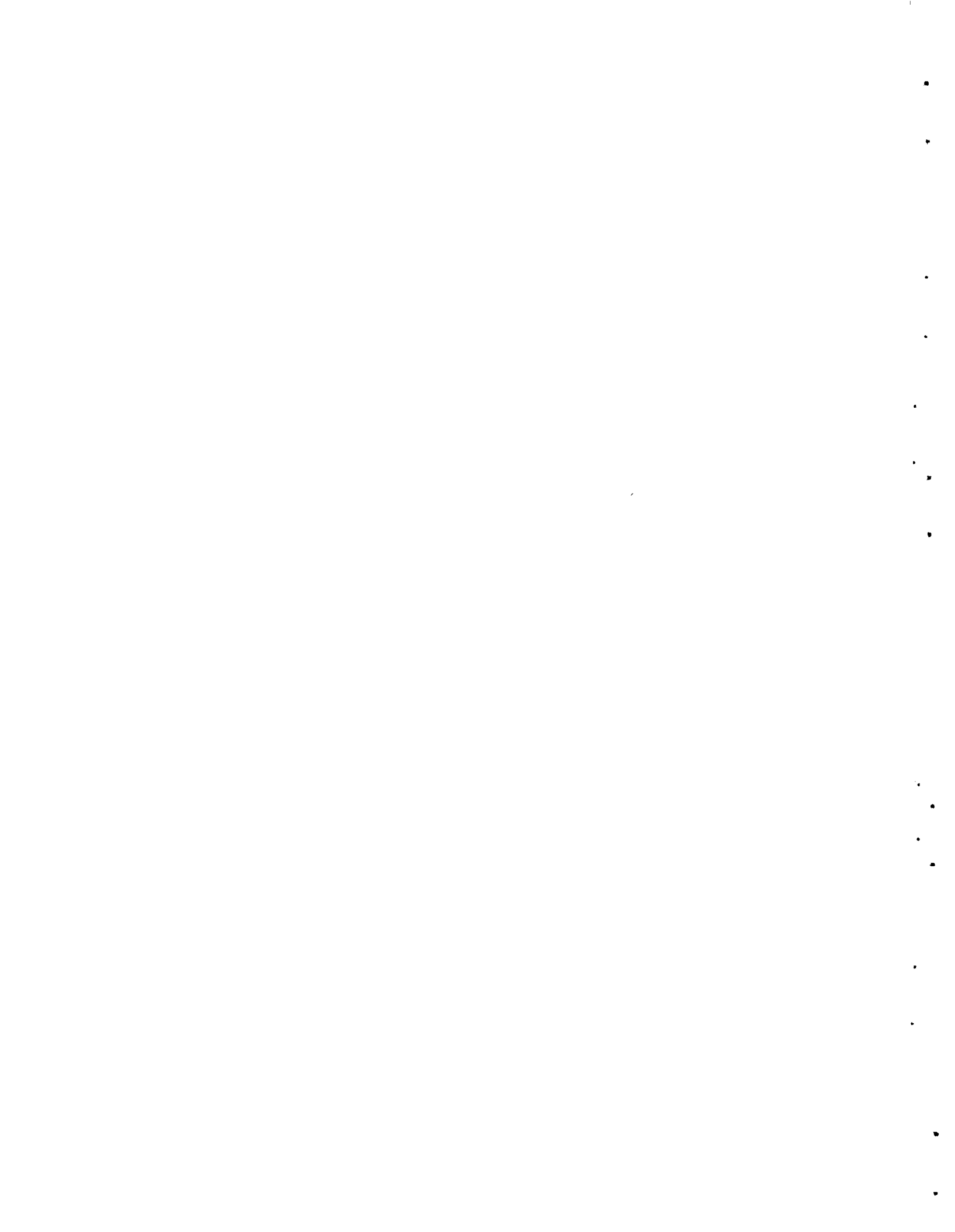




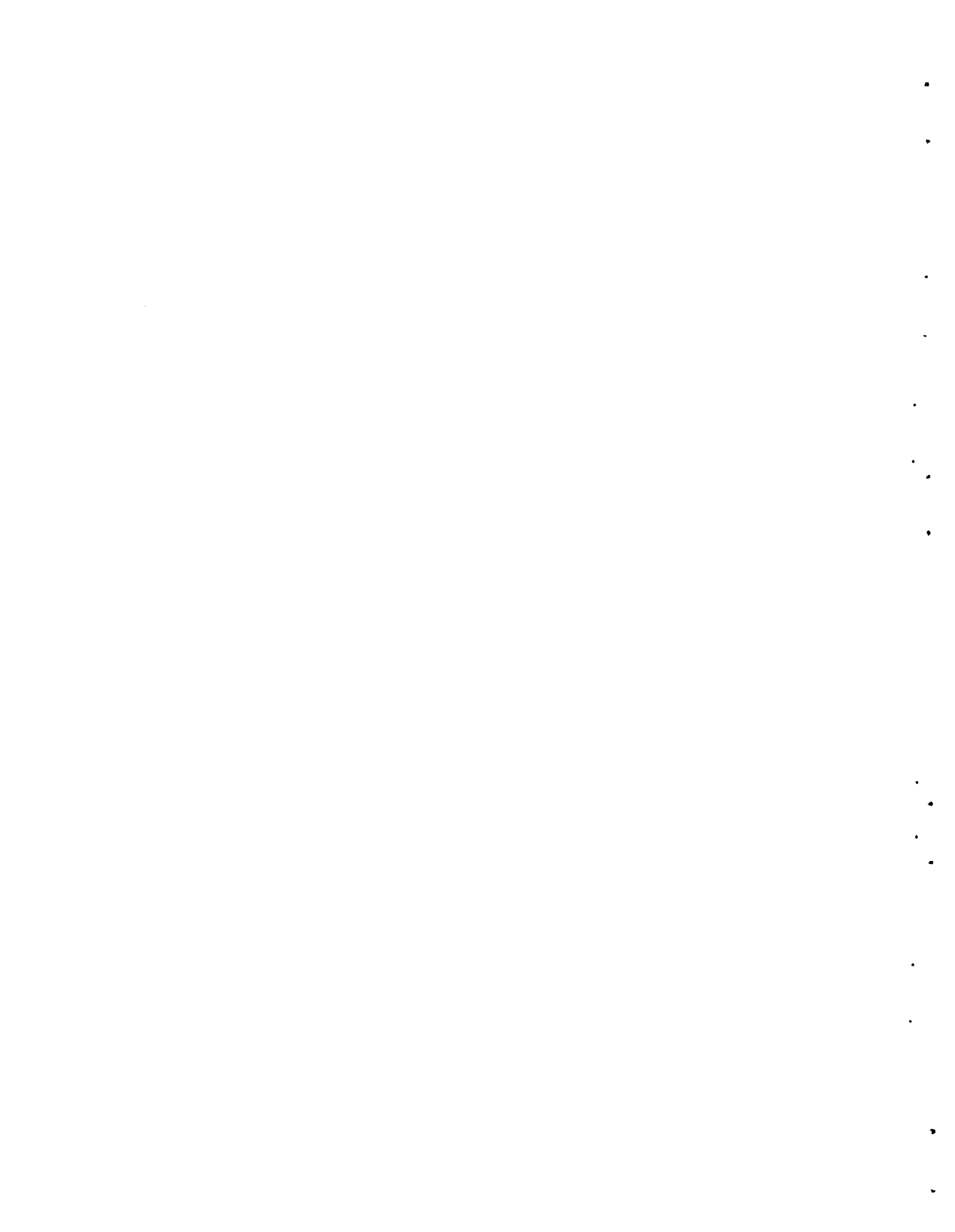
TABLE IV

POWER CHARACTERISTICS FOR VARIOUS PWR LATTICE PARAMETERS

Economic Optimums for Pu Recycle	Lattice Parameter Variations	Power Ratio			
		First Recycle (Zero Exposure)	First Recycle (10,000 Mwd/MT)	Steady State Recycle, (Zero Exposure)	Steady State Recycle, (10,000 Mwd/MT)
		$\left( \frac{\text{Power from Plutonium Recycle Assembly}^{**}}{\text{Power from U}^{235}\text{-Enriched Assembly}} \right)$			
75-80%	(Fuel )90 (Density,)70 (% T.D. )50	1.35 1.41 1.49	1.09 1.06 1.11	0.92 0.95 1.02	0.84 0.85 0.86
0.53 - 0.56"	(Rod )0.50*** (Pitch,)0.55 (in. )0.60	1.21 1.34 1.46	0.94 1.08 1.18	0.83 0.91 0.98	0.78 0.85 0.94
0.40 - 0.44"	(Rod )0.209*** (Radius,)0.193 (in. )0.177	1.32 1.51 1.65	1.10 1.20 1.30	0.93 0.99 1.08	0.87 0.96 1.05

\*\*Composition of recycled plutonium is 62% Pu<sup>239</sup>, 17% Pu<sup>240</sup>, 16% Pu<sup>241</sup>, 5% Pu<sup>242</sup>.

\*\*\*Approximate lattice parameter for U<sup>235</sup>-enriched refueling.



flake material. The cleaned strainer basket was replaced and moderator flow returned to normal. The filter cartridges in the moderator bypass filter were also replaced.

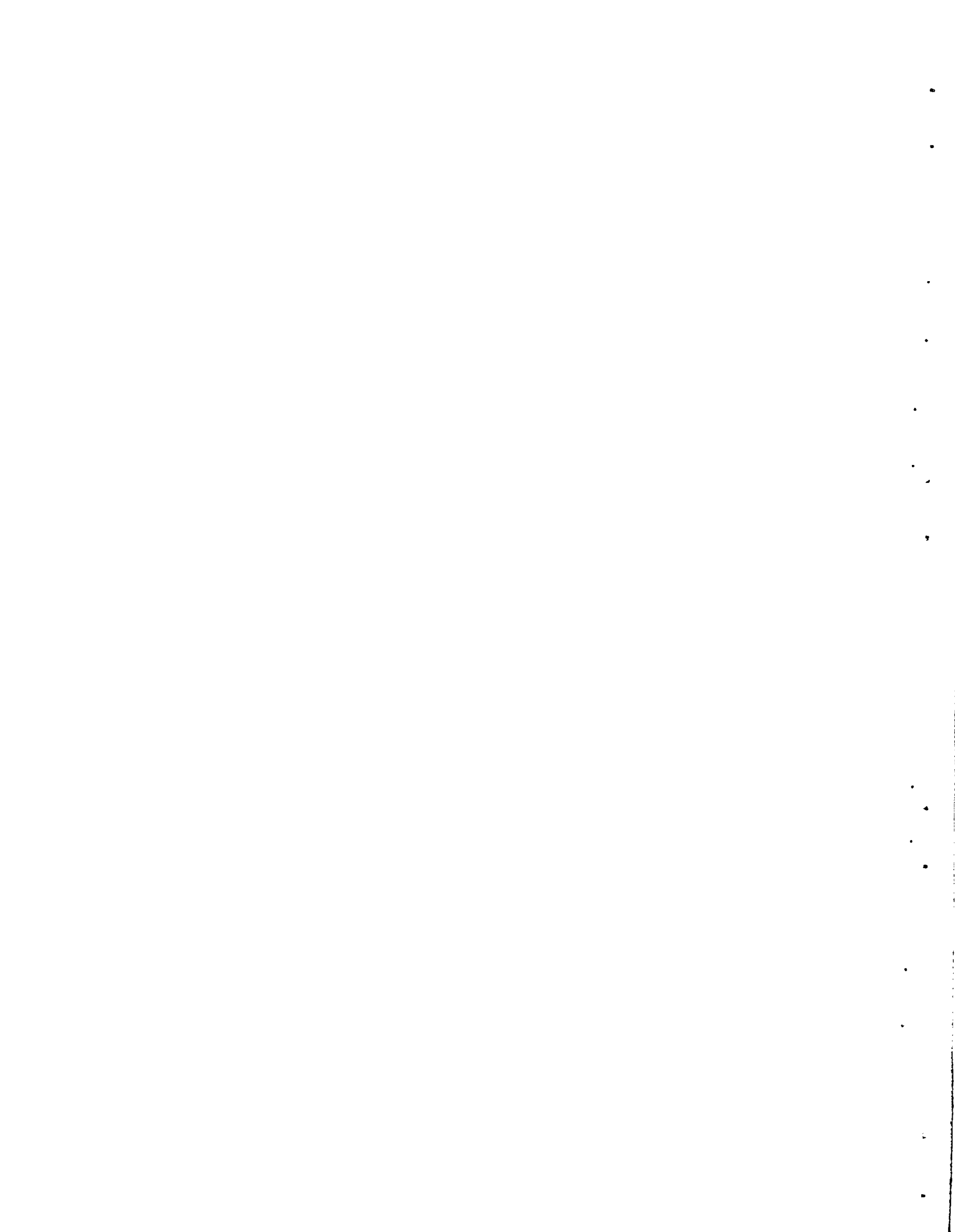
4. The boron addition system installation has been completed and system checkout was in progress at month end. The boron removal system installation continues with remaining work including the connection of the boron removal ion exchange unit to the flow control valve manifold, checkout of the boron removal system, and deuterization of the boron removal ion exchanger.
5. Cleanup ion exchange units for the primary and moderator systems were deuterized and placed in service. The reflector cleanup ion exchanger was also placed in service.
6. Installation of the relocated top and bottom shield cleanup system was completed and returned to service.
7. The charcoal filter units of the process area exhaust filter system were replaced.
8. A low resistance to ground was found on one phase of the underground cable supplying emergency backup electrical power from the 38<sup>4</sup> Bldg. Until the cable is replaced, the old line will be used. The limitation this puts on the operation is that the rupture loop cannot be operated with fuel in the reactor test section.

Heavy water loss recorded for the month was 2744 pounds. All but 150 pounds of this loss actually occurred September 29, 1965, during the FERTF fuel failure incident but was not revealed until now due to miscalibration of the primary system D<sub>2</sub>O storage tanks.

#### Maintenance Experience

Significant maintenance items for the month included the location and repair of numerous top face leaks on the dry gas system. A total of 3438 craft manhours were utilized during the June outage as follows:

FERTF Fuel Failure	329
Decontamination	133
Repair	1 358
Modification and Improvement (including capital work)	754
Operations Assistance	388
Preventive Maintenance	476
	<u>3 438</u> manhours



Improvement Work StatusWork Completed

Core Blanket Filters  
Electrical Diesel Fuel Return Pump  
PRTR Critical Test Instrumentation  
Re-route TKA-5 Discharge  
Export Steam Expansion Joint Repair  
1550 Dry Gas Filter

Work Partially Completed

New Instrument Power Supply  
Traveling Flux Wire Probes  
Reactor Hall Crane Work Platform  
Effluent Monitor System Calibration Modifications  
Diesel Well Pump - Remote Start  
Instrumented Fuel Element Installation  
Relocate IX-4  
Helium Compressor Compensating Pump  
RL Annex Ventilation Enclosure  
Second Moderator Temperature Probe

Design Work Completed

Second Moderator Temperature Probe  
Corrosion Probe Installation in Core Blanket System  
Corrosion Monitoring Probe Installation in Thermal and  
Biological Shield System  
Underwater TV Installation

Design Work Partially Completed

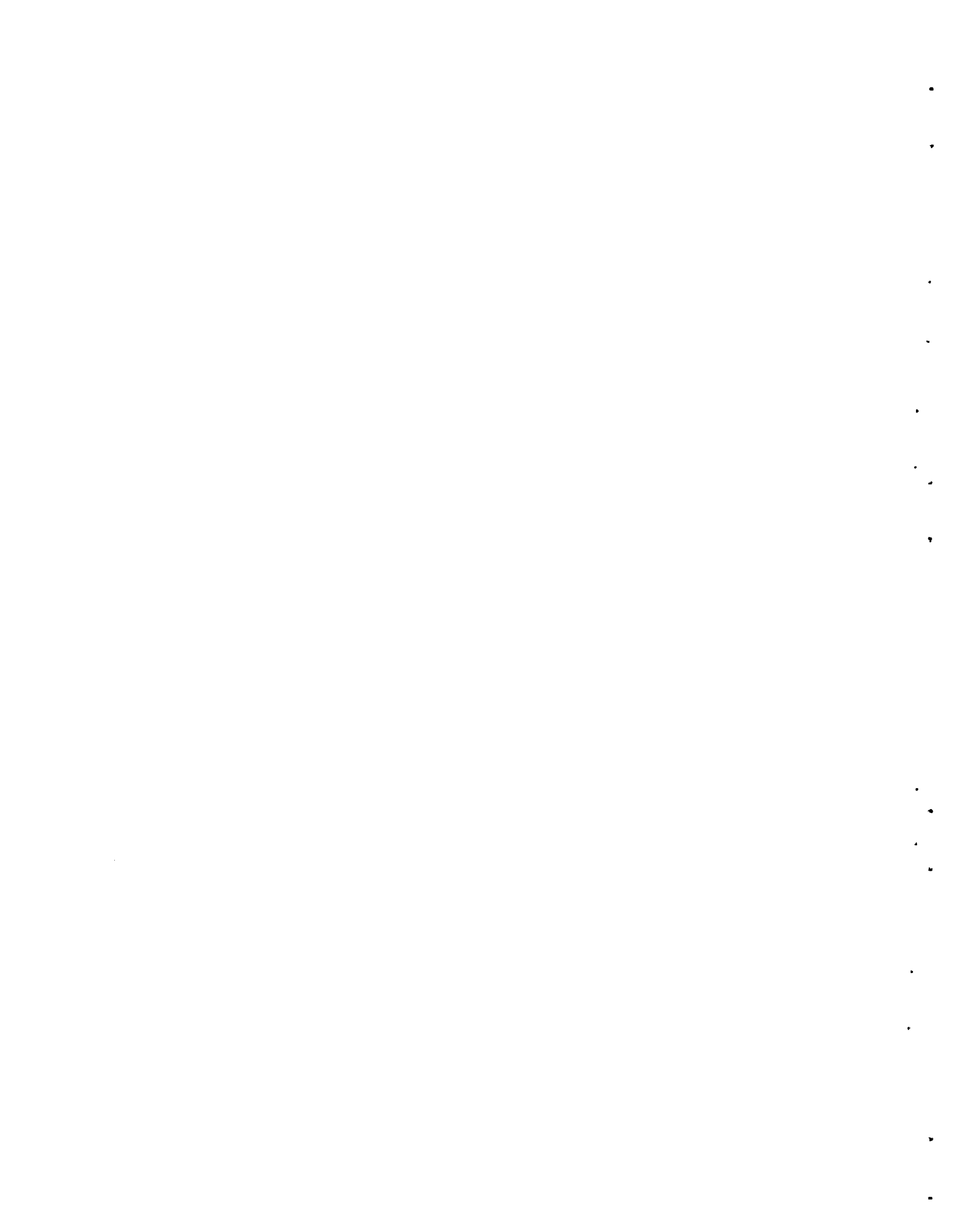
Analysis of HX-1 and Primary Pump Supports  
Rupture Loop Decontamination Equipment  
D<sub>2</sub>O Addition to Primary from Outside C.F.

Process Engineering and Reactor Physics

The presentation of the batch core orientation briefings is essentially complete.

The moderator level probe has been installed and tested. The Time Domain Reflectometer has been received and installed in the Control Room. Sensitivity of the probe has been excellent. Measuring the response of the moderator level to opening of the dump valves, shutdown valve, etc., has been satisfactory. A "noise" problem in the probe has prevented satisfactory testing of the level control mode of operation, and a revision to the equipment may be required to overcome this problem.

A summary description of plans for approach to power and initial power operation has been prepared for transmittal to the AEC.



Studies of neutron flux power calibrations for the Critical Tests were issued. While the flux per watt of power in the core will vary inversely with the number of fuel elements, the flux per watt at the peripheral chamber positions will not be strongly affected. Therefore, the chamber calibrations will be roughly constant throughout the loading and borating of the core.

PRTR Test 125, Irradiation of Zr-2 - 1/2% Niobium Pressure Tube, and PRTR Test 133, Special Burnup Study Fuel Elements, were approved and issued.

The tapered section of process tube 5696 from process channel 1556 was sent to the Radiometallurgy Laboratory. A replica was obtained from the galled area which indicated that the defect was caused by dropping the process tube aligning tool (H-3-13396) into the process tube. Metal buildup is estimated at 0.020".

Changes to the Operating Safety Limits for PRTR were received from AEC-RLOO substantially as proposed in our April transmittal and were distributed within BNW.

#### Project CAH-119 - PRTR Storage Basin Addition and Experimental Facilities Modification

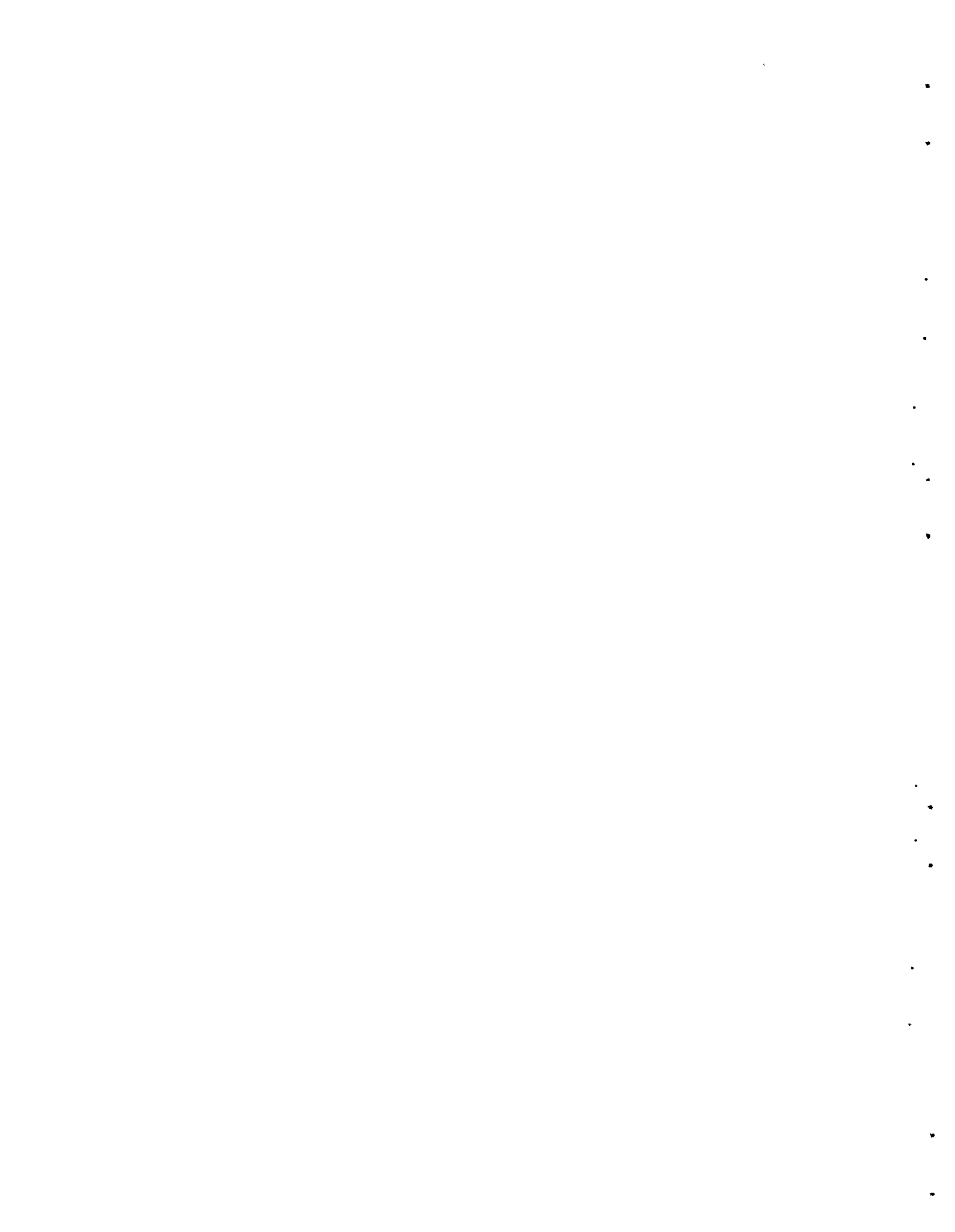
This project is to provide a storage basin addition and equipment for experimental work and additional storage space. The ventilation system has been accepted with minor exceptions and the absolute filters were successfully tested using dioctylphthalate smoke. The building portion is 100% complete, but minor exceptions and additions remain to be done. The demineralizer sump pump was replaced, the underwater lights revised, and other minor items were completed.

During the month comments were submitted on AMF's detailed design drawings for the underwater fuel handling equipment. Fabrication is scheduled to start on receipt of drawing approvals.

#### Project BCP-007 - PRTR Waste Handling

This project is to provide improved waste handling capability and control of reactor systems during off-standard situations. Scope requirements and cost estimates for Phase II have been completed. Preparations of a project proposal revision to include the new items has been started.

The Phase I work review was completed during the month, and engineering work on the 14 items is under way. Engineering review of the drawings for the MH #2 pump, TW tank bypass, and new sump pump installations was completed. Procurement of long delivery items has been initiated. Existing instrument drawings have been marked up for revision to include new instrumentation as required on this project. Procurement specifications have been prepared and transmitted to the Project Engineer for obtaining bid proposals on the equipment.





## EBWR DEMONSTRATION PROGRAM

### Analysis of PRCF Experiments

Calculations are being done to complete the experiment-theory correlations for the EBWR experiment in the PRCF. Radial and axial flux shapes have been calculated with program HFN. Worths of various materials and the reactivity as a function of moderator height have also been calculated with HFN.

Calculations are also being done to evaluate the one dimensional transport theory code DTF-IV.

### INDUSTRIAL ASSISTANCE

#### Westinghouse Physics Tests

Five hundred of a planned total of 1200  $UO_2 - 2 \text{ wt\% } PuO_2$  rods were packaged and shipped to Westinghouse. Three hundred more are to be shipped by July 1, 1966, and 400 will be shipped during September. The rods are to be used by the Westinghouse Reactor Evaluation Center (WREC) in zoned loading studies along with 2.7%  $U^{235}$ -enriched  $UO_2$  rods.

#### Mark I-R Pellet Fuel Rods

A purchase order was placed with General Electric Company for design and fabrication of 77 Mark I-R high power density fuel rods containing pelleted  $UO_2 - PuO_2$  fuel. Two 19-rod clusters assembled from these rods will be included in the Batch Core Experiment, and the remaining rods will be irradiated in the FERTF in a specially designed basket tube element.

### ADVANCED SYSTEMS

#### $U^{233}$ FUELING OF A FAST COMPACT REACTOR (J. C. Fox)

A parametric study emphasizing fuel composition, size, and weight requirements for a 10 Mw(t) liquid metal-cooled fast compact reactor fueled with  $UO_2$  molybdenum cermet has been completed. Results of the study have been interpreted and a rough draft of a formal report written.

The nuclear parameter survey for a series of compact reactors fueled with  $Pu^{239}$ ,  $U^{233}$ , and  $U^{235}$  fuel cermet has been completed. A report, BNWL-283, "Neutronics Characteristics of Selected Compact Fast Reactors," by W. W. Little and R. W. Hardie is being published.

.

.

.

.

.

.

.

.

.

.

.

.

.

.

NUCLEAR SAFETYCONTAINMENT SYSTEMS EXPERIMENT (J. M. Batch)Experimental Facilities

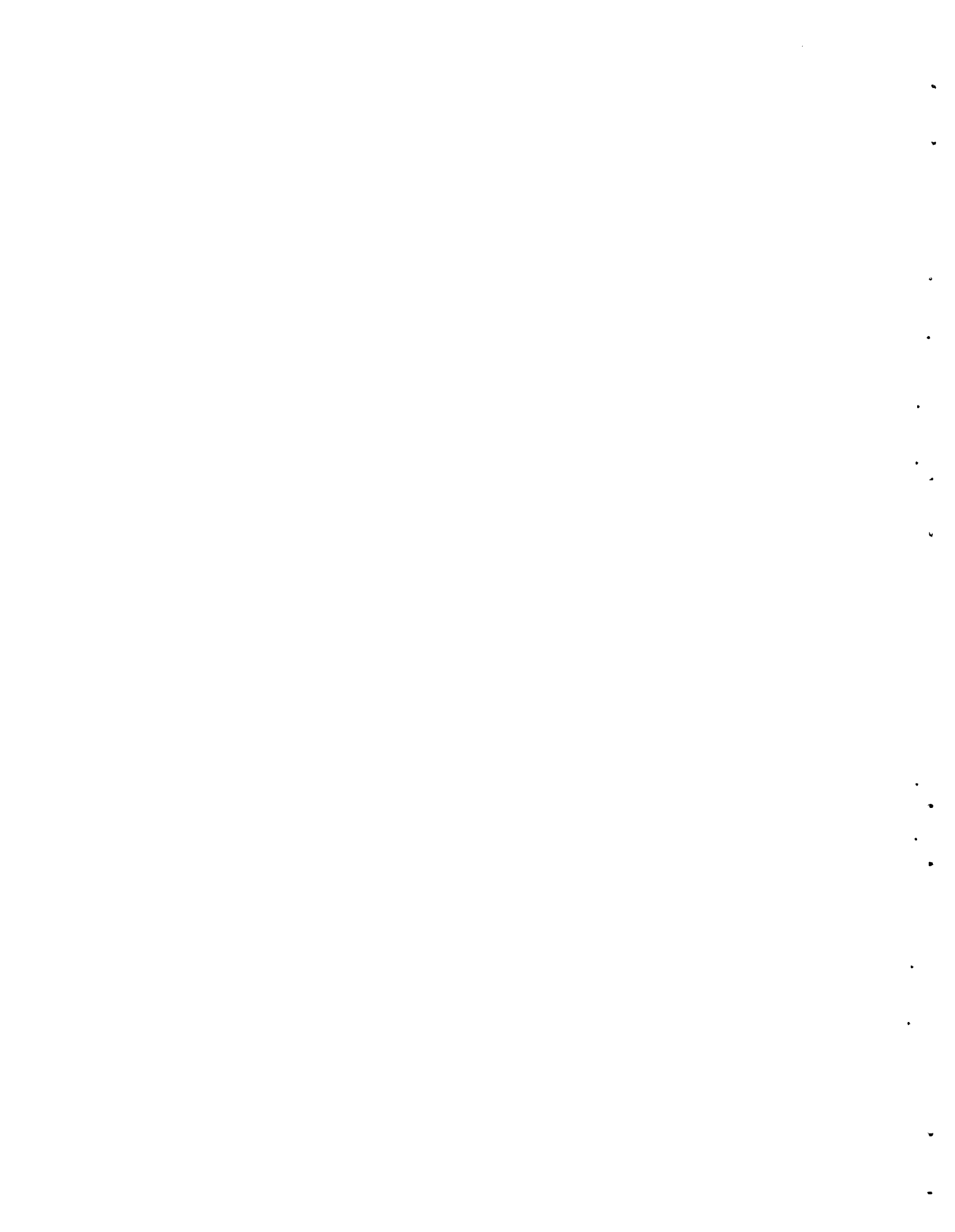
Construction activities were concentrated on the building and utilities for the installation of the reactor simulator vessel outside the containment vessel. Design of the shelter building and utilities was completed. Foundations for the building and for the simulator support were completed and building erection started. Design of the loop piping and structural support for the simulator was 80% completed. Utility runs were started as was the high pressure loop.

The sight glasses on the containment vessel for liquid level measurements, ladders inside the containment vessel, the Dowtherm loop, the external portion of the aerosol sampling system, and the main header for the high pressure nitrogen gas were completed with minor exceptions. Work was started or continued on the aerosol injection line and control panel, on the Maypacks and associated holders, and on the system for suspending the samplers and instrument sensors in the containment vessel.

Aerosol Studies

The fission product aerosol which will be used in CSE tests studying fission product transport in containment will be generated by volatilizing radioactively labeled stable fission product elements or compounds and passing these through the hot zone of a secondary furnace containing molten clad unirradiated  $UO_2$ . This second furnace has two purposes: to add a source of cladding and fuel particles, and to provide a high temperature region for ionization, decomposition, or other reaction of the aerosol. All previous tests in the Aerosol Development Facility (ADF) have used stainless steel clad  $UO_2$ . Because many reactors use or propose to use Zircaloy clad fuel, it is necessary to determine whether the type of cladding used in the CSE aerosol mixture is important. Therefore, a containment test was made in the ADF using Zircaloy-2 clad  $UO_2$ . Comparison with previous tests using Type 304 stainless steel cladding with otherwise similar conditions showed no difference in iodine containment behavior attributable to cladding type. This is not intended to imply that behavior of iodine released from irradiated  $UO_2$  is independent of cladding type. Irradiation history and metal-water reactions may be of importance in this case.

The CSE Maypack efficiency for retaining  $I_2$  and HI at various mass loadings and flow rates while sampling air and steam-air atmospheres was studied. Tentative conclusions are: (1) Continued flow of clean air or steam-air through a loaded Maypack will elute some of the iodine from the glassfiber filter and move it to the silver screens or charcoal; (2)  $I_2$  masses over about 5 mg loaded at a flow rate of 0.5 SCFM may result in some penetration of the silver screens; and



(3)  $I_2$  in steam-air atmosphere is retained on the glass fiber filter (Gelman Type A) in a manner similar to HI. The filter appears to have a limited capacity for adsorption of these vapors as evidenced by the decreasing percentage retained with increasing mass loadings.

#### Gamma Energy Analytical System

Computer program alterations were made to reduce the typed input data necessary to perform automatic gamma energy analyses. Other small program bugs related to the separate line timing of background and stored spectra were observed and corrected. Barium-lanthanum-140 standards were filed for two of the detector systems and a routine procedure set up to check instrument variables on a daily basis.

Discussions were held with Applied Mathematics and Radiological Sciences personnel on problems relating to the statistics of computed analytical results and channel grouping of multicomponent spectra.

#### Multiplexer Code

The multiplexer code has been checked out with preliminary dynamic voltage tests. These consisted of monitoring the sinusoidal line voltage and a ramp voltage originating from an oscilloscope sweep. From these tests and others, it was determined that the four analog amplifiers were badly out of adjustment, and this was corrected. Because of this, some long term reproducibility and stability checks are planned for the system using a precision voltage source.

The multiplexer code uses a series of tables to control the scanning sequence. These tables are packed binary to conserve storage and hence are quite inconvenient for a user to generate. Thus, an auxiliary code has been written and debugged which types out queries to the user for typed-in information which the code uses to generate the required tables. The result is a punched tape which can later be easily read into the computer with the optical reader.

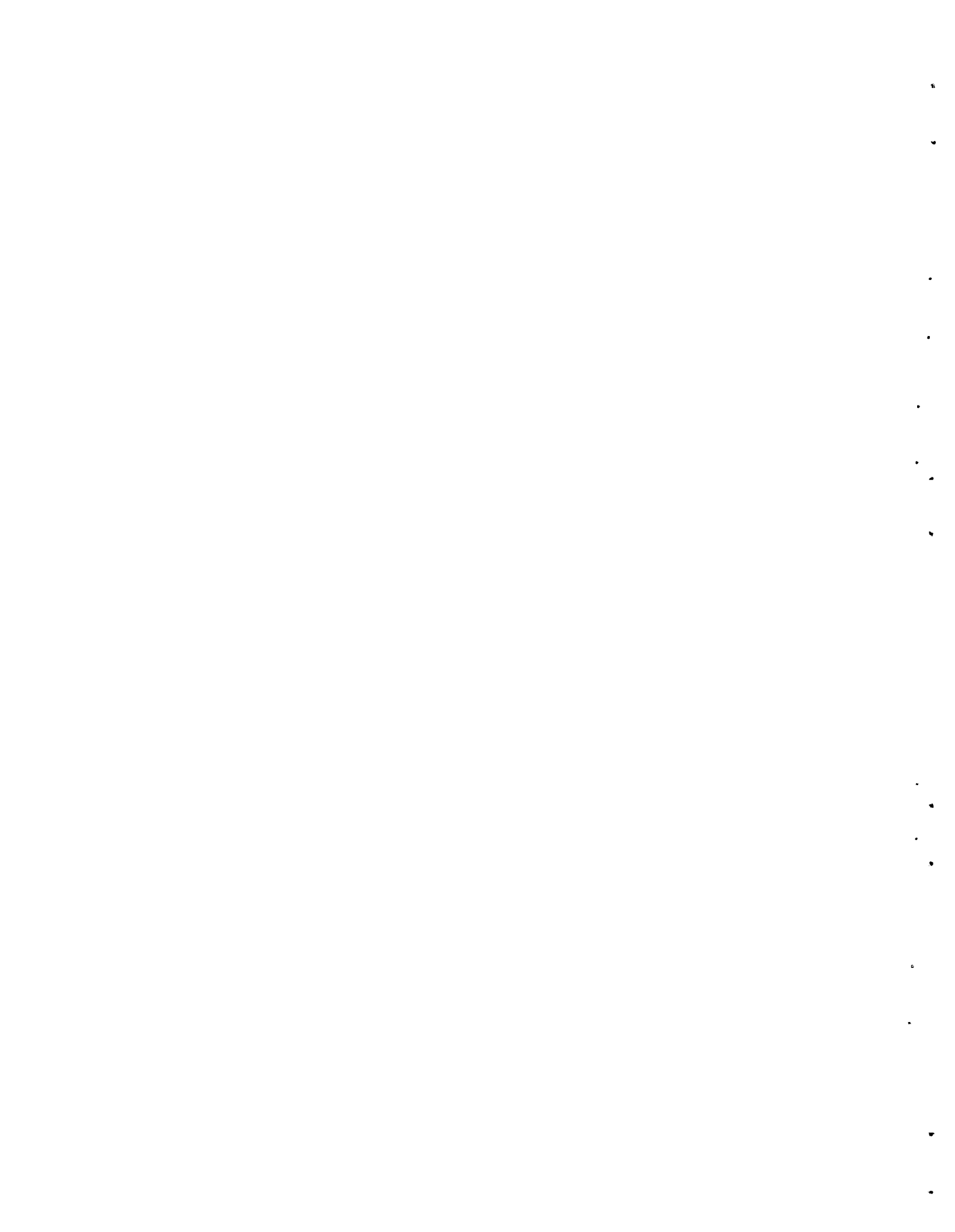
#### Autoclave Testing

Testing of Phenoline 302 painted carbon steel coupons in steam at 135 °C continued. At 1275 hours exposure, one coupon cracked--the other remained intact. This is considered acceptable service life for CSE conditions.

A sample of the electrical cable proposed for use on the CSE Maypack cluster solenoid valves was tested in steam at 135 °C for 1340 hours. The radiation cross-linked polyalkene jacket darkened and became slightly gummy, but remained flexible, tough and had good electrical resistance.

#### Leak Rate Testing

Preliminary tests were concluded and sensors removed from the containment vessel to permit access by construction personnel. The



high results by the reference volume method reported last month were determined to result from a numerical error. Data have been recalculated and reasonable agreement found.

### Decontamination

A decontamination program to aid in the determination of containment system safety parameters was begun during the past month. Initial efforts have been directed toward the adaptation of vapor phase cleaning techniques to the cleanup of containment system surfaces. Preliminary studies have been made in a small pilot plant facility with steam and  $\text{NH}_4\text{OH}$ ,  $\text{NaOH}$ , and  $\text{NaBr}$ . Decontamination factors on painted surfaces were two or less. Much greater efficiency was obtained with iodine contamination on stainless steel; D.F.'s ranged up to 12.

### Contamination Mechanisms

A study of contamination mechanisms with autoradiography was begun during the past month to aid in the study of containment system safety parameters. Autoradiographs of painted surfaces contaminated with radioactive iodine are consistent with general adsorption or uniform deposition of extremely fine particles and/or deposition with subsequent reaction with the painted surface on which is superimposed the deposition of relatively large agglomerates. Additional autoradiographic studies are planned to further define iodine deposition mechanisms and to determine those affecting the deposition of other radionuclides.

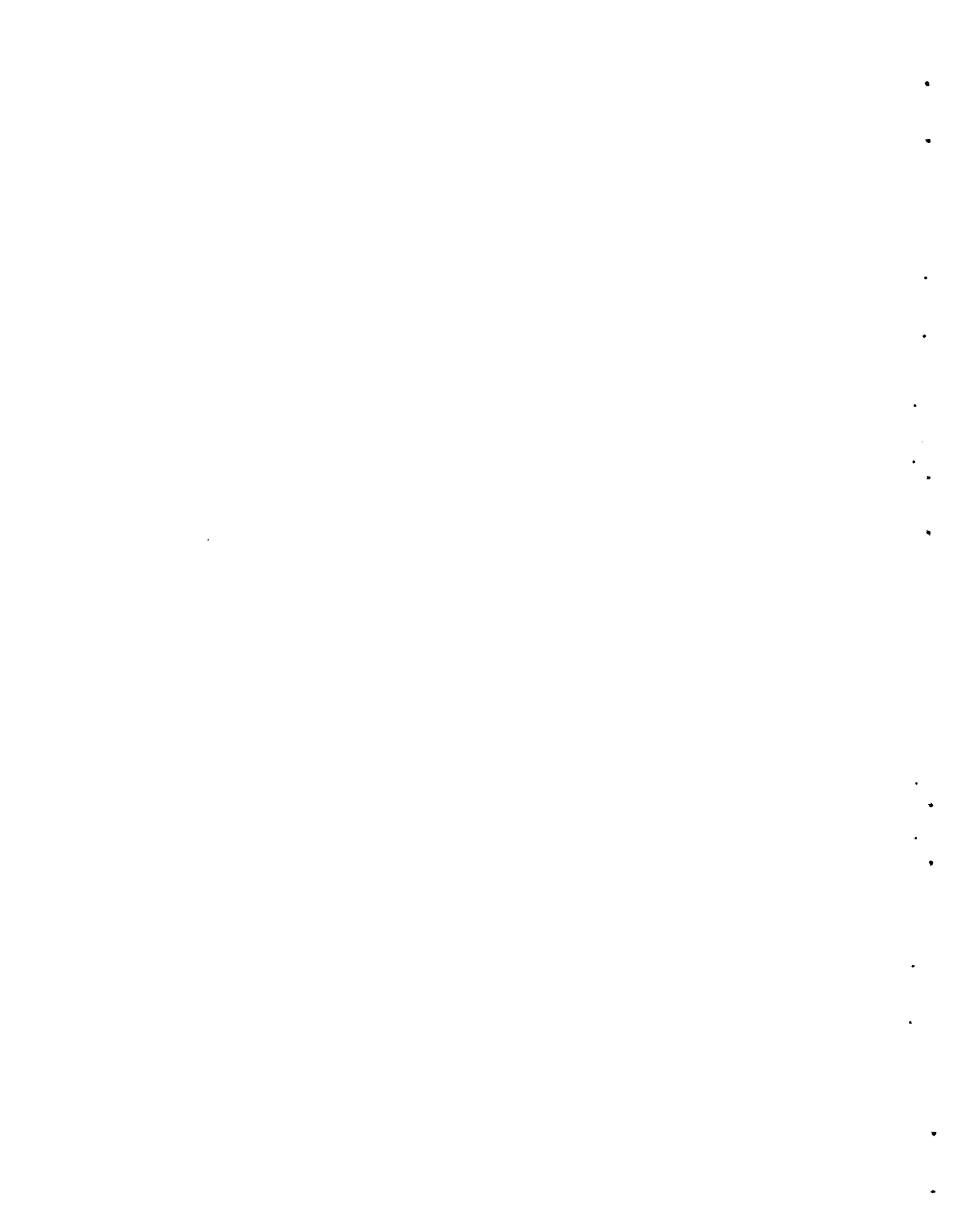
### PRESSURE VESSEL CRACK MONITORING (J. C. Spanner)

#### Detection of Metal Overstress by Acoustic Emission

Further work has been conducted on the development of a system to monitor for crack growth in reactor pressure piping by detecting the attendant acoustic emission.

Data derived from type 304L stainless steel, double cantilever beam, crack propagation specimens show a consistent pattern of maximum acoustic emission activity as the formation of a macrocrack is approached. Once the crack is formed and caused to grow, the abundance of acoustic emission decreases significantly. The high density of signals preceding formation of a visible crack may derive from formation of micro cracks and joining of these to form a macro crack. Once the gross crack is formed, if it propagates primarily by transgranular failure, the level of acoustic emission may drop appreciably. Obviously this pattern of events requires careful metallurgical analysis to correlate the acoustic emission with the metallurgical sequence. Such examination is planned as the next investigative step. This pattern of events is quite significant to the end objective of the program if it can be substantiated as being logical metallurgically.

The relative merits of accelerometers, conventional omnidirectional PZT-5 elements, epoxy bound PZT-5 powdered elements, and the





electrostatic transducer are being evaluated as acoustic emission sensors. The following performance characteristics have been observed to date:

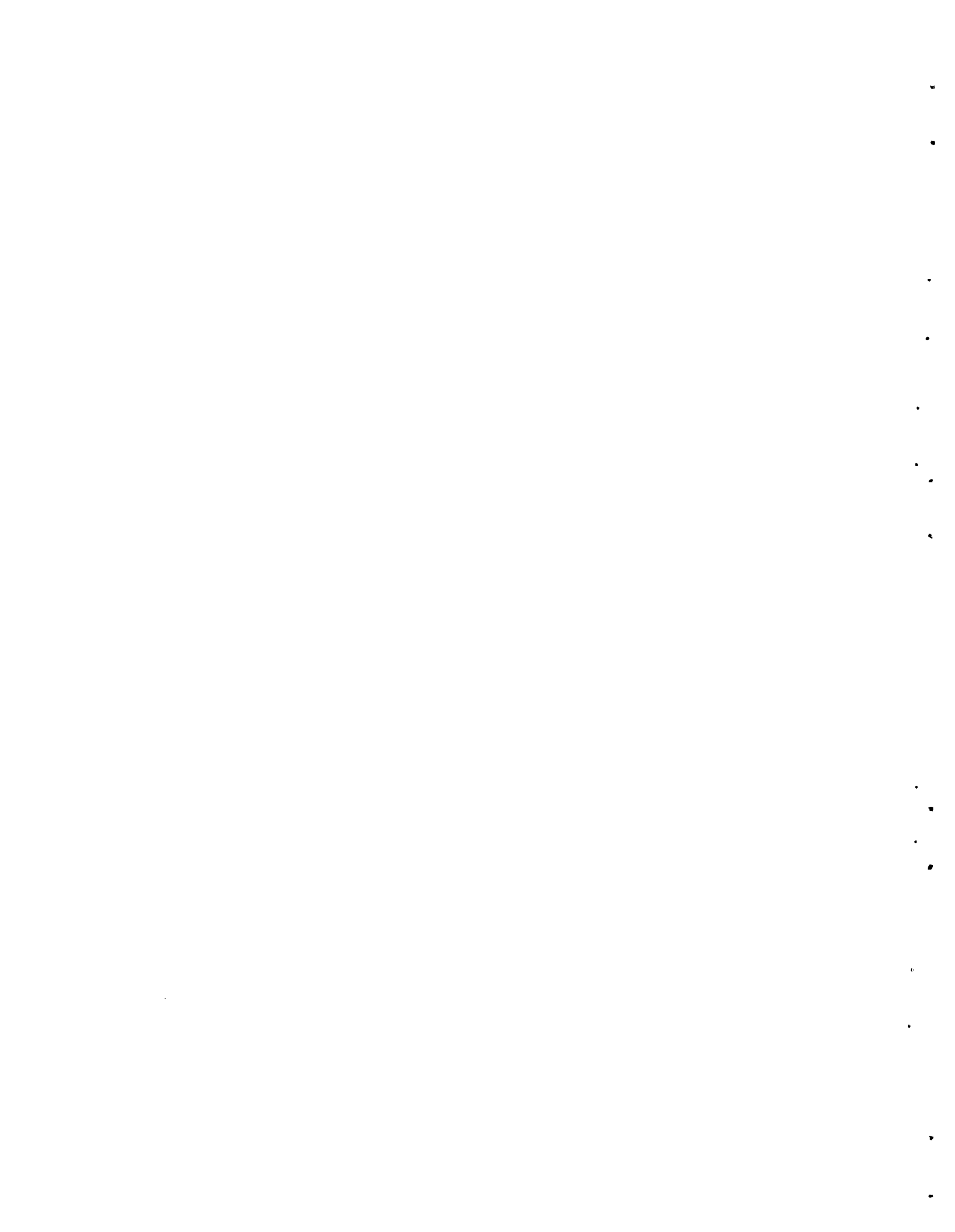
1. The epoxy bound PZT-5 powder appears to have the broadest frequency response, followed by electrostatic element, the omnidirectional PZT-5 element, and the accelerometer units.
2. The accelerometer is the most sensitive within its frequency limits (<30 KHz); however, for broadband response the omnidirectional PZT-5 element was most sensitive, the epoxy bound PZT-5 powder was second (i.e., about 1/3 the conventional PZT-5), and the capacitor third (i.e., about 1/5 the conventional PZT-5).
3. Epoxy bound PZT-5 powder still appears superior in amplitude directionality when polarized in both the longitudinal and shear modes.
4. For ease of bonding and reproducibility, the epoxy bound PZT-5 powder appears best since the mixture is molded directly on the specimen surface.
5. The capacitor transducer is best able to withstand high temperature service.

A factor of 10 improvement in the electrostatic transducer sensitivity was accomplished by changing from the accelerometer design to a ball-bearing electrode which is self-aligning with the mica dielectric sheet and the specimen surface. The sensitivity of this transducer is now approaching a usable level.

Problems were encountered with the back electrode of the epoxy bound PZT-5 powder elements; however, newly designed shapes appear to have solved the major problem of the wire post loosening up in the cured material.

The final step in this evaluation will be simultaneous monitoring of a double cantilever beam test with one each of the candidate transducers. When this is completed, evaluation results will be summarized including specific recommendations for future development work.

While conducting tests to detect fuel spacer vibration in a mockup of a pressurized reactor process tube, observations were made which are significant to this program. Signals generated by small impacts on the tube wall were transmitted quite readily across a rolled joint between the tube and a nozzle fitting. It was also found that the hydraulic noise in a pressurized, high temperature system is lower than anticipated. Additional data were obtained to permit checking the accuracy of locating the signal source in a pipe system by comparing time of signal arrival at various sensors. These data have not yet been analyzed.



Compilation of the first quarterly report on the acoustic emission program is in progress.

## RADIOACTIVE RESIDUE PROCESS DEVELOPMENTS (A. M. Platt)

### High Level Waste

#### Waste Solidification Engineering Prototypes (WSEP)

After completion of the phosphate glass Run A, the equipment was disassembled remotely and transferred to the Engineering Development Laboratory 102 for additional design verification tests. Remote installation and assembly of the pot solidification equipment established the final prototype equipment arrangement for the first radioactive run. Remote disassembly and reassembly of 90% of the other equipment was performed satisfactorily. Minor tool and procedure modifications are being completed as a result of the testing. In other tests the cooling capacity of the resistance-heated pot furnace was 6 kilowatts with the pot wall temperature at 260 °C during air cooling. The solids feeder system for the spray solidifier melter has been installed and is ready for final testing. The water flush system for the feed line was fabricated and installed.

A study was continued to formulate an optimal set of experimental designs to obtain specific information on storage properties of radioactive wastes.

#### Process Chemistry

Laboratory studies on the effects of variations from flowsheet composition on the processing of PW-2 waste showed that a 15% increase in selected feed components (increase in PO<sub>4</sub> and SO<sub>4</sub>, decrease in Li, Na, Al and Ca) can increase sulfate evolution by a factor of two. A similar study of the effect of non-flowsheet rate of addition of NaPO<sub>3</sub> to the melter showed that an increase of phosphate concentration by a factor of four in the melter is required to double the rate of sulfate evolution. A survey of PW-2 waste stability toward solids formation was made as a function of initial acidity and degree of concentration.

Run B in the WSEP will be an ORNL Rising Level Glass run with PW-1 waste as the feed. Phosphate, sodium, and lithium will be added for fluxing and lowering the melting point. Corrosion tests with melts having various additive compositions are being made to aid in selecting operating conditions and receiver pot material. In these tests, 310 stainless steel appears to have better corrosion resistance than 304L.

#### Glass Studies

Data for the mixed phosphate-borate-silicate matrix system have been submitted for statistical correlation. Preliminary mathematical analysis has revealed the need for data on several additional compositions, and these are currently being prepared.



Work continued on measurement (with the high temperature dilatometer) of the thermal expansion properties of a large number of samples of glasses and microcrystalline solids corresponding to various proposed WSEP compositions. One sample, prepared in the 324 Building equipment, showed a very unusual hysteresis behavior. It expanded on heating but contracted much less on cooling (actually expanded over a portion of the descending temperature range). This behavior could obviously have serious consequences for the integrity of a relatively inelastic container.

In other work, an evaluation is being made of the French and British type of glasses--from the standpoint of use with waste of Hanford Purex composition. (Hanford waste contains a much higher concentration of inerts than either British or French Purex waste.) It appears that the lower corrosivity and leachability of the British and French glasses will have to be weighed against the larger volume of waste they will produce.

#### COLUMBIA RIVER SEDIMENTATION STUDIES (J. M. Nielsen)

Calibration of a 9-inch well crystal and scintillation-counting system was completed for use on samples from the Columbia River estuary. A revised computer program (GEM) was prepared for use with this detector. This system measures specific activities of 1 dpm per gram or less for radionuclides of interest in this study. Because of the larger volume capability of this well crystal, less sample evaporation will be necessary with an accompanying reduction in cost.

In an effort to establish the chemical forms of radionuclides in Columbia River sediment, media suitable for gradient density separation of the samples into organic and inorganic fractions are being sought. The liquid, 2-bromoethanol (specific gravity 1.77) which was initially recommended for this purpose was found to be unsuitable due to its solvent action on the radionuclide-containing compounds of the sediment.

#### WASTE SOLIDIFICATION CONDENSATE TREATMENT (G. J. Alkire)

Experiments were started to determine the most effective method for dissolving the centrifuged residue from the hydrous-oxide ferricyanide scavenging scheme so that the solution containing fission products can be recycled to the headend of the solidification process.

Preliminary work showed that  $H_2O_2$ ,  $NaHSO_3$ , and hydroxylamine in dilute  $H_2SO_4$  will readily dissolve the hydrous oxides. The hydroxylamine- $H_2SO_4$  system appears to be the most effective method. Present efforts are being directed toward optimizing reagent concentrations for most effective dissolution. The effects of the dissolution on the ferricyanide precipitate are being investigated using  $Cs^{137}$  as a tracer.

Further research will be required to determine if accumulation of ferricyanides in the system gives rise to hazardous conditions.

•

•

•

•

•

•

•

•

•

•

•

•

•

•

•

•

Preliminary experiments were made on methods for treating the high volume condensate generated in the WSEP process. Three methods tried were sorption on minerals, ozone sparging, and air sparging in permanganate solutions.

Pyrolusite ( $MnO_2$ ) was used as the sorbent in the first mineral sorption experiments. Radioruthenium, the principal contaminant, was sorbed to less than 5% breakthrough for 40 column volumes and less than 30% breakthrough for 70 columns at pH 5. Other minerals such as those having high  $Fe_2O_3$  content will be used in future studies.

Results of ozone sparging showed that a 2%  $O_3$  sparge at 300 ml/min flow rate will reduce the ruthenium concentration by 99.9% in two hours. For the same flow rate, the time required for equivalent reductions can be reduced by about 60% if 0.1 M  $AgNO_3$  is added to solution. Air sparging in a solution containing  $KMnO_4$  was also shown to be effective. About 95% reduction of the ruthenium concentration was effected by sparging in a 0.001 M  $KMnO_4$  solution for two hours. Greater reductions will take place in a shorter period of time if the  $KMnO_4$  concentrations are increased. For example, a ruthenium reduction of 97.5% was observed in 50 minutes for 0.1 M  $KMnO_4$ . For all sparging experiments, temperatures from 90 to 95 °C were employed.

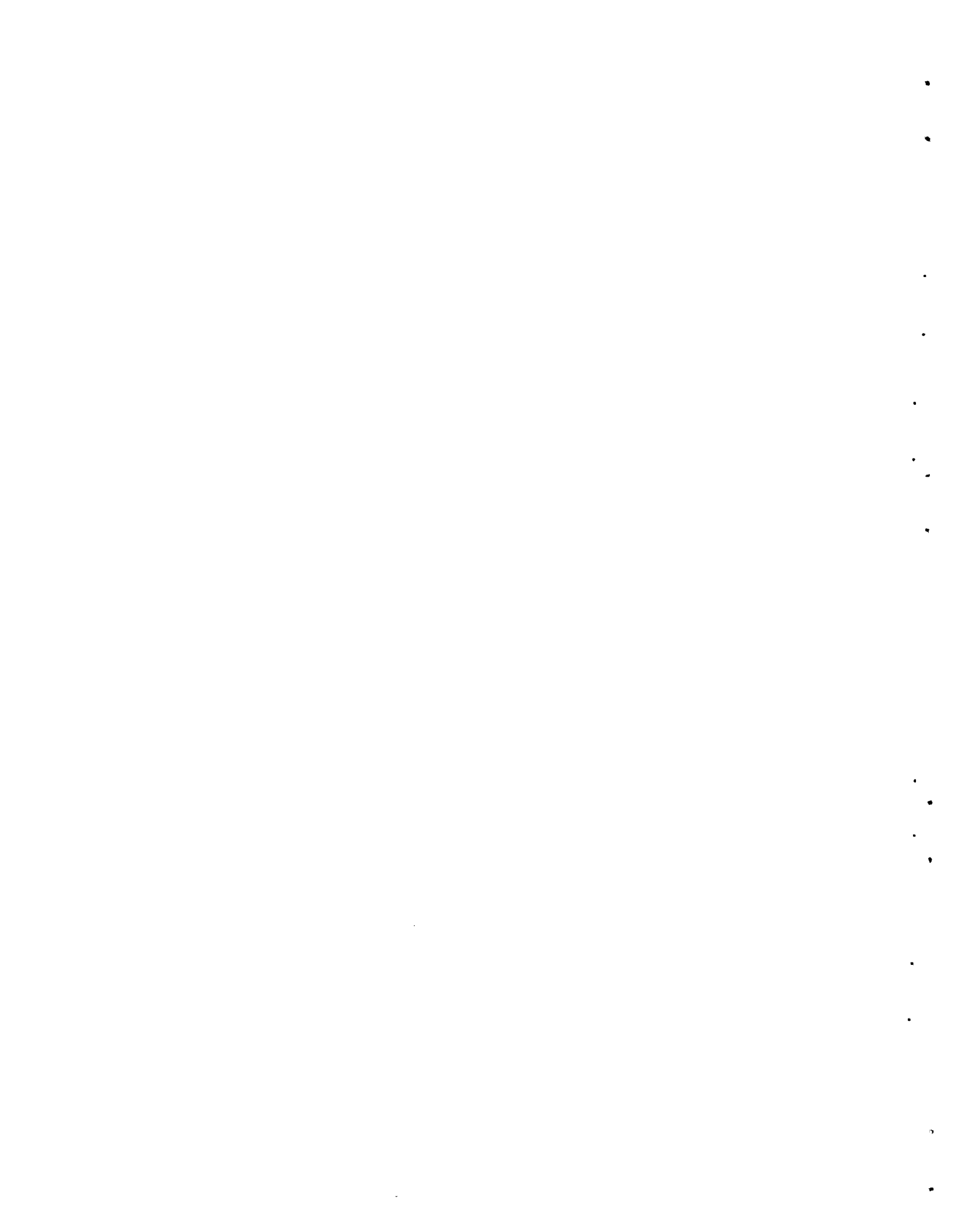
#### RADIOACTIVE SHIPMENT HAZARDS (L. C. Schwendiman)

The release experiments were completed on the samples of simulated high level waste spiked with actual waste material. Diffusion theory is being used to correlate the observed release to theoretical mass transfer by diffusion theory is being used to correlate the observed release to theoretical mass transfer by diffusion in the molten ceramic phase. Based on an assumed diffusivity of  $10^{-7}$   $cm^2/sec$ , diffusion rates for cesium were found to be in fairly close agreement with the measured release rates, 1 to 2% per hour. This diffusivity is within the range expected for alkali metals.

#### FISSION PRODUCT AEROSOL CONTAINMENT

##### Removal of Organic Iodide with Hydrazine (L. C. Schwendiman)

Hydrazine sprays were used in the 114-liter aerosol chamber to remove methyl iodide. For each experiment the chamber was initially brought to approximately 75 °C and contained a  $CH_3I$ -steam atmosphere. Next, approximately four liters of room temperature solutions were sprayed through the chambers at a recycle rate of approximately 300 ml/min. After the hydrazine had been sprayed into the chamber, the air temperature was approximately 45 °C. Solutions of both a 37% hydrazine and a combination of 35% hydrazine and 5% ammonium hydroxide removed virtually all the  $CH_3I$  from the chamber atmosphere. A 5% hydrazine, 5% ammonium hydroxide solution removed 75 to 87% of the  $CH_3I$  from the chamber atmosphere.





Installation of the piping on the large aerosol chamber was essentially completed and electrical work was under way. Still remaining are the construction of the greenhouse, installation of the stirrer and iodine generator, and a large trapping system.

#### Physical Chemistry of Hydrazine-Methyl Iodide Reaction (L. L. Burger)

The gas chromatograph-electron capture detector for methyl iodide was found to respond linearly to methyl iodide concentrations up to  $3 \times 10^{-10}$  g of methyl iodide. With the present sensitivity it was possible to extend reaction studies to concentrations of about 1.6 mg per m<sup>3</sup>.

The rate of reaction of methyl iodide with the equilibrium vapors over the water and sodium hydroxide solutions of hydrazine was measured. The time for 50% removal was quite rapid (0.8 min) over 95% hydrazine and much slower for 36 and 52% hydrazine. The presence of NaOH appeared to slow the reaction even further. The effect was not dependent on concentration of NaOH in the range 0.05 to 0.2 M.

In several cases the concentration was followed over several half-lives and in all but one case the concentration of methyl iodide decreased exponentially according to

$$C = C_0 e^{-kt}$$

in which  $C_0$  = initial concentration and  $C$  = concentration at time  $t$ .

The reaction proceeded to virtually complete removal of methyl iodide. In one case less than 0.02% of the methyl iodide remained.

#### DISPOSAL OF REACTOR OFF-GAS INTO SOIL SYSTEMS (W. A. Haney)

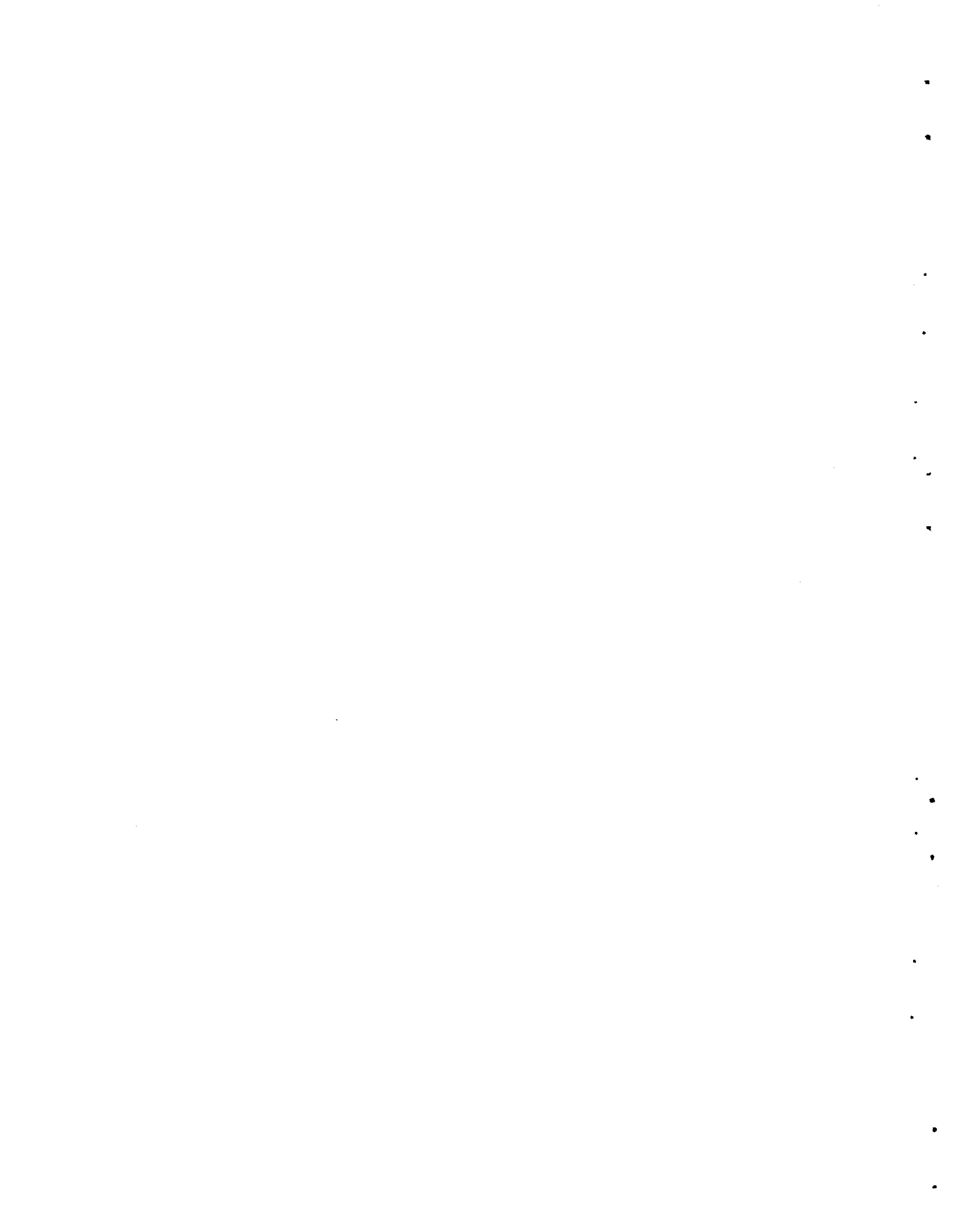
A solution was obtained for a single-well geometry in a uniform infinite medium which should allow the injection-well radius to be accurately defined (a property which an earlier solution lacked). The solution will be used to calculate flow rates and travel times for wide ranges of geometric variables, injection pressures, and temperatures.

The numerical scheme for calculating flow rates from finite difference solutions to compressible gas flow problems was found to be correct. Inconsistencies which are being experienced in mass flow rate calculations must be in either the formulation of the problems or in the approximations arising through use of finite difference solutions to such problems. The cause of the inconsistencies is being sought.

#### REACTOR SAFETY ANALYSIS AND EVALUATION (R. G. Wheeler)

##### Subsize Vessel Failure Analysis

This portion of the program is concerned with evaluating the failure behavior of irradiated low-alloy steel reactor pressure vessels from tests on subsize-vessel specimens.



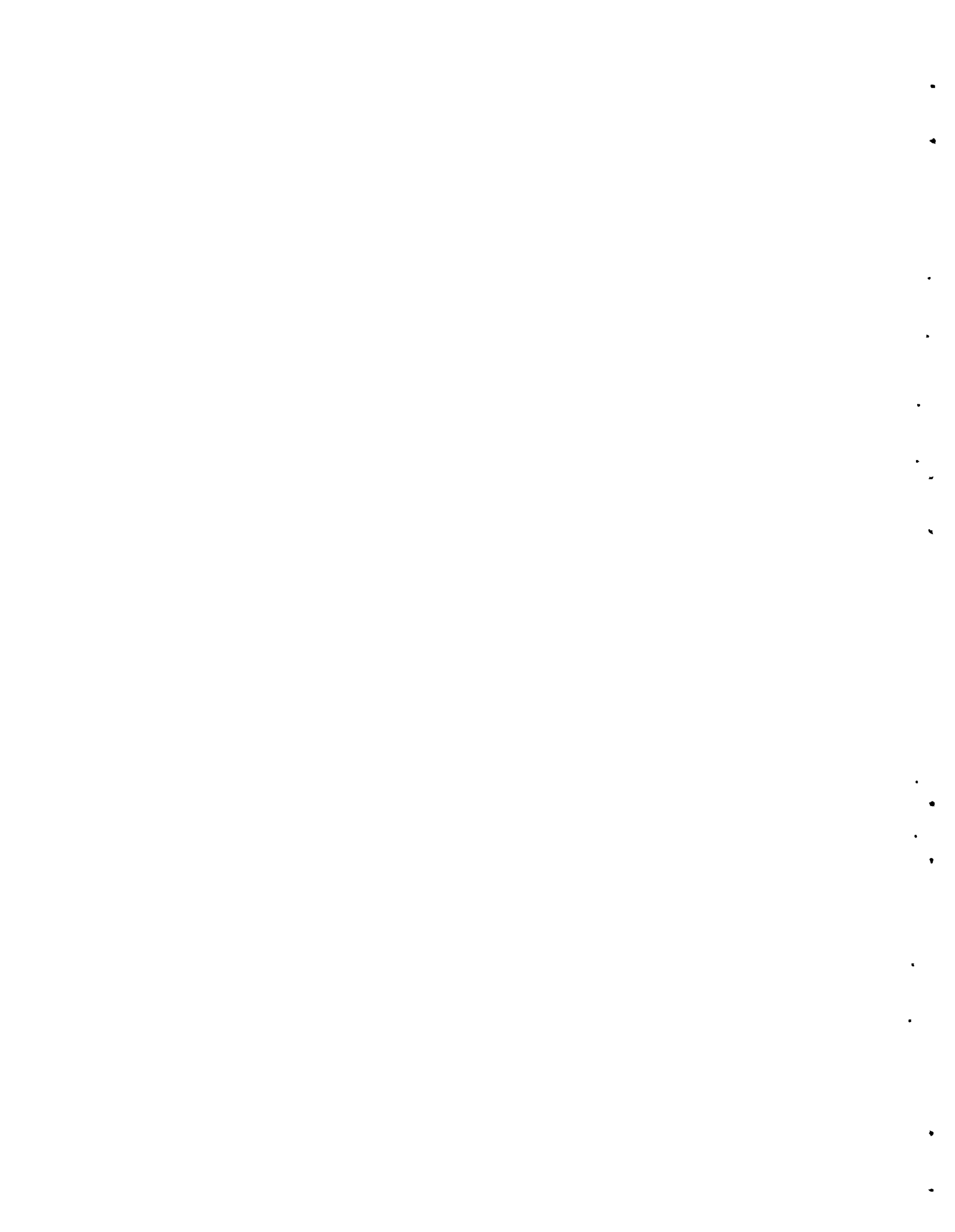
During this period the compliance testing of the subsize-vessel specimens was continued, the low cycle fatigue growth of cracks in subsize-vessel specimens was continued, and the first two irradiated A212B subsize-vessel specimens were burst tested. The large amount of compliance data obtained to date has not been adequately analyzed. The analysis of this data will be near completion next month (July). Preliminary results from the crack growth studies are very encouraging. The usefulness of these crack growth tests for irradiated specimens will depend on the nondestructive monitoring equipment being able to pick up a repeatable acoustic emission signal. These preliminary tests on unirradiated specimens have produced a repeatable acoustic signal during the fatigue test.

The results of the burst tests of the irradiated A212B specimens are most encouraging. The specimens were obtained from a GEH-10 basket that had been exposed in the M3 position of the ETR for one reactor cycle. Preliminary dosimetry studies indicate these specimens received an exposure of approximately  $2.5 \times 10^{18}$  nvt ( $E > 1$  Mev). The temperature of the specimens during the reactor exposure was between 400 and 500 °F (204.4 and 260 °C).

The specimens were 18" long with a 2.0" inside diameter, and both specimens had longitudinal slots 0.06" wide by 1.0" long milled 0.2" through the 0.25" thick specimen wall. The specimens were internally pressurized to failure of the 0.05" thick web under the slot. The opened webs provided through wall thickness cracks with sharp crack tips. A rubber cylinder, called a mouse patch, was placed inside the specimen and provided a water tight seal of the cracks during the burst tests. The loading of the specimens produced an approximate axial stress to hoop (circumferential) stress ratio of 1/2.

One specimen was burst tested at 86 °F (30 °C) and the other specimen was burst tested at 66 °F (19°C). The specimen tested at 86 °F failed in a ductile manner with the crack propagating only a short distance. The specimen tested at 66 °F failed in a brittle manner with the crack propagating the full length of the specimen. The 86 °F failure occurred at a hoop stress of 55,400 psi. The failure of the irradiated specimen at 86 °F is very similar to the 80 °F failure of an unirradiated specimen. The unirradiated specimen failed at a hoop stress of 42,400 psi. Modified drop-weight tear tests of this material indicated the NDT temperature of the unirradiated A212B to be -40 °F. These two burst tests indicate the NDT temperature of the irradiated specimens is 76 °F (24.4 °C).

Ultrasonic monitoring techniques were applied to these burst tests to study the acoustic emission generated during failure over a band width of 50 kc to 1 mc. Signals generated within the specimens are picked up mechanically by a piezoelectric source and converted to electronic pulses. The pulse information is amplified at the transducer impedance to that of a cable leading to a unit with filtering, integrating, and amplifying capabilities. At the time of the test the pulse information is monitored using a memory type oscilloscope and stored on magnetic tape. The two burst tests of irradiated specimens



produced a significant amount of acoustic signals. Similar burst tests of unirradiated A212B specimens at the same temperatures produced a negligible amount of signal. It was previously found that satisfactory acoustic signals from burst tests of unirradiated A212B specimens were received only at temperatures below  $-20^{\circ}\text{F}$ . It has been demonstrated that ultrasonic monitoring techniques to study acoustic emission can be applied successfully to irradiated specimens during failure. The shift in NDT due to the irradiation exposure is seen to correspond to the shift in temperature below which ultrasonic signals are received over a bandwidth of 50 kc to 1 mc.

#### CUSTOMER

ASSISTANCE TO PHILLIPS PETROLEUM COMPANY (W. L. Hampson, Jr.)

##### Np-Al Capsules

Four capsules, each having a different neptunium concentration, are being fabricated for resonance integral measurements. The neptunium is in the form of Al-Np alloys, 0.5 to 5 wt% Np. The alloys are cast and rolled into sheets 0.030" thick. Coupons, 4-1/2" long, are cut from the sheet and formed into 0.86" diameter tubes. Each tube is inserted into an aluminum can.

ASSISTANCE TO GENERAL ATOMIC (W. L. Hampson, Jr.)

##### PuO<sub>2</sub> - Graphite Compacts

Process development and tooling were nearly completed for the fabrication of 12 rods containing PuO<sub>2</sub> - graphite compacts. The rods will be used for critical tests. The 12 rods will consist of six pairs with three different PuO<sub>2</sub> concentrations and two separate isotopic (Pu<sup>240</sup>) compositions. Two rods containing pure graphite compacts were fabricated for standards and to test fabrication procedures. The remaining development problem concerns obtaining and insuring uniform plutonium distribution within and among compacts.

U. S. NAVAL RESEARCH LABORATORY (R. E. Dahl)

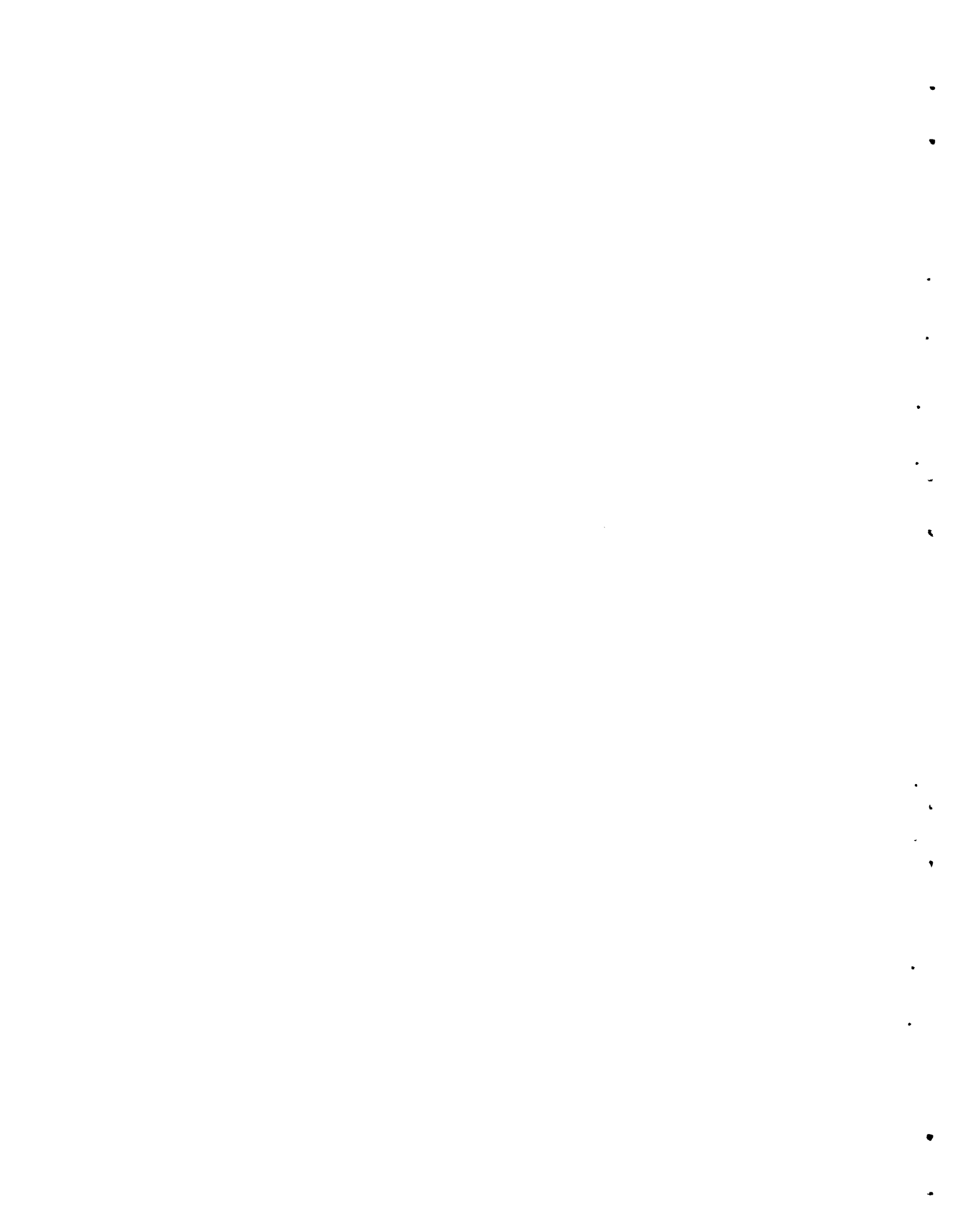
##### Effects of Uncertainties in the Differential Cross Section of the Fe<sup>54</sup> (n,p)Mn<sup>54</sup> Reactions

There is a substantial uncertainty in the differential cross section for the Fe<sup>54</sup>(n,p)Mn<sup>54</sup> reaction which unfortunately has a considerable effect in exposure rates for damage studies of reactor pressure vessels. Three investigators have used essentially the same cross section measurements of the Fe<sup>54</sup>(n,p)Mn<sup>54</sup> reaction but have fared dissimilar lines through the measured points. The resulting fission-average cross sections are 68 mb, 82 mb, and 97 mb. The principal differences are caused at the low energy end of the iron-activation curve since the fast neutron flux is high in this region.



Determination of neutron exposure for several reactor pressure vessels has been based on fluxes calculated from activation of iron monitors placed at or near the reactor pressure vessel walls. Iron monitors have been widely utilized for exposure determinations because the  $\text{Fe}^{54}(\text{n},\text{p})$  reaction is the most reliable monitor which can be used to accurately detect fast neutrons over extended times.

Estimates of the pressure vessel flux of the SM-IA reactor, which is currently undergoing safety review, are based on data from activation of iron monitors. Spectral-averaged cross sections have been calculated with the three differential cross-section curves discussed above and a spectrum which was determined with a transport-theory analysis. Values for these spectral-average cross sections differed by about 35%. Since the estimated safe life of the reactor pressure vessel is directly proportional to the flux at the pressure vessel, uncertainties in the  $\text{Fe}^{54}(\text{n},\text{p})$  cross section are very important in the safety analysis of this reactor and could be similarly important in safety analysis of other reactor systems.





DISTRIBUTIONNumber of Copies

3	<u>AEC Division of Technical Information Extension</u>
1	<u>Aerofjet-Nucleonics</u> P. O. Box 77 San Ramon, California G. W. Titus
1	<u>Aeroprojects, Inc.</u> W. B. Tarpley
1	<u>Air Force Materials Laboratory</u> Wright-Patterson AFB S. W. Bradstreet
1	<u>Allis Chalmers Manufacturing Co.</u> Virginia D. Rose
1	<u>Ames Laboratory</u> F. H. Spedding
3	<u>Argonne National Laboratory</u> R. M. Adams C. E. Stevenson R. C. Vogel
1	<u>Armour Research Foundation</u> W. Loewe
3	<u>Atomics International</u> A. A. Jarrett (2) H. Pearlman
1	<u>Atomic Power Development Associates, Inc.</u> W. H. Jens
2	<u>The Babcock and Wilcox Company</u> Lynchburg, Virginia H. S. Allen R. A. Webb
1	<u>Battelle Memorial Institute</u> D. L. Morrison
1	<u>Bechtel Corporation</u> R. F. Griffin
4	<u>Brookhaven National Laboratory</u> A. E. Castleman Elizabeth J. Edwards C. J. Raseman D. G. Schweitzer

.

.

.

.

.

.

.

.

.

.

.

.

.

.

- 2        Carolinas-Virginia Nuclear Power Associates  
          H. T. Babb
- 1        Columbia University, New York  
          J. E. Casterline
- 1        Combustion Engineering  
          P. O. Box 500  
          Windsor, Connecticut  
          W. P. Chernock
- 1        Dow Chemical Company, Rocky Flats  
          J. R. Seed
- 7        DUN  
          J. R. Carrell  
          D. R. Hogle (Atomics International)  
          C. G. Lewis  
          W. M. Mathis  
          H. G. Spencer  
          J. R. Spink  
          W. K. Woods
- 1        Ebasco Services, Inc.  
          T. A. Flynn, Jr.
- 2        E. I. duPont de Nemours and Co.  
          W. B. Scott
- 5        General Atomic Division  
          S. L. Koutz  
          E. Creutz  
          D. B. Coburn  
          D. V. Ragone  
          A. J. Goodjohn
- 1        General Electric Co.,  
          Advanced Technology Laboratory, Bldg. 5  
          Schenectady, N. Y.  
          J. L. Michaelson
- 2        General Electric Company, Pleasanton  
          L. P. Bupp  
          E. A. Evans
- 9        General Electric Company, Richland  
          W. J. Dowis  
          R. E. Dunn  
          G. L. Hammons  
          H. H. Hopkins  
          M. Lewis  
          J. S. McMahon  
          J. W. Nickolaus  
          J. W. Riches  
          R. E. Tomlinson



2        General Electric Company, San Jose  
         K. P. Cobern  
         S. Naymark

2        General Electric Company  
         2151 1st St., San Jose, California  
         C. H. Robbins  
         E. R. Kilsby

1        General Electric Company, APED  
         San Jose, California  
         R. B. Richards

2        IIT Research Institute  
         10 West 35th St.,  
         Chicago, Illinois  
         W. J. McGonnagle  
         T. A. Zaker

1        Knolls Atomic Power Laboratory  
         W. Cashin

1        Los Alamos Scientific Laboratory  
         H. F. Redman

1        Massachusetts Institute of Technology  
         Manson Benedict

1        National Bureau of Standards  
         C. Muehlhause

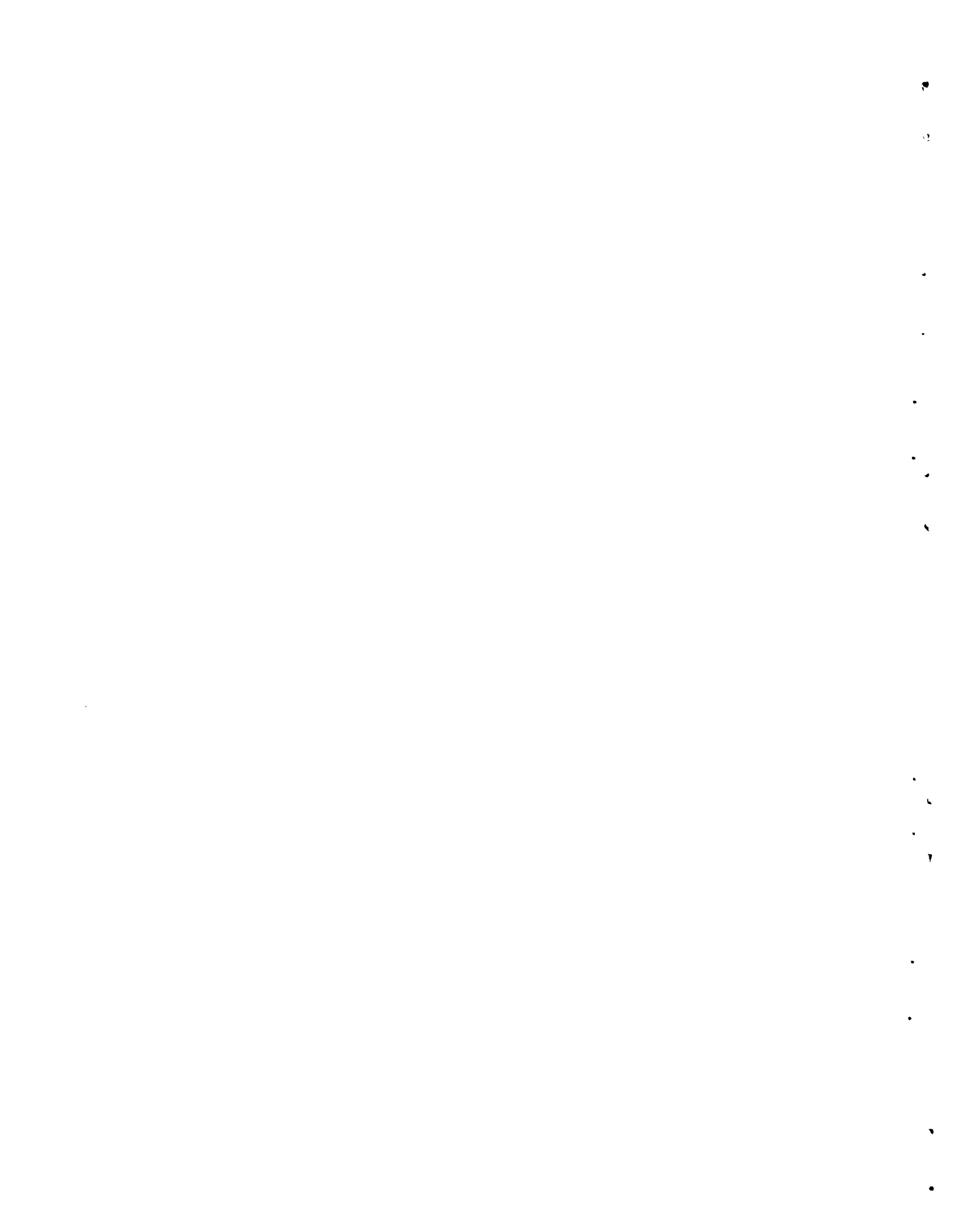
1        Nuclear Development Corporation of America  
         W. A. Loeb

1        Nuclear Materials and Equipment Corporation  
         C. S. Caldwell

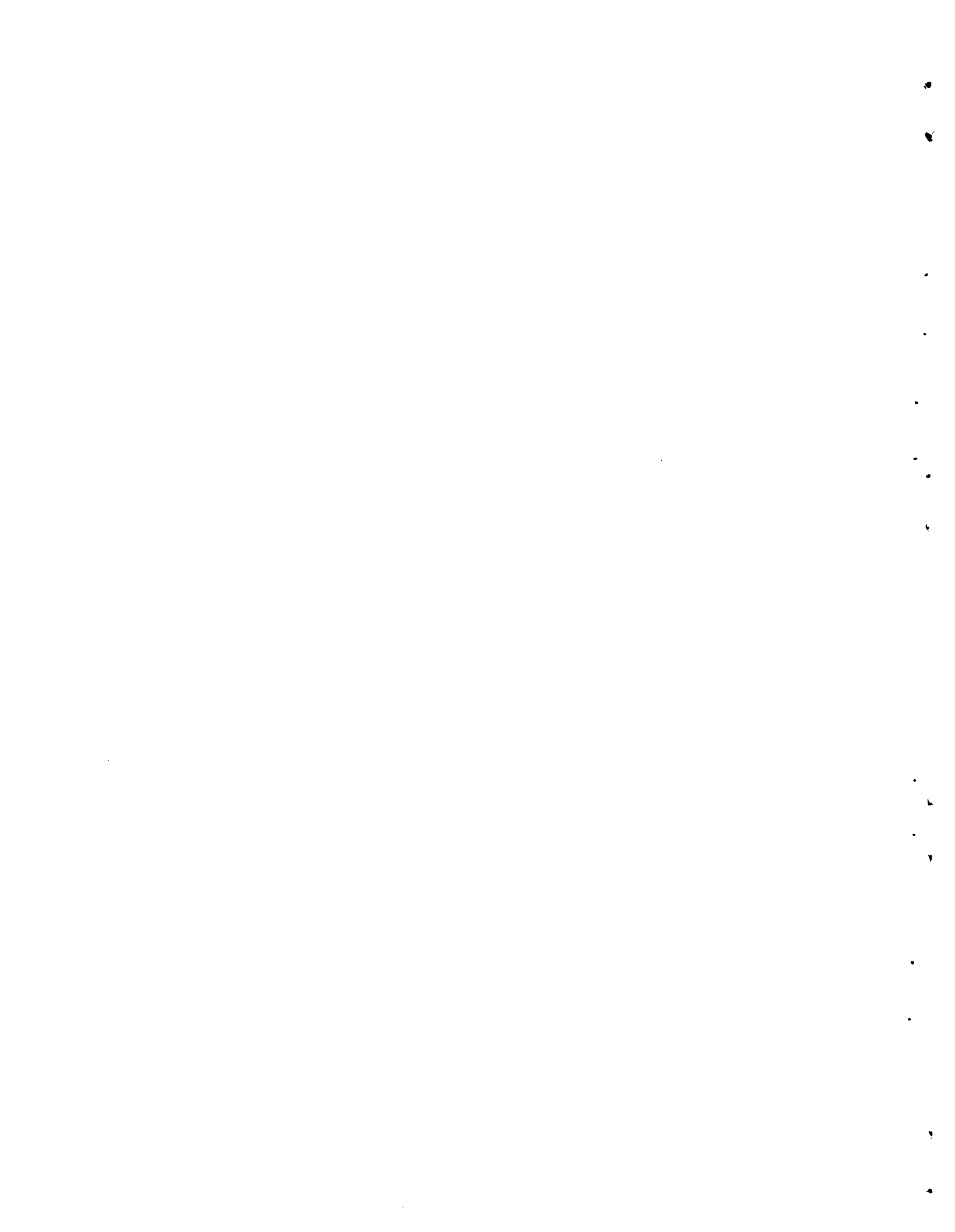
2        Oak Ridge Operations Office  
         D. F. Cope  
         W. J. Larkin

10       Phillips Petroleum Company  
         G. Bright (2)  
         W. E. Nyer (2)  
         F. Schroeder (2)  
         T. R. Wilson (2)  
         D. R. de Boisblanc  
         E. O. Mills

4        Richland Operations Office  
         P. M. Midkiff  
         C. L. Robinson  
         R. K. Sharp (2)



- 1        Sargent and Lundy  
W. A. Chittenden
- 7        Union Carbide Corporation (ORNL)  
F. L. Culler  
W. B. Cottrell  
J. H. Frye  
R. W. McClung  
O. Sisman  
D. B. Trauger (2)  
M. S. Wechsler
- 1        United Nuclear Corporation  
C. Graves
- 1        University of California  
V. E. Schrock
- 1        University of Minnesota  
H. Isbin
- 1        University of Texas  
G. W. Watt
- 1        USAEC, Canoga Park  
R. W. Richards
- 1        USAEC-AECL, Chalk River, Canada  
M. N. Hudson
- 1        USAEC, Chicago Operations Office  
Argonne, Illinois  
D. M. Gardiner
- 1        USAEC, Division of Compliance  
Region IV, P. O. Box 15266, Denver  
J. W. Flora
- 1        USAEC, Division of Compliance  
Washington  
L. Kornblith, Jr.
- 1        USAEC Headquarters, Washington  
Space Electrical Propulsion Office  
Col. G. K. Dicker
- 3        USAEC, Idaho Operations Office  
J. F. Kaufmann  
D. C. King  
D. E. Williams





2        USAEC, New York Operations Office  
         A. J. Rizzo  
         C. Stahle

1        USAEC, San Francisco Operations Office  
         211 Bancroft Way  
         Lt. Col. J. B. Radcliffe, Jr.

1        USAEC, Savannah River Operations Office  
         H. B. Rahner

1        USAEC, Toronto Technical Representative  
         D. G. Boyer

17       USAEC, Washington  
         Advisory Committee on Reactor Safeguards  
         R. F. Fraley

1        USAEC, Washington  
         Civilian Reactors, Division of Reactor Development  
         and Technology  
         A. Giambusso

7        USAEC, Washington  
         Division of Licensing and Regulation  
         E. G. Case  
         J. J. DiNunno

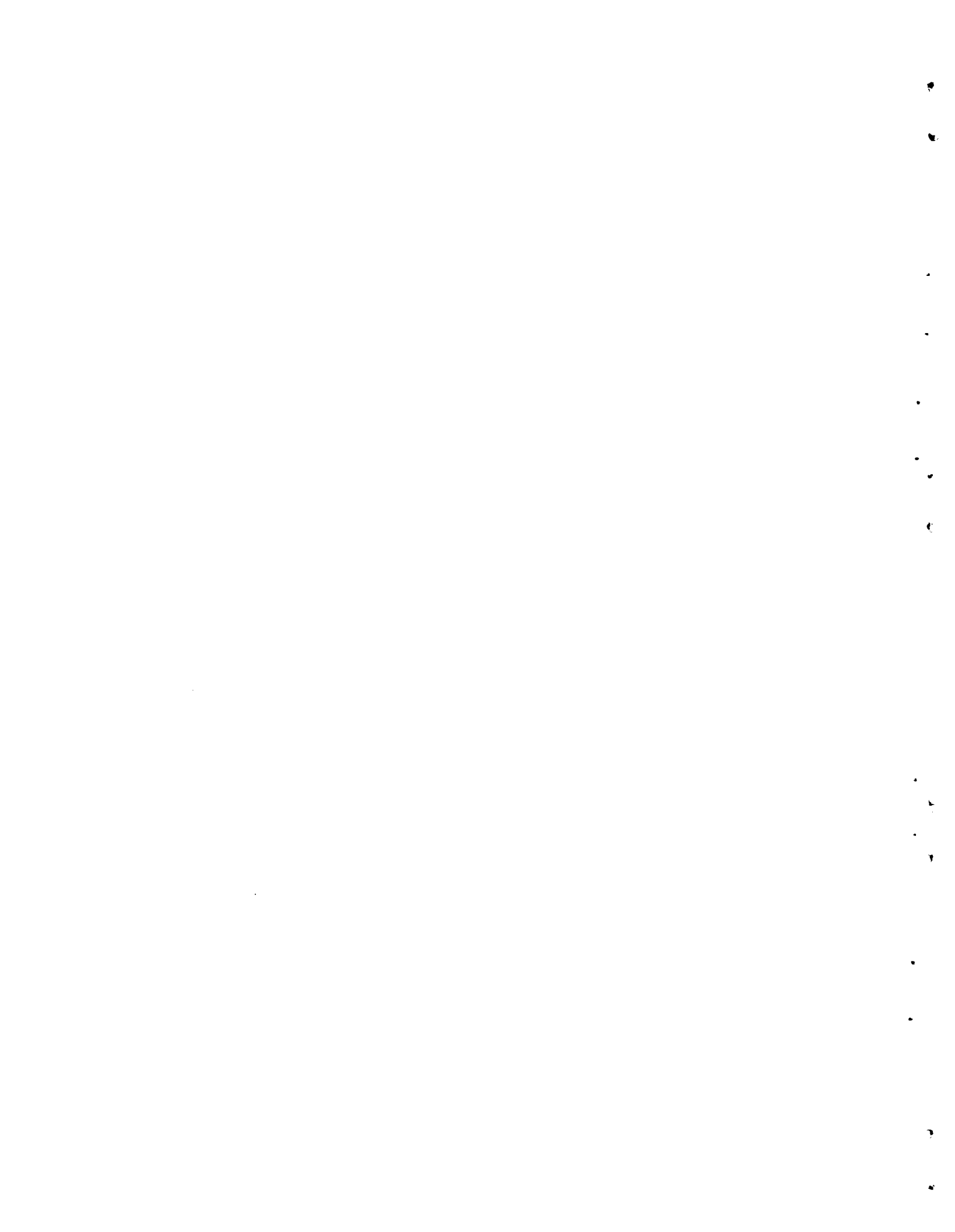
3        USAEC, Washington  
         Division of Production  
         F. P. Baranowski

20       USAEC, Washington  
         Division of Reactor Development and Technology  
         Col. K. Cooper  
         J. E. Robb  
         S. A. Szawlewcz  
         M. Shaw (16)  
         G. W. Wensch

1        USAEC, Washington  
         Division of Research  
         G. A. Kolstad

1        USAEC, Washington  
         Naval Reactors Branch  
         Division of Reactor Development and Technology  
         R. S. Brodsky

1        USAEC, Washington  
         Office of Assistant General Counsel for Patents  
         R. A. Anderson



4

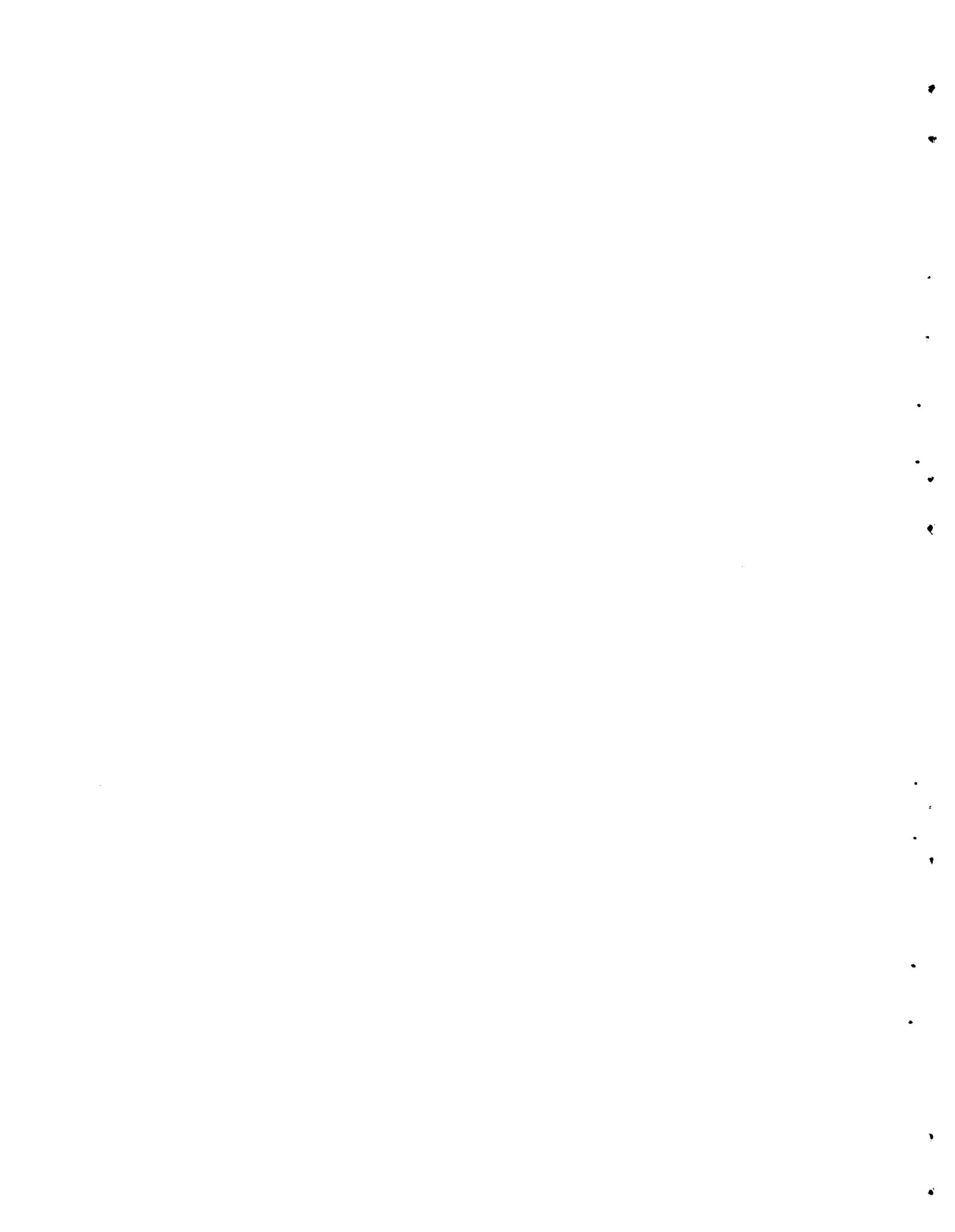
Westinghouse Electric Corporation

R. H. Fillnow  
R. G. McGrath  
E. J. Kreh  
R. A. Wieseemann

75

Battelle-Northwest

F. W. Albaugh  
G. J. Alkire  
R. J. Anicetti  
J. M. Atwood  
J. A. Ayres  
J. M. Batch  
T. K. Bierlein  
J. G. Bradley  
S. H. Bush  
J. J. Cadwell  
E. D. Clayton  
T. B. Correy  
F. G. Dawson  
L. J. Defferding  
D. R. de Halas  
R. F. Dickerson  
R. L. Dillon  
K. Drumheller  
E. A. Eschbach  
S. L. Fawcett  
J. R. Fishbaugher  
W. E. Foust  
J. C. Fox  
G. C. Fullmer  
E. P. Galbraith  
S. M. Gill  
S. Goldsmith  
L. A. Hartcorn  
H. Harty  
R. E. Heineman  
R. J. Hennig  
H. L. Henry  
P. L. Hofmann  
E. R. Irish  
A. R. Keene  
L. W. Lang  
D. D. Lanning  
H. V. Larson  
G. A. Last  
R. D. Leggett  
J. E. Minor  
T. C. Nelson  
C. E. Newton  
R. E. Nightingale  
H. M. Parker  
R. S. Paul  
L. T. Pedersen  
A. M. Platt



W. D. Richmond  
W. E. Roake  
C. A. Rohrman  
L. C. Schwendiman - C. E. Linderoth  
W. A. Snyder (5)  
A. J. Stevens  
R. W. Stewart  
W. H. Swift  
C. R. Tipton  
L. D. Turner  
C. M. Unruh  
E. E. Voiland  
F. W. Van Wormer  
M. T. Walling  
R. G. Wheeler  
R. D. Widrig  
F. W. Woodfield  
D. C. Worlton  
Technical Information Files (3)  
Technical Publications (2)

